

THESIS FOR THE DEGREE OF DOCTOR OF PHILOSOPHY

# Predicting the Long-Term Insulation Performance of District Heating Pipes

CAMILLA PERSSON

Division of Building Technology  
Department of Civil and Environmental Engineering  
CHALMERS UNIVERSITY OF TECHNOLOGY  
Gothenburg, Sweden, 2015

Predicting the Long-Term Insulation Performance of District Heating Pipes  
A. CAMILLA PERSSON  
ISBN: 978-91-7597-172-8

© A Camilla Persson, 2015

Doktorsavhandlingar vid Chalmers tekniska högskola  
Ny serie nr 3853  
ISSN: 0346-718X

Division of Building Technology  
Department of Civil and Environmental Technology  
Chalmers University of Technology  
SE-412 96 Göteborg  
Sweden  
Telephone: +46 (0)31-772 1000  
<http://www.chalmers.se>

Printed by Chalmers Reproservice  
Göteborg, Sweden, 2015

# Predicting the Long-Term Insulation Performance of District Heating Pipes

CAMILLA PERSSON

Division of Building Technology

Department of Civil and Environmental Technology

Chalmers University of Technology

## *ABSTRACT*

The aim of the studies that comprise this thesis was to predict the heat loss over time from a range of district heating pipes insulated with closed-cells foam. The thermal conductivity of the foam changes over time when it is not diffusion-tight encapsulated against the environment, as diffusion alters the cell gas composition until it reaches equilibrium with the surrounding air. Over the first thirty years of use the insulation capacity of a straight pipe of medium size insulated with polyurethane foam decreases by about 10%. The insulating gases cyclopentane and carbon dioxide initially present in the foam cells diffuse out of the foam over time, while nitrogen and oxygen from the air diffuse into it. Complete ageing increases the thermal conductivity of the insulation by about  $10 \text{ mW}\cdot\text{m}^{-1}\cdot\text{K}^{-1}$ , but it is a slow process that takes several years. Equilibrium is not even reached after 100 years. In this work models have been derived that can be used to predict the long-term heat flow from the pipes and investigate the influence of factors that have an impact.

Finite difference models for the pipes alone are presented, which consider the variation of the cell gas composition over the foam cross section. All gases are considered in the gas phase. But cyclopentane is also considered in dissolved state, as well as potentially in liquid state depending on the amount and the temperature present. In order to determine the solubility of cyclopentane in the polyurethane matrix of the foam measurements were performed. The solubility was found to decrease with temperature. About 50% of the cyclopentane was dissolved at room temperature, while only about 35% was dissolved at  $50^\circ\text{C}$ . There is a weak coupling between the heat conduction (i.e. temperature) and the gas diffusion (i.e. cell gas content) due to the fact that the thermal conductivity is dependent both on the temperature and the cell gas content, which has been taken into consideration. Both single and twin pipe geometry have been studied. Complex mathematics in the form of a coordinate transformation is needed to perform the predictions for twin pipe geometry.

To model installed pipes, a stationary model for annularly insulated pipes in the ground has been developed, which also involves complicated mathematics. The temperature is represented by series expansions; in each region with differing thermal conductivity a separate expansion is used. The expansions are matched to each other at the region boundaries and chosen to fulfil the boundary conditions.

Finally, the measured cell gas status of aged pipes and the results obtained by modelling based on assumptions of their initial status and ageing conditions have been compared. It was found that the actual aged pipes contained less oxygen and more carbon dioxide than predicted. This is probably due to oxidation. It is interesting to note that not only the oxygen but also the carbon dioxide content is influenced by

oxidation. By consuming oxygen and producing carbon dioxide the oxidation will slow down the decrease of the insulation performance.

**Keywords:** polyurethane foam, insulation capacity, long-term performance, thermal conductivity, heat conduction, diffusion, cyclopentane, solubility coefficient

### *LIST OF PUBLICATIONS*

The thesis is based on the following papers/reports, referred to by Roman numerals I-VI in the text:

- I Environmental aspects on heat losses from district heating pipes – a comparison between single and twin pipes

Co-authors: Fröling M., Mangs S, Ramnäs O. and Jarfelt U.  
Proceedings of the 8<sup>th</sup> International Symposium on District Heating and Cooling, Trondheim, Norway, August 14-16, 2002

- II Multipole method to compute heat losses from district heating pipes

Co-author: Claesson J.  
Proceedings of the 7<sup>th</sup> Nordic Symposium on Building Physics, Reykjavik, Iceland, June 13-15, 2005

- III Prediction of the Long-Term Insulating Capacity of Cyclopentane-Blown Polyurethane Foam

Co-author: Claesson J  
Proceedings of the 8<sup>th</sup> Nordic Symposium on Building Physics, Copenhagen, Denmark, June 16-18, 2008

- IV Solubility of cyclopentane in PUR-foam and implications for district heating pipes

Co-authors: Jarfelt U. and Ramnäs O.  
Proceedings of the 11<sup>th</sup> International Symposium on District Heating and Cooling, Reykjavik, Iceland, August 31<sup>st</sup> - September 2<sup>nd</sup>, 2008.

- V Prediction of Heat Losses from District Heating Twin Pipes

Co-author: Claesson J.  
Proceedings of the 11<sup>th</sup> International Symposium on District Heating and Cooling, Reykjavik, Iceland, August 31<sup>st</sup> - September 2<sup>nd</sup>, 2008.

- VI Used district heating pipes – measured and modelled ageing compared  
Co-author: Olle Ramnäs  
Report 2014:12, Department of Civil and Environmental Engineering, Chalmers University of Technology

The details of the mathematics in papers II – V are described more thoroughly in the background reports:

- BII Claesson J. and Persson C. (2005) *Steady-State Thermal Problem of Insulated Pipes Solved with the Multipole Method*, Report 2005:3, Department of Civil and Environmental Engineering, Division of Building Technology/Building Physics, Chalmers University of Technology
- BIII-IV Persson C. and Claesson J. (2005) *Heat loss from a district heating pipe – coupled radial heat conduction and diffusion through the polyurethane foam insulation*, Report 2005:14, Division of Building Technology/Building Physics, Chalmers University of Technology
- BV Claesson J. and Persson C. (2008) *Numerical solution of diffusion problems using conformal coordinates. Application to district heating pipes*. Report 2013:2, Department of Civil and Environmental Engineering, Chalmers University of Technology

Other publications by the author (previously Holmgren):

Fröling M. and Holmgren C. (2002) Environmental impacts from production of district heating pipes – report written in Swedish: Miljöbelastning från produktion av fjärrvärmerör, Report FOU 2002:82, the Swedish District Heating Association.

Fröling M., Svanström M. and Holmgren C. (2002) Life Cycle Performance of District Heating Distribution Networks, Proceedings of the 8th International Symposium on District Heating and Cooling, Trondheim, Norway, August 14-16

Jarfelt U., Holmgren C., Nilsson S., Mangs S. and Ramnäs O. (2002) Comparison of Long-Term Thermal Performance of Polyurethane Foam Blown with HFC-365 mfc and Cyclopentane, Proceedings of Polyurethanes Conference 2002, Salt Lake City, Utah, USA, October 13-16

Fröling M., Holmgren C. and Svanström M. (2004) Life Cycle Assessment of the District Heat Distribution System. Part I: Pipe Production, International Journal of Life Cycle Assessment, vol. 9 no. 2, pp 130-136

Claesson C., Holmgren C., Jarfelt U. and Ramnäs O. (2004) A new method of laying district heating pipes, Proceedings of the 9th International Symposium on District Heating & Cooling, Helsingfors, Finland, August 30-31

Jarfelt U., Ramnäs O., Persson C. and Claesson C. (2004) Insulation properties of flexible district heating pipes – report written in Swedish: Flexibla fjärrvärmerörs isoleringsegenskaper, Report FOU 2004:117, the Swedish District Heating Association

Persson C., Reidhav C., Jarfelt U. and Ramnäs O. (2006) Insulating performance of flexible district heating pipes, Proceedings of the 10th International Symposium on District Heating and Cooling, Hanover, Germany, September 3-5

Fröling M., Persson C. and Svanström M. (2006) Life Cycle Assessment of the District Heat Distribution System, Part 3: Use phase and overall discussion, International Journal of Life Cycle Assessment 11 (6) pp. 437-446

Mangs S., Ramnäs O., Persson C., Jarfelt U. and Fröling M. (2006) PET and PUR Foam Insulated District Heating Pipes – Study: Environmental Comparison, EuroHeat&Power – English Edition 1 (3), pp. 26-31



## TABLE OF CONTENTS

---

1	INTRODUCTION .....	1
1.1	Aim .....	2
1.2	Content .....	3
1.3	Structure .....	3
1.4	Acknowledgements .....	3
2	POLYURETHANE FOAM .....	5
2.1	Manufacture .....	5
2.1.1	Foam .....	5
2.1.2	Pipes .....	6
2.2	Structure .....	7
2.2.1	Cell gas .....	7
2.2.2	Matrix .....	8
2.2.3	Density and cell size .....	8
2.3	Thermal conductivity .....	9
2.3.1	Value at 50°C .....	9
2.3.2	Modes of heat transfer .....	9
2.3.3	Conduction through the cell gas .....	10
2.3.4	Conduction through the matrix and radiation .....	15
2.3.5	Overall thermal conductivity of the foam .....	17
3	THERMAL MODELS OF THE PIPES .....	19
3.1	The heat conduction equation .....	19
3.2	Single pipes .....	20
3.2.1	Stationary temperature within an insulation of constant thermal conductivity .....	20
3.2.2	Stationary temperature with radially varying thermal conductivity of the insulation .....	22
3.2.3	Temperature profile with time variation .....	23
3.3	Twin pipes .....	24
3.3.1	Coordinate transformation .....	24
3.3.2	Stationary temperature profile .....	26
3.3.3	Temperature profile with time variation .....	26
3.4	Pipes in the ground .....	27
3.4.1	Steady state solution for annularly insulated pipes in the ground .....	27
3.4.2	Other steady state solutions .....	30
3.4.3	Coupling of ground and pipe models .....	30
3.5	Factors that influence the heat flows from the pipes .....	31
3.5.1	The pipe geometry .....	32
4	AGEING .....	34

4.1	The diffusion equation .....	35
4.2	Transport coefficients in polyurethane foam .....	37
4.2.1	Diffusion coefficient ( $D_{\text{eff},c}$ or $\delta_{\text{eff},c}$ ) .....	38
4.2.2	Permeability coefficient ( $\delta_{\text{eff},p} = P_{\text{foam}}$ ) .....	41
4.2.3	Solubility coefficient (S).....	42
4.3	Permeability coefficients for the polyethylene casing.....	44
4.4	Ageing of single pipes .....	44
4.4.1	Diffusion in radial coordinates.....	44
4.4.2	Complete radial model with coupled heat and mass transfer .....	47
4.4.3	Example of an ageing single pipe .....	48
4.5	Ageing of twin pipes.....	50
4.5.1	Model ascribing all transport resistance to the casing. ....	50
4.5.2	Model of ageing using conformal coordinates.....	51
4.6	Factors that influence the ageing of pipes.....	52
4.6.1	Transport resistance of the different materials.....	52
4.6.2	Cyclopentane content.....	53
4.7	Modelled cell gas content after ageing compared to measured content of used pipes .....	55
5	SUMMARY AND DISCUSSION.....	60
5.1	Improvements of the models.....	61
5.2	Discussion of other insulation options.....	61
	REFERENCES .....	63
	APPENDIX A Thermal conductivities and viscosities – an additional literature study.....	71

# 1 INTRODUCTION

---

Old district heating networks that have been renovated and expanded may contain several different distribution solutions originating from various time periods, e.g. concrete ducts, asbestos cement pipes and pipes with sliding insulation or an air gap to the insulation. This thesis focuses on predicting the insulation performance of the type of district heating pipe generally used in fairly new network installations, i.e. a steel fluid pipe insulated with polyurethane foam covered by a polyethylene casing (Figure 1) [EN253:2009]. The foam fills the volume between the fluid pipe and the casing, acting as a bond between them. This type of pipe has been used since the late 1960s - early 1970s [e.g. Sørensen 2001, Werner 1999]. So-called twin pipes comprising two fluid pipes within the same casing also exist. The single pipe geometry is generally used for large fluid pipe dimensions in order to make the pipes manageable, whereas the twin pipe geometry is employed for smaller fluid pipes.

The pipes are set in the ground with a cover depth of about 0.4-0.6 m depending on the surroundings (green area or street) [Laying instructions FVF D:211]. Shallower burial of pipes has been investigated to make installation cheaper and faster and has also been employed e.g. by Göteborg Energi [Nilsson et al. 2006].

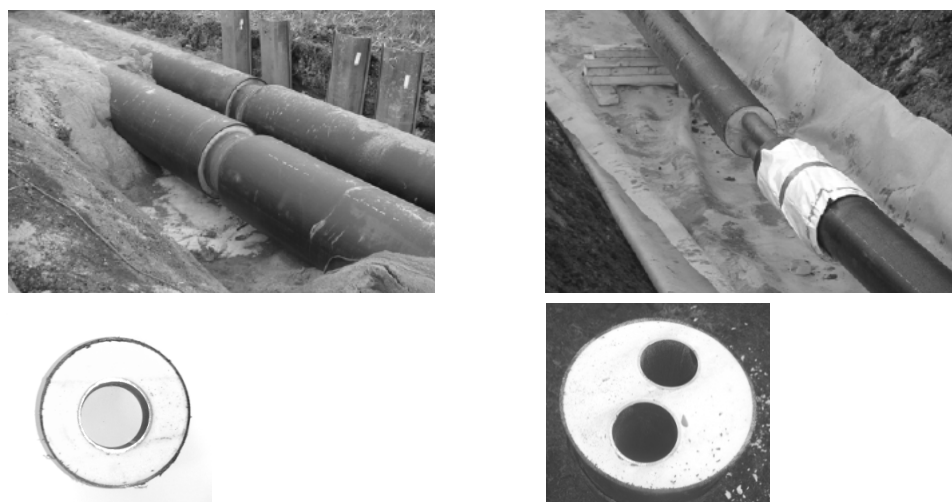


**Figure 1.** Single and twin district heating pipes.

The pipes are designed to withstand hot water transport at a maximum temperature of 120°C and a maximum pressure of 1.6 MPa (16 bar) for at least 30 years. The forward temperature in Swedish district heating networks is usually about 65-120°C and the

return temperature approximately 30-65°C. The temperatures vary depending on heat demand; for example, they differ between summer and winter.

In order to obtain a well-functioning district heating network that transports heat from the centralized heat generation to customers and fulfils their heat demand, it is important that distribution losses are not too high. The heat should be released where needed. The relative heat loss from plant to customer, i.e. heat lost/(heat lost+heat for use), in district heating networks is about 10% [Frederiksen and Werner 1993]. The heat loss from transport through large transit pipes is only a few percent, while it is about 20% in areas with detached houses and up to 40% when the energy demand in such areas is low.

Both the cost and the environmental performance of the distribution are closely linked to the heat loss. Depending on how new and well insulated the network is, the heat loss cost has been estimated at about 20-40% of the total distribution cost, which also includes the investment in the construction of the network, as well as pumping and maintenance costs [Frederiksen and Werner 1993]. The environmental impact related to the lost, unused heat depends on the type of heat production. For average district heat production, the network's heat loss has been found to account for a considerable proportion of the network's life cycle environmental impact; over 50% of most of the studied environmental impacts [Fröling et al. 2006, Nielsen 2001].

Well-insulated buildings have a low heat load. Improvements in insulation standards [EPBD2: Directive 2010/31/EU, ER 2010:39 Mission 13: National strategy for low-energy buildings] have a negative impact on district heating distribution conditions. At the beginning of the 21<sup>st</sup> century, the connection of small buildings such as semi-detached or detached houses to district heating was the subject of much debate in Sweden and a research programme Sparse district heating (in Swedish: Värmegles fjärrvärme) financed by the Swedish District Heating Association and the Swedish Energy Agency was introduced between 2002-2006. Increased demand for low-energy buildings has made the discussion less relevant. A low heat load results in a low linear heat density, i.e. little heat sold/trench metre, which leads to a high relative heat loss. The cost and environmental impact per distributed useful sold heat thus increases in line with the heat load decrease. District heating works best in areas with a high heat load.

Much work has been carried out in order to make the heat transport as efficient as possible. Better district heat distribution solutions than those employed at present are constantly being sought. Calculations can be used to make predictions of how changes in pipe design, installation and temperature levels influence heat loss from the network.

### **1.1 Aim**

The aim of this thesis was to develop simple but accurate calculation models to predict heat flow over time from different district heating networks in order to evaluate various distribution solutions. It was necessary to determine the heat flow and how the pipes aged. Single and twin pipes were considered.

One task was to illustrate how the cell gas content varies over the cross section of the foam and how it changes with time. Special attention has also been paid to

investigating the influence of the amount and distribution of the insulating gas in gas, liquid and dissolved states respectively.

## **1.2 Content**

Based on the initial cell gas content and boundary temperatures, the single and twin pipe models determine the heat flow and temperature profile over the pipe's cross section. They also predict the cell gas composition profiles over time and how these influence the heat flow. For the single pipe the calculations were made in the radial cylindrical coordinate, while for the twin pipe a coordinate transformation was used to obtain a simpler geometry. The development over time was in both cases calculated using explicit finite differences.

A model that determines the steady state temperature around annularly insulated pipes in the ground and the heat flows from the pipes is also presented. This model has been coupled to the single pipe model to determine the temperatures of the casings of the pipes set in the ground.

## **1.3 Structure**

The thesis begins by describing the insulation within the pipe before it gradually expands to include whole pipes and pipes laid in the ground. Chapter two focuses on the polyurethane foam insulation, i.e. what properties make it a good insulation material and how the thermal conductivity of the foam can be modelled.

The third chapter deals with heat conduction. First heat conduction within the pipes is treated. It is explained how to determine temperature profiles over the pipes' cross-sections and heat flows from the pipes, both for the single and twin pipe geometry. This is followed by a description of how the temperature around pipes installed in the ground can be modelled and the corresponding heat flows from the installed pipes determined. Special emphasis is put on a model derived for annularly insulated pipes. Finally, the chapter concludes with a discussion of what influences the heat loss from the pipes, e.g. the extent to which the different materials contribute to the insulation and the influence of the laying.

The fourth chapter covers the ageing of the pipes. It includes a description of how ageing can be modelled and the material parameters involved. Examples of influencing factors are also presented; a discussion about the share of the transport resistance of the different materials, the influence of the cyclopentane content of the foam and the quality of the casing material. Results from modelled ageing and measurements on actual aged pipes are then compared before the thesis concludes with a short summary and discussion. Suggestions for future work to improve modelled ageing predictions are presented and other potential insulation materials are briefly discussed.

## **1.4 Acknowledgements**

I would like to take this opportunity to acknowledge those who helped and guided me, had patience with me, encouraged and had trust in me during my years as a PhD student.

- My supervisors all through the work: Ulf Jarfelt and Olle Ramnäs
- The mathematical expert Johan Claesson

- The district heat distribution research group at Chalmers of which I was a member:  
Ulf Jarfelt, Olle Ramnäs, Morgan Fröling, Magdalena Svanström, Sara Mangs, Charlotte Reidhav and Stefan Forsaeus Nilsson
- The reference group made up of dedicated people from the industry. Special thanks to Göran Johansson at Powerpipe System AB for collaboration in connection with two of my papers [IV, Fröling et al. 2004]
- The staff at the Division of Building Technology

This work was financially supported by the Swedish District Heating Association and the Swedish Energy Agency.

## 2 POLYURETHANE FOAM

---

For many years straight district heating pipes have been almost exclusively insulated with polyurethane foam, a material developed to conduct as little heat as possible, i.e. with as low a thermal conductivity as possible. The foam functions both as “a glue” that mechanically bonds the casing and service pipe together and as insulation in the pipe construction. This chapter describes the material and its insulation performance; how the thermal conductivity of the material can be modelled and what influences its conductivity.

### 2.1 Manufacture

#### 2.1.1 Foam

The foam is made by mixing polyol, blowing agent, surfactant and catalyst with diisocyanate [Oertel and Abele 1994]. The polyol and diisocyanate react exothermically to form the polyurethane. The released heat vaporizes the physical blowing agent, a low boiling liquid with low thermal conductivity, today usually cyclopentane. The gas creates small bubbles in which it becomes trapped when the polyurethane stiffens. These gas filled cells are of vital importance for the insulating power of the foam. Thus, the blowing agents are treated in some detail in this thesis. In addition to the physical blowing agent, small amounts of water added to the mix and water from air humidity also contribute to foaming as a chemical blowing agent. Water reacts with the isocyanate to form a urea link in the polyurethane and carbon dioxide. The stabiliser and the catalyst are added in order to achieve the desired foam structure with small, closed and uniform cells.

##### 2.1.1.1 Blowing agent alternatives

Cyclopentane blown polyurethane foam insulation is now state of the art in Europe. Until the negative effect of chlorofluorocarbons (CFCs) on the stratospheric ozone layer was discovered, fluorotrichloromethane (CFC-11) was used as a blowing agent [Svanström 1997]. It was attractive due to the low thermal conductivity ( $\lambda_{25} = 8.4 \text{ mW}\cdot\text{m}^{-1}\cdot\text{K}^{-1}$  [McMenamin et al. 2009]), low permeation rate through the foam, relatively high saturation vapour pressure, suitable boiling point (23.8°C), low-order toxicity and non-flammability. CFC-11 has been classified as the first generation blowing agent with a low thermal conductivity, high ozone depletion potential (ODP) and high global warming potential (GWP) [NIST Chemistry webbook]. After recognition of the high ODP of CFCs, dual blown (CFC-11/increased amount of water) polyurethane foam was initially utilised to reduce ozone depletion. Fully water blown foam was also used for district heating pipes. Although this is a good alternative from many perspectives, the thermal conductivity of carbon dioxide ( $\lambda_{25} =$

16.6 mW·m<sup>-1</sup>·K<sup>-1</sup> [McMenamin et al. 2009]) is higher than that of most other blowing agents.

In order to increase the degradability in the atmosphere, one or several of the halogen atoms of the CFC molecule can be replaced by hydrogen atoms. The new molecules, hydrochlorofluorocarbons (HCFCs), thus have lower ODP and GWP than the CFCs. HCFCs belong to the second generation of blowing agents with low thermal conductivity, low ODP and moderate GWP. Fluorodichloroethane (HCFC141b,  $\lambda_{25} = 9.9 \text{ mW}\cdot\text{m}^{-1}\cdot\text{K}^{-1}$  [McMenamin et al. 2009]) can be mentioned as a frequently used blowing agent. In some non-European countries, HCFC141b is still employed as a blowing agent.

The hydrocarbon cyclopentane is classified among the third generation of blowing agents. It is by far the most common blowing agent for foams in district heating pipes today. The thermal conductivity of cyclopentane will be discussed in detail later. Some pipe producers were reluctant to use cyclopentane as a blowing agent. One reason was that pipe manufacturers need to change to an explosion proof installation in order to handle cyclopentane, as it is highly flammable. Hydrofluorocarbons (HFCs) have been marketed as alternatives [Mangs 2005]. Together with cyclopentane they belong to the third generation of blowing agents with moderate thermal conductivity, zero ODP and moderate GWP. Some HFCs used as blowing agents are pentafluorobutane (HFC365mfc), heptafluoropropane (HFC227fa), pentafluoropropane (HFC245fa), tetrafluoroethane (HFC134a) and difluoroethane (HFC152a). They all have  $\lambda_{25}$ -values around 12–14 mW·m<sup>-1</sup>·K<sup>-1</sup> [McMenamin et al. 2009]. On the positive side they do not contribute to ozone depletion and have high saturation vapour pressures, enabling them to be present in the cell gas in large numbers. However, a disadvantage is that all HFCs are moderate greenhouse gases and their phasing out is under discussion.

A fourth generation of blowing agents with low thermal conductivity, zero ODP and moderate to low GWP has been developed. Except for methylformate (Foam Supplies Inc, Ecomate,  $\lambda_{25} = 10.7 \text{ mW}\cdot\text{m}^{-1}\cdot\text{K}^{-1}$  [Murphy et al. 2005]) all members of this generation are hydrofluoroolefins (HFOs) or hydrochlorofluoroolefins. As olefin molecules are unsaturated they are more reactive and easily broken down in the atmosphere, thus having moderate to low GWP. A few years ago chlorotrifluoropropene was introduced by Honeywell (Solstice LBA,  $\lambda_{20} = 10.2 \text{ mW}\cdot\text{m}^{-1}\cdot\text{K}^{-1}$  [Honeywell 2013]) and also by Arkema (Forane 1233zd, in its development phase known as AFA L1,  $\lambda_{25} = 10 \text{ mW}\cdot\text{m}^{-1}\cdot\text{K}^{-1}$  [Arkema 2013, Lynch 2014]). Hexafluorobutene has been introduced by DuPont (Formacell 1100,  $\lambda_{25} = 10,7 \text{ mW}\cdot\text{m}^{-1}\cdot\text{K}^{-1}$  [Loh et al. 2012, Quintero 2012]).

It should be borne in mind that apart from low thermal conductivity, zero ODP and low GWP, other factors must also be considered in the search for the best blowing agent: e.g. flammability, vapour pressure (boiling point), solubility, cost efficiency, toxicity (working environment) etc.

### 2.1.2 Pipes

Pipes are produced in different dimensions. The dimension of a pipe is given by the nominal diameter (DN) of the steel fluid pipe and the outer diameter of the casing. The degree of insulation of a pipe is normally indicated by an insulation series

ranging from 1 to 4, where a high series indicates thick insulation. The insulation thickness varies between about 30 mm and almost 200 mm.

Pipes can be produced one by one in the traditional way or continuously. When each pipe is insulated separately, the fluid pipe is centred in the casing pipe and the ends are sealed before the foam is injected into the cavity between the pipes. When the pipes are continuously produced, the foam can either be sprayed onto the pipe or into a movable mould before the casing is extruded onto the foam. The two different production methods lead to variations in the cell structure of the foam within the pipe.

There is batch and spatial variability of the insulation in the pipes. One reason for the spatial variability is that when the foam is blown between expansion boundaries, it becomes compressed close to them. The density is lower within the core than on the surface layers, where the cells become compressed in one direction and a thin film of solid polymer, i.e. “a skin”, can form close to the boundary. The increased amount of solid material at the interfaces raises their thermal conductivity but helps to prevent diffusion.

Storage of pipes before use may lead to spatial variability due to ageing, e.g. caused by gas diffusion and transport in channels where adherence between materials is lacking, increasing the thermal conductivity near the pipe ends [Persson et al. 2006].

## **2.2 Structure**

### *2.2.1 Cell gas*

The cell gas of cyclopentane-blown foam contains cyclopentane, carbon dioxide and air in different proportions. Initially the cell gas contains a high level of insulating gases, but if the foam is not diffusion-tight encapsulated, the diffusion strives to level out the concentration differences between the foam and the surrounding air. The proportions of carbon dioxide and cyclopentane will decrease over time until after many years the cells are completely air-filled. It will take more than 100 years for the polyurethane foam of a district heating pipe without a diffusion barrier to become air-filled.

Instead of being solely cyclopentane-blown, some foams are blown with cyclopentane mixtures, i.e. co-blown with isopentane or n-pentane [Jarfelt and Ramnäs 2006, Dohrn et al. 2007]. Small amounts of carbon monoxide are present in the cell gas of some types of foam. Occasionally more than 10 vol% of carbon monoxide is present in the cell gas [Olle Ramnäs, personal communication].

The total cell gas pressure of the cyclopentane-blown foam of new district heating pipes is normally between 100-130 kPa at room temperature. In exceptional cases very high pressures up to 200 kPa, or low pressures of around 70 kPa, have been measured. The cell gas contains a few vol% of air, about 30-40 vol% of cyclopentane (including small amounts of other hydrocarbons, probably impurities from the cyclopentane), about 50-70 vol% of carbon dioxide and 0.5-1 vol% of water vapour. It is interesting to note that the oxygen/nitrogen-ratio of the cell gas in most new foams is higher than that of air.

Isocyanate reactions are not complete in all types of foam directly after manufacture. A continued reaction gives rise to a gradually increasing amount of carbon dioxide

and consequently a rise in total cell gas pressure during the first weeks or months after production.

The partial pressure of cyclopentane in the cells is normally very close or equal to its saturation pressure at room temperature. The partial pressure of cyclopentane cannot be higher than its saturation pressure, e.g. about 34 kPa at 20°C or about 42 kPa at 25°C [Smith and Srivastava 1986]. In some foams up to 40% of the total amount of cyclopentane in the cell is present as a condensed liquid at room temperature. However, about half of the total amount of cyclopentane added to foam is dissolved in the polymer matrix [IV].

### 2.2.2 Matrix

The polyurethane matrix is the solid material in the foam that encloses the gas filled cells. The matrix is made up of cell windows separating two cells and struts where three cells meet. The cell windows are thin (<1 µm), while the struts are relatively thick (about 30 µm) [Hilyard and Cunningham 1994]. In the simplest foam models, the matrix consists of parallel planes or rectangles. However, more complicated geometrical objects have also been used. Despite the fact that it does not fill space the pentagonal dodecahedron structure (Figure 2) has been employed to describe the cell structure, e.g. to determine the cell size and strut fraction of foams or to model radiation. Other cell structures occasionally used are the rhombic dodecahedron and the truncated dodecahedron (or tetrakaidecahedron).

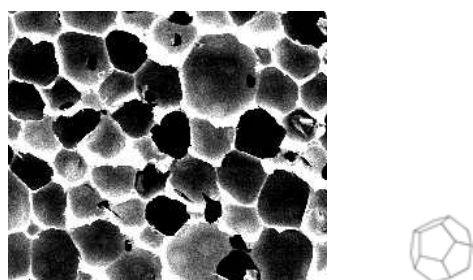


**Figure 2.** The cellular structure of the polyurethane foam; SEM photo and pentagonal dodecahedron cell model. The diameter of the cells in the photo is about 140 µm.

### 2.2.3 Density and cell size

The old district heating pipe standard stated that the density of the polyurethane foam should be greater than 60 kg·m<sup>-3</sup> [EN253:2003]. The cell size should be less than 0.5 mm in the radial direction and the percentage of closed cells at least 88%. In the new standard these requirements have been replaced by functional demands.

A German study found that most district heating pipes had foams with densities of around 80 kg·m<sup>-3</sup> (6 pipes), while only 3 pipes had lower densities. The cell sizes were between 0.25-0.30 mm [Besier et al. 2008]. In another study of foams for district heating pipes, the foam densities were found to be around 55-75 kg·m<sup>-3</sup>, where the cell sizes of the rigid foams were 0.26-0.31 mm, while the micro-cellular/semi-flexible foams had cell sizes of 0.10-0.25 mm [Jarfelt and Ramnäs 2006].

Recent foam development has led to lower density foams with smaller cells. A low foam density decreases heat conduction through the matrix, but usually increases the heat transfer by radiation. The latter transfer is reduced by a small cell size.

When the cell size decreases, a larger share of the solid material becomes situated in the cell windows. The cell windows either remain about as thick as before or break, resulting in open-cell foams. This redistribution of the solid material at cell size decrease leads to higher solid conduction that to some extent counteracts the decreased radiation [Smits 1994, Glicksman and Stewart 1997].

### 2.3 Thermal conductivity

The thermal conductivity of a material  $\lambda$  [ $\text{W}\cdot\text{m}^{-1}\cdot\text{K}^{-1}$ ] describes the magnitude of the heat flow  $q$  [ $\text{W}\cdot\text{m}^{-2}$ ] through the material for a certain temperature difference  $T$  [K] across the material; Fourier's law for homogeneous and isotropic materials, eq. 1.

$$q = -\lambda \cdot \nabla T = -\left( \lambda \cdot \frac{\partial T}{\partial x}, \lambda \cdot \frac{\partial T}{\partial y}, \lambda \cdot \frac{\partial T}{\partial z} \right) \quad [\text{W}\cdot\text{m}^{-2}] \quad (1)$$

Thus, an insulation material should have as low a thermal conductivity as possible.

#### 2.3.1 Value at 50°C

The 2003 version of the standard for rigid district heating pipes stated that the thermal conductivity of the polyurethane foam at 50°C should be less than or equal to 33  $\text{mW}\cdot\text{m}^{-1}\cdot\text{K}^{-1}$  [EN253:2003]. Since the development of foams with a better insulation performance, the  $\lambda_{50}$ -value has been lowered to 29  $\text{mW}\cdot\text{m}^{-1}\cdot\text{K}^{-1}$  in the 2009 standard version [EN253:2009].

In 2006 three raw material producers were asked to supply a board of their best insulating foam [Jarfelt and Ramnäs 2006]. The best foam had a thermal conductivity of 24  $\text{mW}\cdot\text{m}^{-1}\cdot\text{K}^{-1}$  at 50°C. By decreasing the foam density and cell size it was estimated that it would be possible to achieve a value of 22  $\text{mW}\cdot\text{m}^{-1}\cdot\text{K}^{-1}$ . In a study of district heating pipe foams on the German market in 2006,  $\lambda_{50}$ -values of between 25 to 29  $\text{mW}\cdot\text{m}^{-1}\cdot\text{K}^{-1}$  were measured [Besier et al. 2008]. The  $\lambda_{50}$ -value varied with the density according to the equation:  $\lambda_{50} [\text{mW}\cdot\text{m}^{-1}\cdot\text{K}^{-1}] = 16.4 + 0.148 \cdot \text{density} [\text{kg}\cdot\text{m}^{-3}]$ . In the 2013 pipe producer catalogues, certified  $\lambda_{50}$ -values of 22  $\text{mW}\cdot\text{m}^{-1}\cdot\text{K}^{-1}$  were stated for flexible pipes (Logstor) and 26  $\text{mW}\cdot\text{m}^{-1}\cdot\text{K}^{-1}$  for traditionally produced pipes (Powerpipe).

#### 2.3.2 Modes of heat transfer

Generally, there are three modes of heat transfer: conduction, radiation and convection. As the foam cells are so small, less than 0.5 mm in diameter, the heat transfer by natural convection within the foam can be neglected. The overall thermal conductivity of polyurethane foam of thicknesses used for district heating pipe insulation is modelled as the sum of the individual contributions of conduction and radiation (eq. 2) [Hilyard and Cunningham 1994]<sup>1</sup>. Conduction takes place both through the matrix and during the gas phase. All heat transfer modes are temperature dependent.

<sup>1</sup> Radiation should not be treated separately for thin foam samples (< about 1 cm), as e.g. low emissivity boundary layers may have a large impact on the heat conduction then. The impact of such layers is small in foam of the thicknesses used for district heating pipes [Hilyard and Cunningham 1994]. The two conduction terms are often treated separately.

$$\lambda_{foam} = \lambda_{conduction}^{gas} + \lambda_{conduction}^{matrix} + \lambda_{radiation} \quad [W \cdot m^{-1} \cdot K^{-1}] \quad (2)$$

### 2.3.3 Conduction through the cell gas

High void volume fraction, also known as porosity, is a characteristic of good insulation materials. As solid materials are much better conductors than gases, a little solid material in the insulation is favourable. The thermal conductivity of solid polyurethane is about one order of magnitude larger ( $210 \text{ mW} \cdot \text{m}^{-1} \cdot \text{K}^{-1}$  [Nielsen et al. 2000]) than that of most gases ( $10\text{-}30 \text{ mW} \cdot \text{m}^{-1} \cdot \text{K}^{-1}$ , at room temperature). To further reduce the thermal conductivity, the foam has closed cells that encapsulate insulating gases with lower thermal conductivity than air. The percentage of closed cells in the foam is usually about 90-95%.

The thermal conductivity due to conduction in the gas phase of the foam is given by the product of the void volume fraction  $f_g$  [-] and the thermal conductivity of the gas mixture in the cells  $\lambda_g$  [ $W \cdot m^{-1} \cdot K^{-1}$ ] (eq. 3).

$$\lambda_{conduction}^{gas} = f_g \cdot \lambda_g \quad [W \cdot m^{-1} \cdot K^{-1}] \quad (3)$$

The porosity is about 94-95% and can be calculated from the density of the solid polyurethane matrix  $\rho_{PUR}$  [ $kg \cdot m^{-3}$ ] and the foam density  $\rho_f$  [ $kg \cdot m^{-3}$ ] according to eq. 4. The density of solid polyurethane is about  $1200\text{-}1250 \text{ kg} \cdot \text{m}^{-3}$  [Nielsen 1998, Ahern et al. 2005].

$$f_g = \frac{\rho_{PUR} - \rho_f}{\rho_{PUR} - \rho_{cell\ gas}} \approx 1 - \frac{\rho_f}{\rho_{PUR}} \quad [-] \quad (4)$$

As the void volume fraction of the foam is so high, conduction in the gas phase represents about 60-80% of the total thermal conductivity, despite the low conductivity of the cell gas.

Decreasing the cell size to around  $1 \mu\text{m}$  or less should make it possible to reduce conduction in the gas phase. This cell size may be achieved by using carbon dioxide as a blowing agent under supercritical conditions. According to Bayer Material Science (2011), the current state of development is  $3\text{-}4 \mu\text{m}$  and the aim is to produce a “nanof foam” with a cell size of  $0.5 \mu\text{m}$ . In such foam with a cell size less than the mean free path of a gas molecule, the heat conduction would in principle only take place in the solid polymer and by radiation.

#### 2.3.3.1 Thermal conductivity of the individual gases

The thermal conductivity of the insulating gases is about  $10 \text{ mW} \cdot \text{m}^{-1} \cdot \text{K}^{-1}$  lower than that of air and increases in line with temperature (Figure 3). A linear approximation of the temperature dependence can be used for small temperature intervals [Reid et al. 1987]. For the  $275\text{-}400\text{K}$  interval, higher order polynomials only yield a slightly better correspondence to measurement data. A survey of the thermal conductivity of nitrogen, oxygen and carbon dioxide is presented in Appendix A.

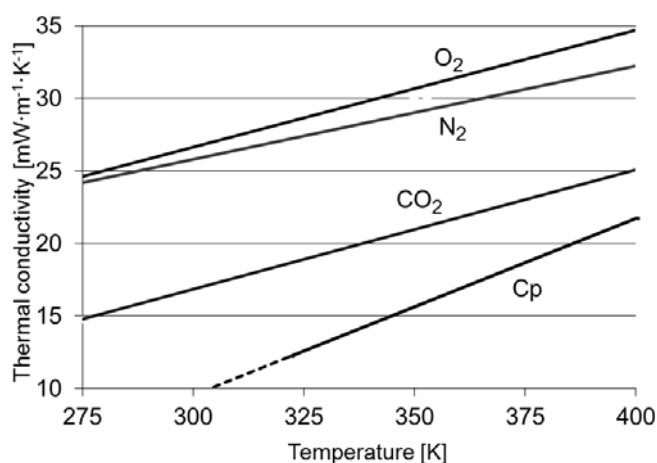


**Figure 3.** Thermal conductivity of oxygen, nitrogen, carbon dioxide and cyclopentane at 100 kPa. All data for the inorganic gases are from NIST [NIST Chemistry webbook]. The data for cyclopentane is from Contreiras Louro (2007).

There is a large variation in the cyclopentane values listed by different sources. Data on cyclopentane can be found in Volkert (1995), Fleurent and Thijs (1995), Brodt (1995), Takada et al. (1998), Heinemann et al. (2000) and Contreiras Louro (2007). A reported span for the thermal conductivity of cyclopentane at 25°C is 8.9-13.8 mW·m<sup>-1</sup>·K<sup>-1</sup> [Merten and Rotermund 1997, Brodt 1995]. Values from Reid et al. (1987) and Nielsen (1998) have been used in the calculations for this thesis [III-V], which may somewhat overestimate the thermal conductivity of cyclopentane (Figure 4).

In Contreiras Louro (2007), a linear equation for the thermal conductivity of cyclopentane at 100kPa is used,  $\lambda = A + B \cdot T$ . In Table 1 the constants A and B are stated for different measurement sets. The corresponding straight lines are shown in Figure 4. However, all these studies were performed at temperatures higher than 338K and a linear approximation of the temperature dependence will probably deviate a few percent at temperatures around 300K. Linear approximations for two other hydrocarbons, butane and 2-methylbutane, deviate a few percent at the two ends of a temperature range of 300 - 420K [NIST Chemistry webbook].

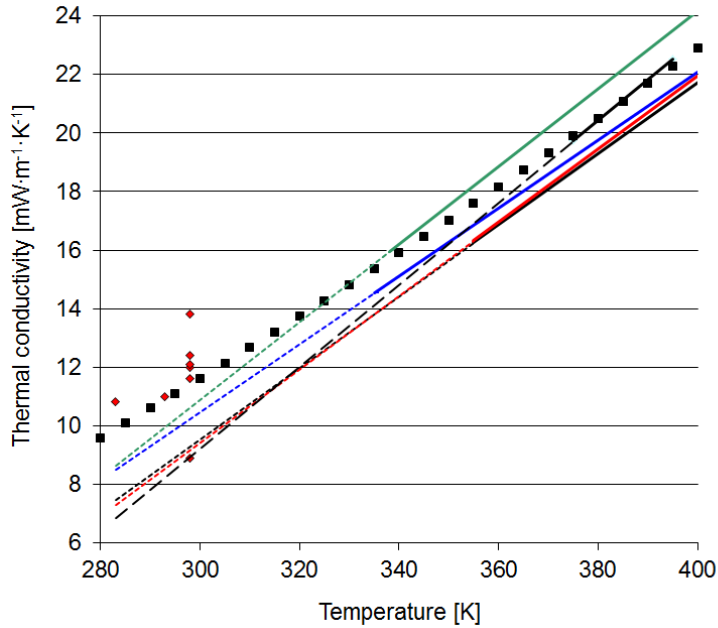


**Figure 4.** The thermal conductivity of cyclopentane at different temperatures and at 100kPa (for temperatures above the boiling point, 322K) or at saturation pressure (for temperatures below 322K). All full and broken lines are based on data from Contreiras Louro (2007). The red line represents her own work and the other lines refer to data from Bayer Technology Services (1995 and 1998). The broken lines are values extrapolated to temperatures below the temperature ranges covered in the studies. The red diamonds represent data from various studies mentioned by Merten and Rotermund (1997). The black squares indicate the values used by Nielsen (1998) and are calculated from an equation and constants presented by Reid et al. (1987).

**Table 1.** Constants of the equation  $\lambda = A + B \cdot T$  [ $\text{mW} \cdot \text{m}^{-1} \cdot \text{K}^{-1}$ ] used for calculation of the thermal conductivity of cyclopentane at 100kPa within the studied temperature range.

A	B	temperature range (K)	Reference
-26.992	0.1218	353 – 394	Contreiras Louro 2007
-28.200	0.1254	353 – 415	Oliveira 2001
-28.986	0.1329	338 – 415	Treckmann and Braden 1995a
-24.392	0.1169	335 – 417	Treckmann and Braden 1995b
-32.701	0.1398	375 – 395	Dohrn 1998

The fact that cyclopentane is liquid at room temperature contributes to difficulties in determining the gas phase thermal conductivity at temperatures below the boiling point. The conductivity of cyclopentane given for 100 kPa and temperatures < 49°C is a theoretical value that can be used for calculations of the conductivity of mixtures with other gases. This value can either be extrapolated from measurements at higher temperatures or from pressures below the saturation pressure or calculated from mixtures with other gases. The pressure does not have a great influence on the thermal

conductivity, e.g. if the pressure is lowered (increased) by around 50% the conductivity only decreases (increases) by 1.5% at a temperature around 350K [Contreiras Louro 2007]. The change is smaller at higher temperatures (1.2% at around 390K). As cyclopentane has a lower thermal conductivity than common hydrocarbon impurities (e.g. pentane and isopentane) sometimes present in a liquid sample, these impurities will cause too high values for not quite pure gas.

### 2.3.3.2 Thermal conductivity of the cell gas

Determination of the conductivity of the cell gas is complicated because different components in a gas mixture affect each other; therefore the total thermal conductivity of the gas mixture differs from the sum of the thermal conductivities of each gas weighed with its mole fraction [Hilyard and Cunningham 1994]. The mutual interactions depend on, e.g. the different molar masses, sizes and polarities of the gases.

Empirical and corresponding state methods are used to determine the thermal conductivity of gas mixtures [Poling et al. 2001, Reid et al. 1987]. Perhaps one of the most popular methods for cell gas is Wassiljewa's equation (eq. 5), which has been used in III-V. In this equation the molar fractions  $y_i$  [-], the thermal conductivities  $\lambda_i$  [ $\text{W}\cdot\text{m}^{-1}\cdot\text{K}^{-1}$ ] of the individual gases  $i$  ( $i=1,2,\dots$ ) and a function of interaction  $A_{ij}$  ( $i=1,2,\dots, j=1,2,\dots$ ) [-] are included. The function of interaction  $A_{ij}$  can be calculated according to the Mason Saxena modification using gas viscosities  $\eta_i$  [ $\text{N}\cdot\text{s}\cdot\text{m}^{-2}$ ] (which are temperature dependent, see Appendix A) (eqs. 6 and 7) or critical temperatures  $T_{crit,i}$  [K] and pressures  $P_{crit,i}$  [Pa] (eqs. 6 and 8).

$$\lambda_g = \sum_{i=1}^n \frac{y_i \cdot \lambda_i}{\sum_{j=1}^n y_j \cdot A_{ij}} \quad [\text{W}\cdot\text{m}^{-1}\cdot\text{K}^{-1}] \quad (5)$$

$$A_{ij} = \varepsilon \cdot \frac{\left[ 1 + \sqrt{\frac{\lambda_{tr,i}}{\lambda_{tr,j}}} \cdot \left( \frac{M_i}{M_j} \right)^{0.25} \right]^2}{\sqrt{8 \cdot \left( 1 + \frac{M_i}{M_j} \right)}} \quad [-] \quad (6)$$

$M_i$  denotes the molar mass [ $\text{g}\cdot\text{mol}^{-1}$ ] of compound  $i$ . The term  $\lambda_{tr,i} / \lambda_{tr,j}$  can be calculated in two ways (eqs. 7-8).

$$\frac{\lambda_{tr,i}}{\lambda_{tr,j}} = \frac{\eta_i}{\eta_j} \cdot \frac{M_j}{M_i} \quad [-] \quad \text{from viscosities} \quad (7)$$

$$\frac{\lambda_{\text{tr}_i}}{\lambda_{\text{tr}_j}} = \frac{\Gamma_j \cdot \left[ e^{0.0464 \cdot \text{Tr}_i} - e^{-0.2412 \cdot \text{Tr}_i} \right]}{\Gamma_i \cdot \left[ e^{0.0464 \cdot \text{Tr}_j} - e^{-0.2412 \cdot \text{Tr}_j} \right]} \quad [-] \quad \text{with critical temperatures and pressures} \quad (8)$$

$$\Gamma_i = 210 \cdot \left( \frac{\text{T}_{\text{crit}_i} \cdot \text{M}_i^3}{\text{P}_{\text{crit}_i}^4} \right)^{\frac{1}{6}} \quad \text{Tr}_i = \frac{\text{T}}{\text{T}_{\text{crit}_i}}$$

The empirical parameter  $\varepsilon$  in equation 6 is usually put to unity when modelling the ageing of foams, which has also been the case in the present work. It corresponds to  $A_{if}=1$ . Calculations with a lower  $\varepsilon$  would have yielded a higher thermal conductivity.

In some studies  $\varepsilon$  has been adjusted to obtain agreement between measured and calculated thermal conductivities of gas mixtures. For a cyclopentane/nitrogen mixture the best correspondence between measured and calculated thermal conductivities at 100kPa was obtained for  $\varepsilon = 0.85\text{--}0.96$  within the 333-413K temperature range. For a *n*-pentane/isopentane mixture the corresponding value was  $\varepsilon = 1.01$  within the whole of this temperature range [Dohrn et al. 2007]. For isobutane/carbon dioxide  $\varepsilon = 0.91\text{--}0.93$  (343-373K) and for *n*-pentane/carbon dioxide  $\varepsilon = 0.903\text{--}0.904$  (343-373K) were obtained after adjustment [Pinto Varanda 2009]. A four parameter ( $A_1, A_2, \dots, A_4$ ) equation has been suggested for  $\varepsilon$  that considers its temperature T [K] and pressure p [Pa] dependence (eq. 9) [Dohrn et al. 2007].

$$\varepsilon = A_1 \cdot e^{A_2 \cdot p} \cdot T^{A_3 \cdot p + A_4} \quad [-] \quad (9)$$

Various parameter values have been obtained for different gas mixtures when the formula is adjusted to fit measurement data.

In addition to Wassiljewa's equation, another empirical relationship used to determine the thermal conductivity of cell gas mixtures is Brokaw's equation [Reid et al. 1987]. It has been used with good correspondence between calculations and measurements for air/CFC-11 mixtures with the Brokaw coefficient set to 0.5 (eq. 10) [Isberg 1988]. This form of Brokaw's method was employed in paper I.

$$\lambda_g = 0.5 \cdot \left( \sum_{i=1}^n y_i \cdot \lambda_i + \frac{1}{\sum_{i=1}^n y_i / \lambda_i} \right) \quad [\text{W} \cdot \text{m}^{-1} \cdot \text{K}^{-1}] \quad (10)$$

Figure 5 depicts the thermal conductivity at 25°C predicted for different air-cyclopentane and air-carbon dioxide gas mixtures by means of Wassiljewa's equation with the Mason and Saxena modification and Brokaw's equations (eqs. 5-8). It is notable that the predicted conductivities are lower than the corresponding values given by a straight line connecting the conductivities of the pure gases. The largest difference in the results of the different methods for the air – cyclopentane mixture is about  $3 \text{ mW} \cdot \text{m}^{-1} \cdot \text{K}^{-1}$ , while it is about  $0.3 \text{ mW} \cdot \text{m}^{-1} \cdot \text{K}^{-1}$  for the air – carbon dioxide mixture.

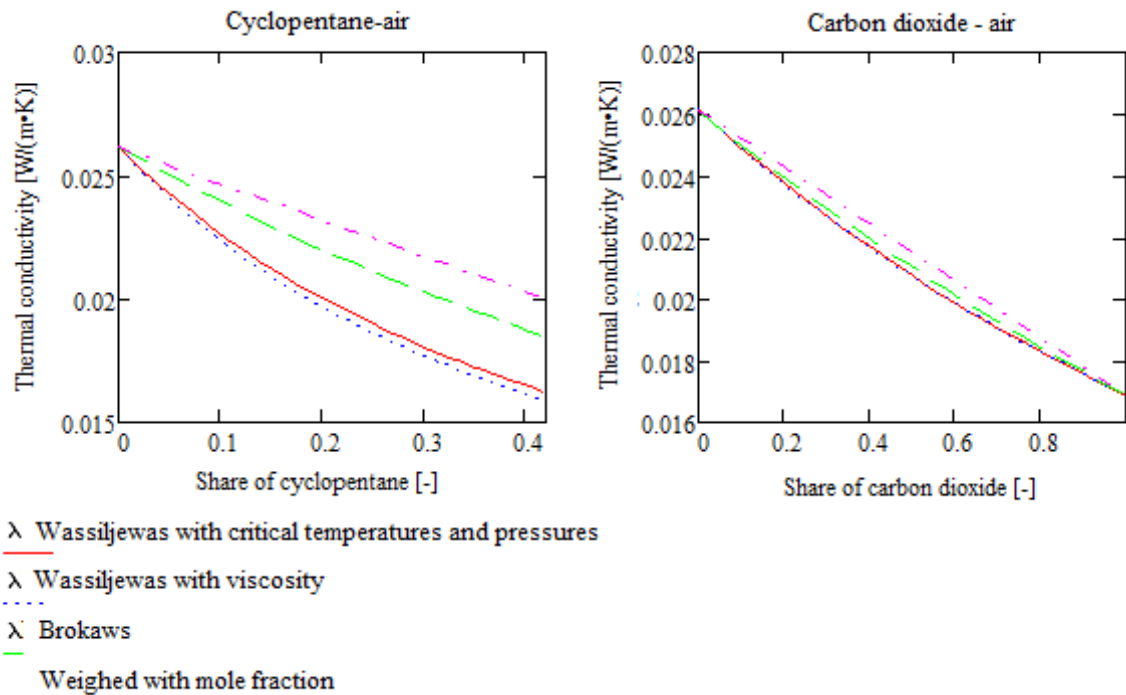


**Figure 5.** Thermal conductivity of air-cyclopentane and air-carbon dioxide mixtures at 25°C predicted by different models ( $\lambda_{25}=11 \text{ mW}\cdot\text{m}^{-1}\cdot\text{K}^{-1}$  for cyclopentane,  $17 \text{ mW}\cdot\text{m}^{-1}\cdot\text{K}^{-1}$  for carbon dioxide and  $26 \text{ mW}\cdot\text{m}^{-1}\cdot\text{K}^{-1}$  for air).

Predictions by means of models have been compared with measurement results of binary mixtures. There is typically at least a few tenths of  $\text{mW}\cdot\text{m}^{-1}\cdot\text{K}^{-1}$  difference between the measurements and the predictions. As mentioned earlier, results obtained by means of Wassiljewa's model have been adjusted to fit the measurements by adjusting the parameter  $\varepsilon$ . Marrucho et al. (2005) studied cyclopentane/nitrogen mixtures. Adjusting by means of  $\varepsilon$  ( $\varepsilon=0.8923$ ) they obtained an overall absolute average deviation of about 1% for Wassiljewa's mixing rule with critical temperatures and pressures. Merten and Rotermund (1997) studied cyclopentane/carbon dioxide and cyclopentane/air mixtures at 40°C. They used Wassiljewa's model with viscosities, a fixed  $\varepsilon=1$  and the thermal conductivity of the cyclopentane calculated based on  $14.8 \text{ mW}\cdot\text{m}^{-1}\cdot\text{K}^{-1}$  thermal conductivity at 25°C (an extreme value according to Fig. 4). Their mean deviation was about  $0.2 \text{ mW}\cdot\text{m}^{-1}\cdot\text{K}^{-1}$  for the cyclopentane/ $\text{CO}_2$  - mixture (max. dev. 0.4) and  $0.7 \text{ mW}\cdot\text{m}^{-1}\cdot\text{K}^{-1}$  for the cyclopentane/air-mixture (max. dev. 1.6).

#### 2.3.4 Conduction through the matrix and radiation

Conduction through the matrix and radiation typically represent about 20-40% of the total thermal conductivity of the foam (approximately  $4\text{-}9 \text{ mW}\cdot\text{m}^{-1}\cdot\text{K}^{-1}$  for foams of  $40\text{-}80 \text{ kg}\cdot\text{m}^{-3}$  density [Olsson 1998],  $12 \text{ mW}\cdot\text{m}^{-1}\cdot\text{K}^{-1}$  [Jarfelt 1998]).

##### 2.3.4.1 Conduction through the matrix

Heat transport by conduction through the polyurethane matrix depends on the thermal conductivity of the polyurethane as well as the amount and distribution of the material.

The thermal conductivity of solid polyurethane at 23°C is about 21 mW·m<sup>-1</sup>·K<sup>-1</sup> (23 mW·m<sup>-1</sup>·K<sup>-1</sup> [Ahern et al. 2005], 19-20 mW·m<sup>-1</sup>·K<sup>-1</sup> [Biedermann et al. 2001], 21 mW·m<sup>-1</sup>·K<sup>-1</sup> [Nielsen et al. 2000]). The temperature dependency of the thermal conductivity is approximately linear (+0.2 mW·m<sup>-1</sup>·K<sup>-1</sup> per °C [Nielsen et al. 2000]). The thermal conductivity is unaffected by differences in the chemical composition of the polyurethane (except for the isocyanate/polyol ratio, with a higher ratio giving lower thermal conductivity), its history and age or small amounts of blowing agent dissolved in the sample.

To calculate the conduction through the polyurethane matrix, Schuetz and Glicksman (1984) used cubic cell models for the windows and struts separately and weighed them together with the material distribution. They assumed that 2/3 of the windows and 1/3 of the struts contributed to the heat transfer, which agrees with the shares aligned in the direction of heat transfer (eq. 11). The strut fraction for polyurethane foam insulation  $f_s$  [-] is roughly 0.90-0.95.

$$\lambda_{conduction}^{matrix} = \left( \frac{2}{3} - \frac{f_s}{3} \right) \cdot (1 - f_g) \cdot \lambda_{PUR} \quad [\text{W} \cdot \text{m}^{-1} \cdot \text{K}^{-1}] \quad (11)$$

Here,  $f_g$  [-] is equal to the porosity or void volume fraction and  $\lambda_{PUR}$  [W·m<sup>-1</sup>·K<sup>-1</sup>] the thermal conductivity of the solid material.

In 1998 Nielsen suggested increasing the contribution by the struts, based on upper and lower limit analyses and averaging in the cubic cell models (eq. 12). According to Nielsen (1998), equations 11 and 12 yield similar results for low density foams <30 kg/m<sup>3</sup>, but differ for the higher density foams (>50 kg/m<sup>3</sup>) used for district heating pipes. Eq. 12 has been employed for the calculations in papers III-V.

$$\lambda_{conduction}^{matrix} = \{0.48 \cdot f_s + 0.66 \cdot (1 - f_s)\} \cdot (1 - f_g) \cdot \lambda_{PUR} \quad [\text{W} \cdot \text{m}^{-1} \cdot \text{K}^{-1}] \quad (12)$$

In 2005 Ahern et al. presented a new approach for determining conductivity due to conduction. They used Maxwell's classical analysis for conducting mixtures in order to take the gas conductivity into account ( $\lambda_{air}/\lambda_{PUR} \approx 0.1$ ) and not neglect it in comparison to the solid one. In their model the gas and solid parts of the conduction are not treated separately. With the model Ahern et al. obtained better agreement with experimental data for water blown polyurethane foam with high void volume fractions that showed a deviation of about 2 mW·m<sup>-1</sup>·K<sup>-1</sup> when modelled by eq. 11. By adding a vertex correction, they also obtained a good fit for lower void volume fractions (<0.95). The contribution from the struts is higher in this model than in the Schultz and Glicksman model.

#### 2.3.4.2 Radiation

The presence of many cells reduces the heat transfer by radiation, as the radiation has to pass several layers. Since the mid-1980s the heat transfer by radiation has been modelled by Rosseland's equation (eq. 13), valid for optically thick, homogeneous and isotropic foams [Schuetz and Glicksman 1984]. It should be noted that the heat transfer by radiation is strongly dependent on the temperature T [K].

$$\lambda_{radiation} = \frac{16 \cdot \sigma \cdot T^3}{3 \cdot E} [\text{W} \cdot \text{m}^{-1} \cdot \text{K}^{-1}] \quad (13)$$

In eq. 13,  $\sigma$  is Stefan Boltzmann's constant =  $5.67 \cdot 10^{-8} [\text{W} \cdot \text{m}^{-2} \cdot \text{K}^{-4}]$  and  $E$  is Rosseland's mean extinction coefficient [ $\text{m}^{-1}$ ].

The extinction coefficient can be determined by measurements. Directional-hemispherical measurements, which take into account diffusely transmitted radiation due to scattering, are the most accurate (accuracy 15%) [e.g. Nielsen 1998, Biedermann et al. 2001]. Rescattering can be neglected, thus the Beer law is valid. The monochromatic extinction coefficient is then obtained by linear regression of the logarithm of the transmission vs. sample thickness or mass divided by area. The mean extinction coefficient is obtained by integration over the wavelengths.

The extinction coefficient can also be modelled. The model (eq. 14) is based on a division of the foam into transparent windows and opaque struts [Hilyard and Cunningham 1994]. The mass extinction coefficient  $e^* [\text{m}^2 \cdot \text{kg}^{-1}]$  is equal to the extinction coefficient  $E [\text{m}^{-1}]$  divided by the foam density  $\rho_f [\text{kg} \cdot \text{m}^{-3}]$ . A mass extinction of  $26.5 \text{ m}^2 \cdot \text{kg}^{-1}$  was used for the present calculations.

$$e^* = \frac{E}{\rho_f} = 4.1 \cdot \varphi \cdot \sqrt{\frac{f_s}{\rho_{PUR}}} \cdot \frac{1}{d_z \cdot \sqrt{\rho_f}} + \frac{1-f_s}{\rho_{PUR}} \cdot E_{PUR} [\text{m}^2 \cdot \text{kg}^{-1}] \quad (14)$$

In eq. 14,  $\varphi [-]$  is an efficiency factor dependent on the strut cross-section,  $f_s [-]$  the fraction of polymer in the struts,  $\rho_{PUR} [\text{kg} \cdot \text{m}^{-3}]$  the solid polymer density,  $d_z [\text{m}]$  a measure of the average cell size,  $\rho_f [\text{kg}/(\text{m}^3)]$  the foam density and  $E_{PUR} [\text{m}^{-1}]$  the polyurethane extinction coefficient.

There is a relationship between the extinction coefficient and the foam density [Olsson 1998]. High density leads to high extinction coefficient values. As the absorption of light depends upon the presence of different chemical structures and polyurethane foam can differ due to the formula used as well as foaming conditions, very different coefficient values have been reported in the literature.

### 2.3.5 Overall thermal conductivity of the foam

For an ordinary polyurethane foam (also studied in papers IV and V as Foam 2), the total initial thermal conductivity increases with temperature from about 23 to around 39  $\text{mW} \cdot \text{m}^{-1} \cdot \text{K}^{-1}$  in the 10-120°C temperature interval (27  $\text{mW} \cdot \text{m}^{-1} \cdot \text{K}^{-1}$  at 50°C). The contributions of the different modes were estimated at (Figure 6):

- conduction in the gas phase  $\lambda_{conduction}^{gas}$  : 13-22  $\text{mW} \cdot \text{m}^{-1} \cdot \text{K}^{-1}$  or about 57% of the total initial heat transfer
- conduction through the matrix  $\lambda_{conduction}^{matrix}$  : 6.2-6.8  $\text{mW} \cdot \text{m}^{-1} \cdot \text{K}^{-1}$  or about 27-17% of the total initial heat transfer
- radiation  $\lambda_{radiation}$ : 3.7-9.9  $\text{mW} \cdot \text{m}^{-1} \cdot \text{K}^{-1}$  or about 16-25% of the total initial heat transfer

The exact values and shares depend on the studied foam and the model used. Uncertainties in input-data and models may cause variations of the order of a few  $\text{mW} \cdot \text{m}^{-1} \cdot \text{K}^{-1}$  in the calculated thermal conductivity. The result illustrates tendencies.

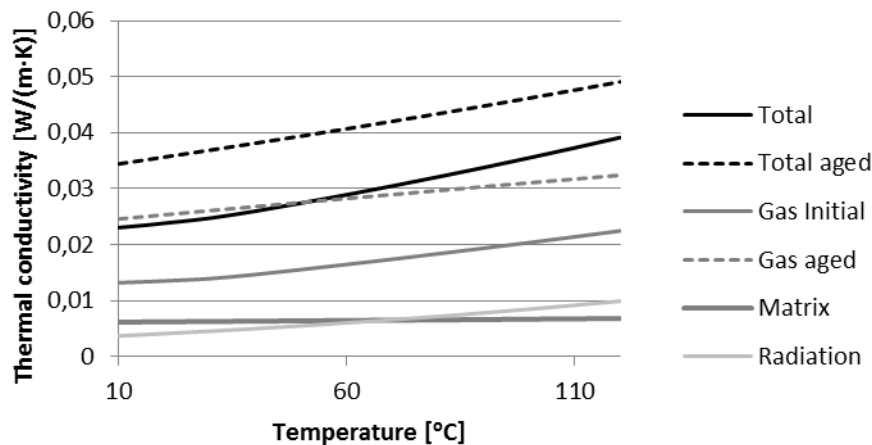


**Figure 6.** Thermal conductivity of new and completely aged (i.e. air filled) cyclopentane blown polyurethane foam (Foam 2 [papers IV, V]) versus temperature, as well as its different contributions: conduction in the gas phase, conduction through the matrix and radiation.

At fully aged conditions, i.e. with the foam cells completely air filled, the total thermal conductivity of the previously studied foam increased by about  $10 \text{ mW}\cdot\text{m}^{-1}\cdot\text{K}^{-1}$  or 50-25% (higher temperature causes less percentage change) to  $34\text{-}49 \text{ mW}\cdot\text{m}^{-1}\cdot\text{K}^{-1}$  (see Figure 6). This end value is of more theoretical interest than practical importance because it will take over 100 years to reach. It is the upper limit of the thermal conductivity. At fully aged conditions, conduction through the cell gas increased by about 87-44% to  $25\text{-}32 \text{ mW}\cdot\text{m}^{-1}\cdot\text{K}^{-1}$ , which represents around 71-66% of the total final thermal conductivity. Conduction through the matrix and radiation remains the same and represents about 18-14% and 11-20% respectively of the aged thermal conductivity of the studied foam.

Pipes used on the German market for 3-25 years had total thermal conductivities at  $23^\circ\text{C}$  of approximately  $25\text{-}40 \text{ mW}\cdot\text{m}^{-1}\cdot\text{K}^{-1}$  [Meigen and Schuricht 2005].

It has become more and more common to use a diffusion barrier between the insulation and casing to hinder the gas transport, especially in small pipe dimensions and flexible pipes. A diffusion barrier can effectively hinder the change in the cell gas content of the insulation.

### 3 THERMAL MODELS OF THE PIPES

---

This chapter deals with prediction of heat flows from district heating pipes and of the temperature within and around them (Figure 7).

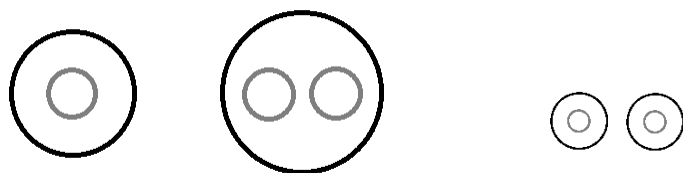


**Figure 7.** Examples of geometries that can be treated by the models presented in the thesis; to the left the single and the twin pipe and to the right an ordinary single pipe network with the pipes buried in the ground.

Heat transfer problems for the pipes alone are treated first. Both steady state and transient solutions are dealt with for the single [papers III, IV, BIII/IV] and the twin pipe [papers V, BV] geometry (Figure 7a). A coordinate transformation has been deduced that facilitates the treatment of the twin pipe geometry. Then pipes laid in the ground are considered (Figure 7b), for which steady state solutions are presented. The temperature profile in the ground and heat flows from the pipes indicated by the steady state models should be considered as a yearly average. A steady state solution for annularly insulated pipes was derived [papers II, BII] and can be used for any number of pipes placed optionally in the ground. Single pipes in the ground can be modelled in a more detailed way by combining the single pipe model with the model for annularly insulated pipes in the ground. The chapter concludes with a discussion on factors that influence the heat flows from the pipes.

#### 3.1 The heat conduction equation

The general equation used for heat conduction is eq. 15. The heating (on the left hand side of eq. 15) is given by the product of the volumetric heat capacity  $c \cdot \rho$  [ $\text{J} \cdot \text{m}^{-3} \cdot \text{K}^{-1}$ ] and the temperature change, while the net heat inflow (on the right of eq. 15) is obtained by the negative divergence of the heat flux  $q$  [ $\text{W} \cdot \text{m}^{-2}$ ]. The heat flux is calculated according to Fourier's law (eq. 16). No internal heat generation is present<sup>2</sup>.

---

<sup>2</sup> The only internal heat generation  $\Delta e$  [ $\text{W} \cdot \text{m}^{-1}$ ] in district heating pipes is the small energy amounts that are used in phase changes of cyclopentane. These are negligible in comparison to the overall heat transfer taking place. The energy released to/absorbed from the cell by condensation/vaporisation is

$$\rho \cdot c \cdot \frac{\partial T}{\partial t} = -\nabla \cdot q \quad [\text{W} \cdot \text{m}^{-3}] \quad (15)$$

$$q = -\lambda \cdot \nabla T \quad [\text{W} \cdot \text{m}^{-2}] \quad (16)$$

### 3.2 Single pipes

Modelling heat losses from the single pipes is quite straightforward, as they have the traditional cylindrical geometry that makes the radial coordinate suitable for use (Figure 8).

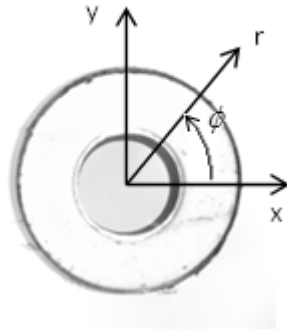


**Figure 8.** The cylindrical geometry of the single pipe and polar coordinates.

#### 3.2.1 Stationary temperature within an insulation of constant thermal conductivity

Assuming constant thermal conductivity of the insulation, the single pipe can be described by an annular cylinder of the insulation material with the temperature at the inner boundary  $T_i$  [K] corresponding to the temperature of the steel fluid pipe and at the outer boundary  $T_e$  [K] corresponding to that of the casing. An analytical solution exists for this simplified case; stationary heat conduction through a cylindrical annulus between  $r_i$  [m] and  $r_e$  [m] of a material with constant thermal conductivity  $\lambda$  [ $\text{W} \cdot \text{m}^{-1} \cdot \text{K}^{-1}$ ] and with constant boundary conditions is given by eqs. 17-19.

$$\frac{d^2 T}{dr^2} + \frac{1}{r} \cdot \frac{dT}{dr} = 0 \quad (17)$$

$$T(r_i) = T_i \text{ [K]} \quad (18)$$

$$T(r_e) = T_e \text{ [K]} \quad (19)$$

---

about  $10^{-6}$  times the energy flow through the cell, i.e. very small in comparison and should be easily transported from/to the cell. The energy released to/taken from the cell due to the condensation/vaporisation was calculated as the change in liquid concentration in the cell between two times multiplied by the enthalpy of vaporisation at standard conditions of cyclopentane  $\Delta \text{vap}H^\circ = 28,784 \text{ kJ/mol}$  [NIST Chemistry webbook] and the cell volume divided by the time interval.

The general solution to eq. 17 is a linear combination of 1 and  $\ln(r)$ , i.e. the temperature is a function of the form  $T(r) = a + b \cdot \ln(r)$ , where  $a$  and  $b$  are constants [Folland 1992]. The solution (eq. 20) is determined with the aid of the boundary conditions (eqs. 18-19).

$$T(r) = T_i + \frac{T_e - T_i}{\ln\left(\frac{r_e}{r_i}\right)} \cdot \ln\left(\frac{r}{r_i}\right) \text{ [K]} \quad (20)$$

The radial heat flow  $q$  [ $\text{W} \cdot \text{m}^{-2}$ ] from the pipe is given by Fourier's law in radial coordinates (eq. 21). The radial heat flow per metre  $Q$  [ $\text{W} \cdot \text{m}^{-1}$ ] from the pipe is obtained by the integral of the flow  $q$  over the pipe's circumference (eq. 22); as there is no angle variation in this case, the integral is equal to the product of the circumference and the flow. The flow  $Q$  can also be stated as a conductance  $K_T$  [ $\text{W} \cdot \text{m}^{-1} \cdot \text{K}^{-1}$ ] times the temperature difference over the ring, as illustrated in Figure 9. The conductance may be expressed as the reciprocal of a thermal resistance  $R_T$  [ $\text{m} \cdot \text{K} \cdot \text{W}^{-1}$ ].

$$q(r) = -\lambda \cdot \frac{dT}{dr} = -\lambda \cdot \frac{T_e - T_i}{r \cdot \ln\left(\frac{r_e}{r_i}\right)} \text{ [W} \cdot \text{m}^{-2}] \quad (21)$$

$$Q = \int_0^{2\pi} q(r) \cdot r \cdot d\phi = 2 \cdot \pi \cdot r \cdot q(r) = K_T \cdot (T_i - T_e) = \frac{1}{R_T} \cdot (T_i - T_e) \text{ [W} \cdot \text{m}^{-1}] \quad (22)$$

$$K_T = \frac{1}{R_T} = \frac{2 \cdot \pi \cdot \lambda}{\ln\left(\frac{r_e}{r_i}\right)} \text{ [W} \cdot \text{m}^{-1} \cdot \text{K}^{-1}] \quad (23)$$

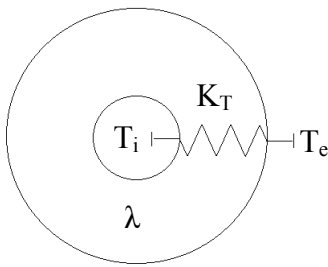


**Figure 9.** Circuit model for the pipe with fixed boundary temperatures at the inner radius  $r_i$  [m] and outer radius  $r_e$  [m] as well as constant thermal conductivity of the insulation.

### 3.2.2 Stationary temperature with radially varying thermal conductivity of the insulation

The thermal conductivity of the insulation normally varies in the radial direction, mainly due to a temperature gradient but also because of e.g., differences in morphology and cell gas content. For cases with radial variation the pipe can be divided into annuli of approximately constant properties and the above solution used for each annulus. The temperature distribution within the pipe and the radial heat flow from the pipe are calculated numerically using finite differences. The insulation between the fluid pipe at  $r_f$  [m] and the casing with the inner radius  $r_{ins}$  [m] are then divided into a sequence of annular regions  $n=1,2,\dots,N$ , so called cells, of approximately constant properties with central radii  $r_n$  [m],  $n=1,2,\dots, N$  and width  $\Delta r$  [m] (see Figure 9). Eq. 24 gives the heat balance for cell  $n$ . The heat flow from a cell  $n$  in the middle of the insulation to cell  $n+1$  is given by  $Q_{n \rightarrow n+1}$  [ $W \cdot m^{-1}$ ] (eqs. 25-26). It passes half of cell  $n$  and half of cell  $n+1$ , the resistance between cell  $n$  and  $n+1$  is thus given by the sum of the two half cells' resistances [e.g. Hagentoft 2001, Claesson 2001]. The two resistances in the denominator of eq. 26 are calculated in accordance with eq. 23. Note that a subscript is used to denote where a property is valid, e.g.  $r_n$  [m] the radial coordinate for cell  $n$ ,  $T_n$  [K] temperature in cell  $n$  and  $\lambda_n$  [ $W \cdot m^{-1} \cdot K^{-1}$ ] thermal conductivity in cell  $n$ . Figure 10 illustrates the thermal network for this case.

$$Q_{n-1 \rightarrow n} - Q_{n \rightarrow n+1} = 0 \quad (24)$$

$$Q_{n \rightarrow n+1} = K_{n \rightarrow n+1} \cdot (T_n - T_{n+1}) \quad [W \cdot m^{-1}] \quad (25)$$

$$K_{n \rightarrow n+1} = \frac{1}{\frac{1}{2 \cdot \pi \cdot \lambda_n} \cdot \ln\left(\frac{r_n + 0.5 \cdot \Delta r}{r_n}\right) + \frac{1}{2 \cdot \pi \cdot \lambda_{n+1}} \cdot \ln\left(\frac{r_{n+1}}{r_n + 0.5 \cdot \Delta r}\right)} \quad [W \cdot m^{-1} \cdot K^{-1}] \quad (26)$$

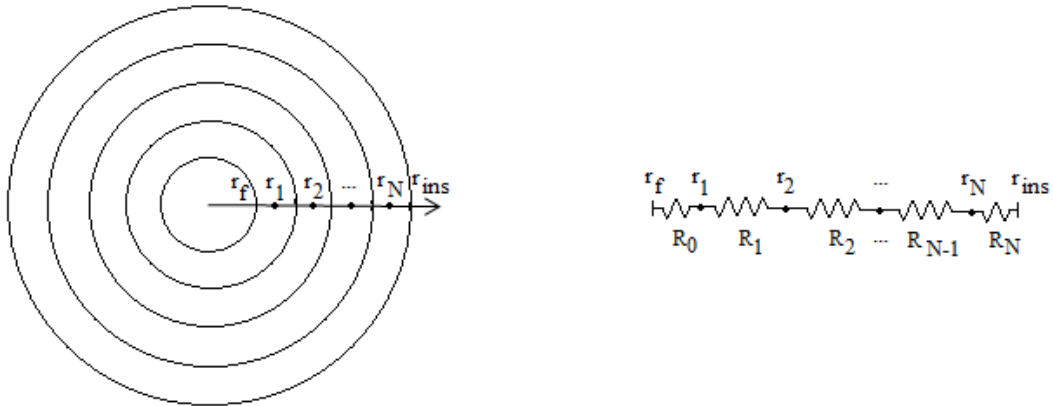


**Figure 10.** The mesh for the insulation of the pipe and the corresponding heat flow model, where  $R_{f \rightarrow 1}$  is denoted  $R_0$ ,  $R_{n \rightarrow n+1}$   $n=1,2,\dots,N-1$  is denoted  $R_n$  and  $R_{N \rightarrow ins}$  is denoted  $R_N$ . The latter shorter denotation is suitable for use at implementation where the properties are stored as vector elements (subscript  $n$  becomes vector element  $n$ ).

At the boundaries heat is only transported through one half cell (eqs. 27-28). Resistances for the fluid pipe and casing (e.g.  $1/(2 \cdot \pi \cdot \lambda_{PE}) \cdot \ln(r_c/r_{ins})$  for the casing with outer radius  $r_c$  [m] in eq. 28) as well as surface heat transfers (e.g.  $1/(2 \cdot \pi \cdot r_c \cdot \alpha)$ ,  $\alpha$  [ $W \cdot m^{-2} \cdot K^{-1}$ ] in eq. 28) may be accounted for by addition of the terms in the denominators of the conductances but are of minor importance.

$$K_{f \rightarrow 1} = \frac{1}{\frac{1}{2 \cdot \pi \cdot \lambda_1} \cdot \ln\left(\frac{r_i}{r_f}\right)} [W \cdot m^{-1} \cdot K^{-1}] \quad (27)$$

$$K_{N \rightarrow ins} = \frac{1}{\frac{1}{2 \cdot \pi \cdot \lambda_N} \cdot \ln\left(\frac{r_{ins}}{r_N}\right)} [W \cdot m^{-1} \cdot K^{-1}] \quad (28)$$

With N cells, N equations are stated for the N unknown temperatures (in the middle) of each annulus. An equation system is thus obtained to be solved for the temperatures. The equation system may be solved by means of matrices such as  $A \cdot T = b$ ,  $T = A^{-1} \cdot b$ ; where the coefficients of the unknown temperatures are put in the correct places in the square matrix A and the constant terms due to the boundary conditions in the vector b. The calculations can be implemented in, for example, the software Mathcad, as has been the case for [papers III, IV and BIII-IV].

The total heat transfer resistance for the pipe is the sum of all annular cell resistances. In this way an effective (or equivalent) thermal conductivity of the foam, i.e. a single thermal conductivity for the whole foam cross section ( $r_{ins}-r_f$  [m]) that would give the same heat loss as the radially varying thermal conductivity, can be derived (eq. 29). The cylindrical geometry makes it most important what type of material is close to the fluid pipe. A good insulation material reduces the heat loss more efficiently if it is placed close to the fluid pipe.

$$\lambda_{eq} = \ln \frac{r_{ins}}{r_f} \cdot \frac{1}{\sum_{n=1}^N \frac{1}{\lambda_n} \cdot \ln \frac{r_f + n \cdot \Delta r}{r_f + (n-1) \cdot \Delta r}} [W \cdot m^{-1} \cdot K^{-1}] \quad (29)$$

### 3.2.3 Temperature profile with time variation

A non-stationary solution is required when changes, e.g. in the thermal conductivity of the insulation or boundary temperatures, take place over time. In such cases the heat flows to and from each annulus may not cancel out as in eq. 24. Instead, the temperature in a cell can increase over time due to a net influx as stated in eq. 30. According to the explicit finite difference method, the temperature increase during a time step is determined based on the flows present at the start of the time step. The temperature is determined at a future time  $t^{nr+1}$  [s], which is specified by a certain number (nr+1) of time steps  $\Delta t$  [s] performed from the initial time  $t_0$  [s];  $t^{nr+1} = t^{nr} + \Delta t = t_0 + (nr+1) \cdot \Delta t$ . The new temperature in the cell  $T_n^{nr+1}$  [K] is given by the temperature change  $T_n^{nr+1} - T_n^{nr}$  [K] during the last time step  $\Delta t$  [s] added to the start temperature of the time step  $T_n^{nr}$  [K] (eq. 31). This method works well as long as the chosen time step

is not too long to ensure numerical stability. The maximum time step is given by eq. 32.

$$\rho_n \cdot c_n \cdot 2 \cdot \pi \cdot r_n \cdot \Delta r_n \cdot (T_n^{nr+1} - T_n^{nr}) = (Q_{n-1 \rightarrow n}^{nr} - Q_{n \rightarrow n+1}^{nr}) \cdot \Delta t \quad [\text{J} \cdot \text{m}^{-1}] \quad (30)$$

$$T_n^{nr+1} = T_n^{nr} + \Delta t \cdot \frac{(Q_{n-1 \rightarrow n}^{nr} - Q_{n \rightarrow n+1}^{nr})}{\rho_n \cdot c_n \cdot 2 \cdot \pi \cdot r_n \cdot \Delta r_n} \quad [\text{K}] \quad (31)$$

$$\Delta t < \min_n \left( \frac{\rho_n \cdot c_n \cdot 2 \cdot \pi \cdot r_n \cdot \Delta r_n}{K_{n-1 \rightarrow n} + K_{n \rightarrow n+1}} \right) \quad [\text{s}] \quad (32)$$

### 3.3 Twin pipes

The twin pipe geometry, with two fluid pipes placed within one casing, is more complex than single pipe geometry, which complicates calculations. A coordinate transformation is performed in order to obtain a suitable geometry in which to perform the heat conduction calculations. The mathematics of the method presented is rather complex. Here, an outline of the main features is provided and the method is presented in more detail in the background report [BV].

#### 3.3.1 Coordinate transformation

The (x,y)- coordinates are transformed by a conformal mapping  $w(z)=u(x,y)+i \cdot v(x,y)$  to the (u,v)-coordinates, in which the twin pipe geometry becomes rectangular [V, BV] (Figure 11). The mapping is derived from a quarter of a pipe and then expanded to a half plane in order to model the whole twin pipe with different forward and return pipe temperatures.

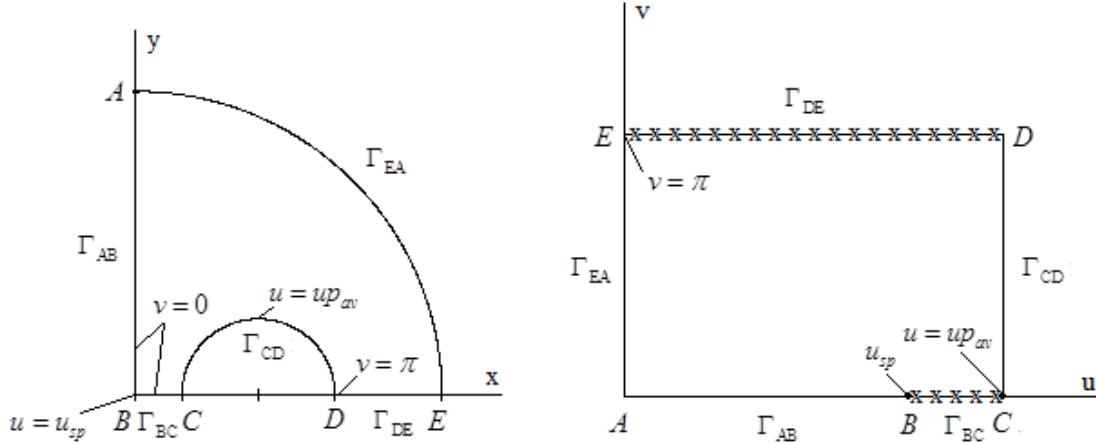


**Figure 11.** The twin pipe geometry in the (x,y)-coordinate system (left) and in the (u,v)-coordinate system (right). The letters A-E indicate corresponding points in the two coordinate systems and the x:s in the right hand diagram symbolize no heat flow boundary conditions.

Assuming that the twin pipe has a casing with a radius  $r_0$  [m] and service pipes placed at  $(\pm x_1, 0)$  of radius  $r_1$  [m], the transformation is given by eqs. 33-35.

$$w(z) = w_0(z) + \sum_{j=1}^J P_j \cdot w_j(z), \quad z = x + i \cdot y \quad (33)$$

$$w_0(z) = -\ln(z - x_1) - \ln(z + x_1) + \ln(x_1 \cdot z - r_0^2) + \ln(x_1 \cdot z + r_0^2) - 2 \cdot \ln(r_0) \quad (34)$$

$$\begin{aligned} w_j(z) &= \frac{r_1^j}{(j-1)!} \cdot \frac{\partial^j}{\partial x_1^j} [w_0(z)], \quad j = 1, 2, \dots, J \\ &= \frac{(r_1)^j}{(z - x_1)^j} + \frac{(-r_1)^j}{(z + x_1)^j} - \frac{(-r_1 z)^j}{(x_1 z - r_0^2)^j} - \frac{(-r_1 z)^j}{(x_1 z + r_0^2)^j} \end{aligned} \quad (35)$$

The transformation (eq. 33) uses line sources in source-sink pairs (eq. 34) to obtain the casing  $r=r_0$  as the u-coordinate curve  $u=0$  and at the same time approximately circular u-curves at the service pipes, especially for small service pipes radii. The line source sources terms are placed at the centre of the service pipes  $z = \pm x_1$  and the line source sinks terms at  $z = \pm x_2 = \pm r_0^2/x_1$ .

To improve the circularity at the service pipes, derivatives of the line sources of different orders, so called ‘‘multipoles’’ are used (eq. 35). These multipoles make zero contribution to the coordinate curve at the casing, maintaining its circularity. The strengths of the multipoles  $P_j$ , i.e. the constants by which they are multiplied, are determined so that the variation in the real part of  $w(z)$  around the service pipes’ circumference  $u_p(\varphi) = \text{Re}(w(x_1 + r_1 \cdot e^{i\varphi}))$  is minimized. This function  $u_p(\varphi)$  (eq. 36) is even in  $\varphi$  and may be expanded in a Fourier cosine series. The variation is minimized by choosing the strength of the multipoles included in the calculations, i.e. up to order  $J$ , so that the first  $J$  Fourier coefficients, excluding the zero order that gives the constant term, becomes zero (eq. 37). An equation system is obtained for determining the strengths  $P_j$  that may be solved by use of matrixes (eq. 38).

$$u_p(\varphi) = u_{p0}(\varphi) + \sum_{j=1}^J P_j \cdot u_{pj}(\varphi) \quad (36)$$

$$\underbrace{\int_0^\pi u_{p0}(\varphi) \cdot \cos(k\varphi) d\varphi}_{-C_k} + \sum_{j=1}^J P_j \cdot \underbrace{\int_0^\pi u_{pj}(\varphi) \cdot \cos(k\varphi) d\varphi}_{B_{k,j}} = 0, \quad k = 1, 2, \dots, J \quad (37)$$

$$B_{k,j} \cdot P_j = C_k, \quad k = 1, 2, \dots, J, \quad j = 1, 2, \dots, J \quad \mathbf{P} = \mathbf{B}^{-1} \cdot \mathbf{C} \quad (38)$$

The function  $w(z)$  that describes the transformation is an analytical function, i.e. satisfying the so-called Cauchy-Riemann’s relations, so that the length scale factors  $h(u, v) = |dz/dw|$  [-] in u and v direction become identical. Then the heat equation has about the same appearance in the conformal and the Cartesian coordinates; the only difference is that the left hand side is multiplied by an area factor  $A(u, v) = h(u, v)^2$  [-], see eq. 39 [BV].

$$A(u, v) \cdot \rho \cdot c \cdot \frac{\partial T}{\partial t} = \frac{\partial}{\partial u} \left( \lambda \cdot \frac{\partial T}{\partial u} \right) + \frac{\partial}{\partial v} \left( \lambda \cdot \frac{\partial T}{\partial v} \right) [\text{W} \cdot \text{m}^{-3}] \quad (39)$$

This equation can be solved numerically with the explicit finite difference method. Here, the problem is two dimensional. The region is divided into cells  $i, j$ . The temperature increase in the cell is caused by the net inflow to the cell (eq. 40). The factor  $h_{i,j}^2 \cdot \Delta u_i \cdot \Delta v_j$  is an approximation of the area of cell  $i, j$  in the  $(x, y)$  coordinate system;  $A_{i,j}$  [ $\text{m}^2$ ]. The heat flows in the  $u$ - and  $v$ -directions are denoted  $Qu$  [ $\text{W} \cdot \text{m}^{-1}$ ] and  $Qv$  [ $\text{W} \cdot \text{m}^{-1}$ ] respectively. The heat flow equations 41-42 are valid for cells  $i, j$  that are not situated at the boundaries, where the conductance are changed, e.g. to only cover half a cell or to zero for no heat flow boundaries.

$$\rho_{i,j} \cdot c_{i,j} \cdot \underbrace{h_{i,j}^2 \Delta u_i \Delta v_j}_{= A_{i,j}} \cdot (T_{i,j}^{nr+1} - T_{i,j}^{nr}) = (Qu_{i-1 \rightarrow i,j}^{nr} - Qu_{i \rightarrow i+1,j}^{nr} + Qv_{i,j-1 \rightarrow j}^{nr} - Qv_{i,j \rightarrow j+1}^{nr}) \cdot \Delta t \quad (40)$$

$$Qu_{i \rightarrow i+1,j} = Ku_{i \rightarrow i+1,j} (T_{i,j} - T_{i+1,j}) [\text{W} \cdot \text{m}^{-1}], \quad Ku_{i \rightarrow i+1,j} = \frac{2 \cdot \Delta v_j}{\frac{\Delta u_i}{\lambda_{i,j}} + \frac{\Delta u_{i+1}}{\lambda_{i+1,j}}} [\text{W} \cdot \text{m}^{-1} \cdot \text{K}^{-1}] \quad (41)$$

$$Qv_{i,j \rightarrow j+1} = Kv_{i,j \rightarrow j+1} \cdot (T_{i,j} - T_{i,j+1}) [\text{W} \cdot \text{m}^{-1}], \quad Kv_{i,j \rightarrow j+1} = \frac{2 \cdot \Delta u_i}{\frac{\Delta v_j}{\lambda_{i,j}} + \frac{\Delta v_{j+1}}{\lambda_{i,j+1}}} [\text{W} \cdot \text{m}^{-1} \cdot \text{K}^{-1}] \quad (42)$$

### 3.3.2 Stationary temperature profile

The stationary temperature for this case can be obtained by starting from a hypothesized temperature profile, i.e. the average temperature of the service pipes and the casing, and looping forward towards a solution. The heat flows to each cell and the temperature change are calculated (eq. 43). As long as the temperature change is not negligible, new temperatures are determined for the cells and the corresponding heat flows and the temperature change calculated. Over relaxation may be used in order to speed up the convergence, which will be reached as long as  $0 < \omega < 2$ . Faster convergence is obtained for values of  $\omega$  above 1, e.g. 1.95 may be chosen.

$$\Delta T = \frac{(Qu_{i-1 \rightarrow i,j} - Qu_{i \rightarrow i+1,j} + Qv_{i,j-1 \rightarrow j} - Qv_{i,j \rightarrow j+1})}{\rho_{i,j} \cdot c_{i,j} \cdot A_{i,j}} \cdot \omega, \quad T_{i,j}^{new} = T_{i,j} + \Delta T_{i,j} \quad (43)$$

### 3.3.3 Temperature profile with time variation

From eq. 40 the new temperature in cell  $i, j$  is calculated according to eq. 44. The time step limit is stated in eq. 45.

$$T_{i,j}^{nr+1} = T_{i,j}^{nr} + \frac{(Qu_{i-1 \rightarrow i,j}^{nr} - Qu_{i \rightarrow i+1,j}^{nr} + Qv_{i,j-1 \rightarrow j}^{nr} - Qv_{i,j \rightarrow j+1}^{nr})}{\rho_{i,j} \cdot c_{i,j} \cdot A_{i,j}} \cdot \Delta t [\text{K}] \quad (44)$$

$$\Delta t < \min_{i,j} \left( \frac{\rho_{i,j} \cdot c_{i,j} \cdot A_{i,j}}{Ku_{i-1 \rightarrow i,j} + Ku_{i \rightarrow i+1,j} + Kv_{i,j-1 \rightarrow j} + Kv_{i,j \rightarrow j+1}} \right) \text{ [s]} \quad (45)$$

### 3.4 Pipes in the ground

This thesis presents steady state solutions for pipes in the ground. Of course in reality, the ground surface and fluid temperatures vary over time. These variations may be seen as disturbances to the average temperatures.

An estimation of how deep in the ground the temperature is affected by a changing surface temperature may be obtained by looking at the solution (eq. 46) for a semi-infinite slab ( $x \geq 0$ ) with a periodically varying surface temperature. The surface temperature varies periodically  $T(0,t) = T_1 \cdot \sin(2 \cdot \pi \cdot t / t_p)$  [K] with time period  $t_p$  and amplitude  $T_1$  [s]. The temperature in the ground will vary with the same time period, but with a smaller amplitude. The maximum temperature will be reached later than at the surface. The temperature variation in the ground is thus less and has a time lag. The periodic penetration depth  $d_p$  is the depth at which the temperature variation decreases to 37% of that at the surface. Periodic penetration depths in the ground for temperature variations with different time periods are presented in Table 2. Yearly temperature variations reach the laying depth of district heating pipes. However, daily temperature variations never reach down to the pipes in the ground.

$$T(x,t) = T_1 \cdot e^{-x/d_p} \cdot \sin \left( \frac{2 \cdot \pi \cdot t}{t_p} - \frac{x}{d_p} \right) \text{ [K]}, \quad d_p = \sqrt{\frac{a \cdot t_p}{\pi}} \text{ [m]}, \quad a = \frac{\lambda}{\rho \cdot c} \text{ [m}^2/\text{s]} \quad (46)$$

**Table 2.** Periodic penetration depth in semi-infinite soil with a thermal diffusivity of about  $1 \cdot 10^6 \text{ m}^2/\text{s}$  [Hagtoft 2001].

$t_p$	24 h	1 month	1 year
$d_p$	17 cm	0.9 m	3.2 m

The steady state temperature solutions presented here may be seen as representing the yearly average temperature around the pipes with corresponding yearly average heat flows from the pipes. They are suitable for determining long-term heat losses from the pipes.

For momentary determinations the seasonal temperature variations need to be considered together with the fluid temperature variations. It would in principle be possible to obtain the temperature solution over time for such a problem by superimposing the solutions for the temperature variations on the steady state solution presented here. These issues have not been studied in this thesis.

#### 3.4.1 Steady state solution for annularly insulated pipes in the ground

In II and the corresponding background report [BII] the steady state problem of annularly insulated pipes with interior surface heat transfer resistance laid in the ground is solved. The solution may be used to determine the temperature field in the ground as well as the heat flows from any number of pipes with annular insulation placed at any location in the ground. The temperature of the fluid in each of the pipes  $n$  ( $n=1,2,\dots,N$ ,  $N$  chosen freely) is  $T_n$  [K] and the temperature of the ground surface  $T_0$  [K]. The thermal conductivity of the ground is  $\lambda$ . Each pipe  $n$  is centred at  $(x_n, y_n)$

and consists of insulation between the inner radius  $r'_{pn}$  [m] and outer radius  $r_{pn}$  [m] of thermal conductivity  $\lambda_n$  [ $\text{W}\cdot\text{m}^{-1}\cdot\text{K}^{-1}$ ]. The surface resistance at the inner radius between the fluid in pipe n and the insulation is  $R_{pn}$  [ $\text{K}\cdot\text{m}\cdot\text{W}^{-1}$ ].

$$\Delta T = \frac{\partial T^2}{\partial x^2} + \frac{\partial T^2}{\partial y^2} = 0, \quad -\infty < x < \infty \quad 0 \leq y < \infty \quad (47)$$

$$T(x, 0) = T_0 \quad (48)$$

$$T_n = T(r'_{pn}, \phi_n) - \beta_n \cdot r'_{pn} \cdot \frac{\partial T}{\partial r} \Big|_{r=r'_{pn}} \quad \beta_n = 2 \cdot \pi \cdot \lambda_n \cdot R_{pn}, \quad n=1, 2, \dots, N \quad (49)$$

The above heat conduction problem is solved by dividing the space into regions with constant thermal conductivity; pipe regions and a ground region. In each region the heat conduction is described by the Laplace equation (eq. 47). Series expansions for the temperature in each region that fulfils the Laplace equation and the internal boundary conditions (eqs. 48-49) are matched at the region boundaries to obtain the solution. The calculations are performed in complex coordinates and the temperature solutions in the regions are given by the real part of complex valued linear combinations of analytic functions (eq. 50). Here  $r_n$  and  $\phi_n$  are the local polar coordinates around pipe n.

$$1, \quad \ln(r_n), \quad \left( r_n \cdot e^{i\phi_n} \right)^{-k}, \quad \left( r_n \cdot e^{i\phi_n} \right)^k \quad k=1, 2, \dots, (\infty), \quad n=1, 2, \dots, N \quad (50)$$

ordinary                      at infinity

A finite number of multipoles ( $k=1, 2, \dots, J$  for multipoles up to order  $J$ ) needs to be chosen for the calculations. Even calculations with multipoles of a low order give good estimations of the heat flows from the pipes [II].

In the pipe regions the calculations are made in local polar coordinates around the pipes. The general solution for the temperature around the pipe contains a constant contribution, a contribution from the line source placed at the pipe and contributions from multipoles placed at the pipe (ordinary and at infinity). The strengths of the ordinary multipoles and the multipoles at infinity are obtained by identifying non-angular dependent and angular dependent terms in the equation for the boundary condition relations between the strengths of the constant contribution and the line source contribution respectively; the constant contribution is expressed as a function of the line source strength and the strengths of the multipoles at infinity as a function of the strength of the ordinary multipoles. The temperature expression in the pipe is written out in eqs. 51-52. Here, the constants  $q'_n$  and  $P'_{nk}$  are yet unknown.

$$T(r_n, \phi_n) = T_n + \frac{q'_n}{2 \cdot \pi \cdot \lambda_n} \cdot \left[ \ln \left( \frac{r'_{pn}}{r_n} \right) - \beta_n \right] + \text{Re} \left\{ \sum_{k=1}^J P'_{nk} \cdot \left[ \left( \frac{r_n}{r_{pn}} \right)^k + \tilde{\beta}_{kn} \cdot \left( \frac{r_{pn}}{r_n} \right)^k \right] \cdot e^{i \cdot k \cdot \phi_n} \right\} \quad (51)$$

$$\tilde{\beta}_{kn} = \frac{\beta_n \cdot k - 1}{\beta_n \cdot k + 1} \cdot \left( \frac{r_{pn}'}{r_{pn}} \right)^{2k} \quad (52)$$

In the ground the calculations are first performed in ordinary complex coordinates. The ground surface at  $y = 0$  is modelled by the method of images. For each pipe  $n$   $n=1,2,\dots,N$  in the ground at  $(x_n, y_n)$  a similar pipe  $n+N$  is put at  $(x_n, -y_n)$ . The distance from pipe  $n$  and from pipe  $n+N$  to any point on the ground surface is then equal. By means of the superposition principle, the temperature solution in the ground is obtained by adding solutions able to describe the temperature around each of the  $2N$  pipes. However, in order to obtain a finite temperature the multipoles at infinity cannot be included in the solution. For the ground the general solution is therefore a linear combination of a constant contribution, contributions from line sources placed at the  $2N$  pipes and contributions from ordinary multipoles placed at the  $2N$  pipes. By identification of terms in the boundary condition at the surface, the constant contribution is determined to the ground surface temperature, the strengths of the line sources at the image pipes to minus the strengths of the ordinary pipes' line sources and finally, the strengths of the multipoles at the image pipes to minus the complex conjugate of the strengths of the ordinary pipes' multipoles. The temperature expression in the ground is written out in eq. 53. Here,  $q_m$  and  $P_{mj}$  are yet unknown constants and  $\bar{P}_{mj}$  the complex conjugate of  $P_{mj}$ .

$$T(x, y) = T_0 + Re \left\{ \sum_{m=1}^N \left[ \frac{q_m}{2 \cdot \pi \cdot \lambda} \cdot \ln \left( \frac{z - \bar{z}_m}{z - z_m} \right) + \sum_{j=1}^J \left( P_{mj} \cdot \left( \frac{r_{pm}}{z - z_m} \right)^j - \bar{P}_{mj} \cdot \left( \frac{r_{pm}}{z - \bar{z}_m} \right)^j \right) \right] \right\} \quad (53)$$

The solution should be continuous at the boundaries between the pipes and the ground. In order to match the solutions in the pipe and ground regions, the temperature expression in the ground is rewritten into local polar coordinates around pipe  $n$  ( $n=1,2,\dots,N$ ). All strengths can be determined by identifying terms in the two different expressions, i.e. from the pipe and the ground region respectively, at the boundary  $r_{pn}$  for the temperature as well as for the heat flow (eqs. 54-58).

Relationships between the strengths:

$$q_n' = q_n \quad n = 1, 2, \dots, N \quad (54)$$

$$P_{nk}' = \frac{\bar{P}_{nk} + \tilde{P}_{kn}}{(1 + \tilde{\beta}_{kn})}, \quad k = 1, 2, \dots, J \quad n = 1, 2, \dots, N \quad (55)$$

$$\tilde{P}_{kn} = \sum_{m=1}^N \sum_{j=0}^{\infty} P_{mj} \cdot \frac{a_{jk} \cdot r_{pm}^j \cdot (-r_{pn})^k}{(z_n - z_m)^{j+k}}, \quad a_{0k} = \frac{1}{k}, \quad a_{jk} = \binom{k+j-1}{j-1} = \frac{(k+j-1)!}{k!(j-1)!} \quad (56)$$

Equations to be solved to determine the strengths:

$$\frac{q_n}{2 \cdot \pi \cdot \lambda_n} \cdot \left[ \ln \left( \frac{r_{pn}}{r'_{pn}} \right) + \beta_n \right] - \frac{q_n}{2 \cdot \pi \cdot \lambda} \cdot \ln \left( \frac{r_{pn}}{|z_n - \bar{z}_n|} \right) + \sum_{\substack{m=1 \\ m \neq n}}^N \frac{q_m}{2 \cdot \pi \cdot \lambda} \cdot \ln \left( \frac{|z_n - \bar{z}_n|}{|z_n - z_m|} \right) \\ - \operatorname{Re} \left\{ \sum_{j=1}^J \bar{P}_{nj} \cdot \left( \frac{r_{pn}}{z_n - \bar{z}_n} \right)^j \right\} + \operatorname{Re} \left\{ \sum_{\substack{m=1 \\ m \neq n}}^N \sum_{j=1}^J \left[ P_{mj} \cdot \left( \frac{r_{pm}}{z_n - z_m} \right)^j - \bar{P}_{mj} \cdot \left( \frac{r_{pm}}{z_n - \bar{z}_m} \right)^j \right] \right\} = T_n - T_0 \quad (57)$$

$$n = 1, 2, \dots, N$$

$$\bar{P}_{nk} = \frac{1 - \tilde{\beta} \tilde{\lambda}_{kn}}{1 + \tilde{\beta} \tilde{\lambda}_{kn}} \cdot \tilde{P}_{kn}, \quad \tilde{\beta} \tilde{\lambda}_{kn} = \frac{(1 - \tilde{\beta}_{kn}) \cdot \lambda_n}{(1 + \tilde{\beta}_{kn}) \cdot \lambda} \quad k = 1, 2, \dots, J \quad n = 1, 2, \dots, N \quad (58)$$

The determination of the line source and multipole strengths may be done iteratively based on an initial estimation of the strengths of the multipoles.

The heat flow from pipe n is given by the line integral of the radial heat flow along the pipe-ground boundary. The total heat flow from pipe n is given by  $q_n$ .

#### 3.4.2 Other steady state solutions

The first problem to be solved by the multipole method intended for district heating pipes concerned pipes with surface resistance in a circular region with surface resistance in a half plane [Myrehed 1989]. The solution can be used to model heat losses from both single and twin pipes in the ground. Zero and first order formulas for heat flows from single and twin pipes were presented by Wallentén (1991). The twin pipe in these formulas is rotated a quarter of a round compared to usual laying, so that the service pipes lie side by side in the ground. This has little influence on the result (<0.2% [Wallentén 1991], <1% [Jonsson 2001]), thus the formulas can be used in real cases. The zero order equations were employed to determine the heat flows from the pipes in paper I. Relative errors in the heat loss from single pipes determined by the zero order formula are estimated at 3% and by the first order formula at 0.5%. Heat flows from twin pipes of varying dimensions laid in the ground predicted by Wallentén's first order multipole formula as well as by finite element (FEM) calculations in two different programs have been compared [Jonsson 2001]. The multipole formula results deviated at most by about 2% from those of the FEM-calculations for the forward pipes and around 20% for the return pipes. The heat flow from the return pipe is calculated by subtracting two numbers of similar magnitude using multipoles. The total heat flow from the pipes differed by a maximum of about 1%.

#### 3.4.3 Coupling of ground and pipe models

The single pipe model can be coupled to the model of the annularly insulated pipes in the ground. The latter model then determines the casing temperature for the pipe model, which reveals the equivalent thermal conductivity of the insulation to be used in the model of the pipes in the ground. From an initial assumption the steady state solution is found by iteration.

The twin pipe model cannot be coupled in the same way to the model presented here for annularly insulated pipes in the ground because the twin pipe does not have cylindrical geometry.

### 3.5 Factors that influence the heat flows from the pipes

The heat flow from the pipes is to a large extent influenced by the temperature levels and the amount and thermal conductivity of the insulation. For a single pipe network a change of 1°C in the temperature levels or of 1 mW·m<sup>-1</sup>·K<sup>-1</sup> in the thermal conductivity of the insulation was found to alter the heat loss by a few percent [II].

The insulation represents practically all of the thermal resistance hindering the heat loss from the pipe. For single pipes an estimation of the share of total thermal resistance caused by the different pipe materials is straightforward due to the simple geometry. The heat flow from the pipe is denoted in eq. 59. It is proportional to the temperature difference  $T_i - T_e$  [K] over it.

The total resistance  $R_{tot}$  [K·m·W<sup>-1</sup>] is the sum of the resistances  $R_j$  for all material layers  $j$  between radius  $r_{j \text{ inner}}$  and  $r_{j \text{ outer}}$ . Table 3 contains data for the calculation. The insulation typically contributes about 99.5% or more of the total thermal resistance of the pipe. The casing typically constitutes some tenths of a percent of the pipe's total thermal resistance and the steel service pipe some hundredths of a percent. For pipes with copper service pipes the thermal resistance of the service pipe is less ( $\lambda_{Cu} \approx 365$  W·m<sup>-1</sup>·K<sup>-1</sup>) and for pipes with PEX-service pipes more; about 1% of the total thermal resistance of the pipe ( $\lambda_{PEX} \approx 0,4$  W·m<sup>-1</sup>·K<sup>-1</sup>).

$$Q = \frac{1}{R_{tot}} \cdot (T_i - T_e) [\text{W} \cdot \text{m}^{-1}], \quad R_{tot} = \sum_{mtrl j} R_j = \sum_{mtrl j} \frac{\ln\left(\frac{r_{j \text{ outer}}}{r_{j \text{ inner}}}\right)}{2 \cdot \pi \cdot \lambda_j} \quad (59)$$

The thermal conductivity of the ground varies depending on the soil and its water content in the range  $\lambda = 0.5 - 2.5$  W·m<sup>-1</sup>·K<sup>-1</sup>. For pipes laid in ground of high to medium thermal conductivity, the ground represents approximately 10% of the total thermal resistance. At really low thermal conductivity (0.5 W·m<sup>-1</sup>·K<sup>-1</sup>) the ground's share might be as high as about 30%. By shallower laying of the pipes (0.4 m instead of 0.6 m), thus decreasing the resistance of the ground, the heat loss may increase by a few percent [II]. Because the laying depth of the pipes changes, heat flows from pipes placed on top of or beside each other differ.

The water flow in district heating pipes is usually turbulent, leading to a high surface heat transfer coefficient at the water-steel interface. For example, the heat transfer coefficient for suitable temperature levels and pipe dimensions for low heat density areas with a 0.5 m·s<sup>-1</sup> speed of flow is between 2000-4000 W·m<sup>-2</sup>·K<sup>-1</sup> [Jonson 2001]. As it makes up at most a few hundreds of a percent of the total thermal resistance, the heat transfer coefficient at the water-steel interface may be neglected.

The heat transfer coefficient at the ground surface  $\alpha_{\text{air-soil}}$  [W·m<sup>-2</sup>·K<sup>-1</sup>] depends on the wind speed. It may with a small error, typically less than <0.01% [Wallentén 1991], be accounted for by using an extra fictive layer of soil of depth  $d = \lambda / \alpha_{\text{air-soil}}$  in the multipole calculations for the ground. One estimation of the heat transfer coefficient is  $\alpha_{\text{air-soil}} = 14.6$  W·m<sup>-2</sup>·K<sup>-1</sup> corresponding to an extra soil layer of about 1 dm [Bøhm 1999].

Using surface heat transfer coefficient representations of the insulation of the pipes instead of insulation layers does not influence the results in calculations of heat flows from pipes in the ground; they only underestimate the flows by a few thousandths of a percent.

**Table 3.** Rough estimates of material properties

	Thermal conductivity [ $\text{W}\cdot\text{m}^{-1}\cdot\text{K}^{-1}$ ]
Steel service pipe	76
PUR-foam	0.03
Polyethylene casing	0.04
Soil	1.5
	Surface heat transfer coefficient [ $\text{W}\cdot\text{m}^{-2}\cdot\text{K}^{-1}$ ]
Water-steel	3000
Air-ground	14.6

### 3.5.1 The pipe geometry

The twin pipe geometry is generally favourable for achieving a low heat loss from the pipe [I, Jonsson 2001, Kristjansson and Bøhm 2006]. In Table 4 heat flows from a few examples of district heating pipes of dimensions available on the market are compared.

**Table 4.** Heat losses from single (Series 2 and 3) and twin pipe networks with data according to appendix in paper VI.

	Heat flow from forward pipe [ $\text{W}\cdot\text{m}^{-1}$ ]	Heat flow from return pipe [ $\text{W}\cdot\text{m}^{-1}$ ]	Total heat flow [ $\text{W}\cdot\text{m}^{-1}$ ]
Twin 2·DN20/140	7.9	0.95	8.8
Single DN20/110	8.6	3.3	11.9
Single DN20/125	7.8	3.1	10.9
Twin 2·DN65/225	14.5	2.7	17.2
Single DN65/160	16.2	6.2	22.4
Single DN65/180	13.9	5.4	19.3
Twin 2·DN200/560	20.7	4.9	25.5
Single DN200/355	24.7	9.4	34.1
Single DN200/400	19.9	7.6	27.5

Forward temperature 80°C, return temperature 40°C. The casing temperatures for the single pipes were calculated based on 8°C ground surface temperature and 0.4 m top filling (green area). The casing temperature for the twin pipe was set equal to the temperature of the casing of the most insulated return pipe in the corresponding single pipe network, in order to calculate an upper limit for the heat flows.

The above comparison was made for insulation thicknesses sold on the market, i.e. determined by the available casing pipe diameters. With the same amount of insulation on two single pipes together as on the twin pipe, the twin pipe geometry would still be favourable.

At high forward temperature compared to return temperature in the twin pipe, the forward fluid heats up the return fluid, which in the calculations is shown as a negative flow from the return pipe. It takes a forward temperature of about 97-117°C depending on pipe dimension to start heating up 40°C return water [Jonsson 2001]. If the return temperature is lowered a lower forward temperature is needed to heat the return.

The heat loss from the twin pipe may be reduced by changing the form of the insulation and/or by displacement of the service pipes within the pipe [Jonsson 2001, Kristjansson and Bøhm 2006]. From an insulation perspective, elliptical (reduction by a few percent), oval or egg-shaped insulation is more favourable for the twin pipe than circular. If the fluid pipes are displaced so that the forward pipe is closer to the centre, the heat flow from the forward pipe is reduced but it may also diminish the total heat flow from the pipe if the repositioning is only a few millimetres. Production and handling aspects of the pipes also need to be considered in practice.

## 4 AGEING

---

The quality of the foam changes as the district heating pipes age. The concept of foam ageing comprises three main aspects:

- thermal degradation as an effect of the temperature
- oxidation due to the presence of oxygen
- changed cell gas content due to diffusion of gases.

It is the last process that primarily influences the heat conduction, which is described more thoroughly in this thesis. The thermal degradation and oxidation impact on the mechanical properties of the foam, e.g. the shear strength and are of importance at high temperatures [GEF Ingenieurgesellschaft Chemnitz mbH et al. 2011]. When foam is exposed to high temperature its colour changes from white-light yellow to dark brown.

If the foam is not diffusion-tight encapsulated its cell gas content will change due to diffusion until the foam becomes completely air filled, see Figure 12. The diffusion strives to equal out differences in the gas content. Cyclopentane and carbon dioxide that are present to a higher degree in the foam than in the surroundings diffuse out and oxygen and nitrogen that have a higher presence in the surrounding air than in the foam diffuse in. The changed cell gas content influences the thermal conductivity of the foam. An increased concentration of air and a decreased concentration of blowing agents in the cell gas impair the insulating properties.

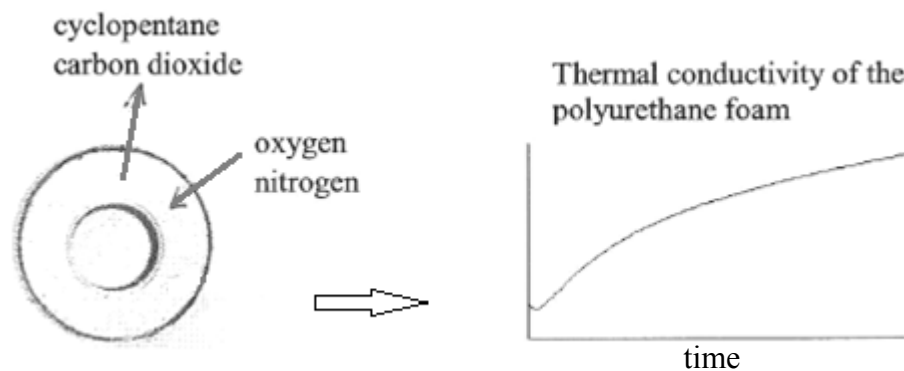


**Figure 12.** Ageing of a district heating pipe

In the modelling it was assumed that the properties of the foam matrix were unchanged, so that the thermal conductivity of the polyurethane matrix and the radiation behaviour of the foam remain the same. While the conduction through the cell gas changes over time due to the changing cell gas composition, the contribution of conduction through the matrix and radiation is fairly constant. Although the small temperature change in the insulation caused by the variation in thermal conductivity somewhat influences its contribution to the conduction, the initial value of the radiation and the conduction through the matrix can be used over the whole ageing time.

The thermal conductivity of polyurethane foam over time may thus be predicted by:

1. Measuring the initial thermal conductivity of the foam ( $\lambda_{foam\ init}$ ) together with its cell gas composition, cell gas pressure and foam density.
2. Calculating the initial contribution of conduction through the cell gas ( $\lambda_{conduction\ init}^{gas}$ ) based on the initial cell gas data as described in Chapter 2.
3. Determining the contribution from conduction through the polyurethane matrix ( $\lambda_{conduction}^{matrix}$ ) and radiation ( $\lambda_{radiation}$ ) by subtracting the calculated initial contribution of conduction through the cell gas from the measured initial foam thermal conductivity:  $\lambda_{conduction}^{matrix} + \lambda_{radiation} = \lambda_{foam\ init} - \lambda_{conduction\ init}^{gas}$  (or model their contribution as described in Chapter 2).
4. Modelling the cell gas composition of the foam over time and the contribution to the thermal conductivity over time from conduction through the cell gas. The effective diffusion and solubility coefficients of the cell gas components must be known.
5. Establishing the total thermal conductivity over time by adding the determined constant contribution ( $\lambda_{conduction}^{matrix} + \lambda_{radiation}$ ) and the modelled contribution over time from conduction through the cell gas ( $\lambda_{conduction}^{gas}$ ).

This chapter begins with a description of the diffusion equation used to model the cell gas composition. Then the data describing the gas transport through the different materials is treated. A measurement method that can be used to determine the gas distribution in the foam is also described. In particular, the solubility of cyclopentane in the polyurethane matrix has been determined in this work. After that models for single and twin pipe ageing are treated. This is followed by a discussion of factors that influence the ageing before the chapter concludes with a comparison between measured cell gas compositions in aged pipes and modelled results.

#### 4.1 The diffusion equation

The cell gas composition of the foam over time depends on the gas diffusion. The gases are assumed to be transported through the foam independently of each other. The general diffusion equation (eq. 60) gives a mass balance for each component in the foam: cyclopentane, carbon dioxide, oxygen and nitrogen. It states that the

increase in total molar mass concentration of a certain component in the foam  $c_{tot}$  [ $\text{mol}\cdot\text{m}^{-3}$ ] is given by the net inflow. No internal generation of the component is considered here<sup>3</sup>. The flow is expressed as the negative divergence of the molar mass flux  $j$  [ $\text{mol}\cdot\text{m}^{-2}\cdot\text{s}^{-1}$ ].

$$\frac{\partial c_{tot}}{\partial t} = -\nabla \cdot j \quad [\text{mol}\cdot\text{m}^{-3} \text{ foam}\cdot\text{s}^{-1}] \quad (60)$$

Each component may be present as a gas and/or a liquid and/or may be dissolved in the matrix. The total amount of a component in the foam is the sum of the gas, liquid and dissolved amounts. Oxygen, nitrogen and carbon dioxide are never present in the liquid phase, but physical blowing agents e.g. cyclopentane with low saturation vapour pressures may condense on the cold external side of the pipe if present at high concentrations. Physical blowing agents are also more soluble in the foam matrix than the permanent gases and are thus present to a larger extent in the matrix. Henry's law may be used to describe the relationship between the concentration of the compound dissolved in the matrix and the partial pressure of the compound in the cell gas.

The gases are assumed to follow the ideal gas law (eq. 61). The general gas law relates the gas phase concentration  $c$  [ $\text{mol}\cdot\text{m}^{-3}$ ] and the partial pressure of the gas [Pa]. In eq. 61  $T$  is the temperature [K] and  $R=8.314$  [ $\text{J}\cdot\text{mol}^{-1}\cdot\text{K}^{-1}$ ] is the general gas constant.

$$p = c \cdot R \cdot T \quad (61)$$

There are two driving potentials for non-isothermal gas diffusion with corresponding diffusion coefficients, e.g. concentration and temperature or partial pressure and temperature (eq. 62 a and b).

$$j = -\delta_c^T \cdot \nabla c - \delta_T^c \cdot \nabla T \quad (\text{a}) \quad j = -\delta_p^T \cdot \nabla p - \delta_T^p \cdot \nabla T \quad (\text{b}) \quad (62)$$

The temperature diffusion coefficients in these expressions are generally disregarded (eq. 63) and the gas flow either described by Fick's 1<sup>st</sup>. law with effective diffusion coefficient  $\delta_{\text{eff},c}$  [ $\text{m}^2\cdot\text{s}^{-1}$ ] or  $\delta_{\text{eff},p}=P_{\text{foam}}$  (also called the permeability of the foam) [ $\text{mol}\cdot\text{m}^{-1}\cdot\text{s}^{-1}\cdot\text{Pa}^{-1}$ ]).

$$j = -\delta_{\text{eff},c} \cdot \nabla c \quad (\text{a}) \quad j = -\delta_{\text{eff},p} \cdot \nabla p = -P_{\text{foam}} \cdot \nabla p \quad (\text{b}) \quad (63)$$

The two different flow equations (eq. 63 a and b) correspond to neglecting different temperature dependent terms and are thus not equivalent for non-isothermal foam.

For a piece of foam with a temperature difference  $\Delta T$  [K] across it, diffusion will take place until the concentration in the foam is equal to the surrounding concentration  $c_e$  [ $\text{mol}\cdot\text{m}^{-3}$ ] according to eq. 63 a. According to this assumption, at equilibrium the

---

<sup>3</sup> In the model the gases are not considered created from or transformed into other substances by internal reactions. However, this takes place in real foam by oxidation. The model could be developed by including this aspect.

partial pressure difference across the foam for an ideal gas (eq. 61) will be  $c_e \cdot R \cdot \Delta T$  [Pa]. If eq. 63 b is used instead, diffusion will take place until the partial pressure is equal on both sides of the foam and a concentration difference in the foam is accepted at equilibrium.

Calculations have been performed for the ageing of district heating pipes both using  $c$  and  $p$  as driving potentials. The heat flow from single pipes with a service pipe temperature of 80°C and a casing temperature of 15°C differed by some tenths of a percent over 30 years depending on the potential used. Hereafter,  $c$  will be employed as driving potential, but  $p$  could just as well have been chosen, as recommended by Wang (2003).

#### 4.2 Transport coefficients in polyurethane foam

When modelling gas transport through cellular materials such as polyurethane foams, two methods may be used; the transport can be modelled from the macroscopic point of view by an effective diffusion or continuum model as in this thesis or from the cellular perspective by a membrane permeation model. From the macroscopic point of view the foam is seen as a homogenous material layer.

Gas transport through a homogeneous layer of solid material takes place by means of three main processes: solution at the surface of the material, migration through the material along the concentration gradient and evaporation at the other side of the material (Figure 13). The whole process is termed permeation. The rate of the gas transport is determined by the transport coefficients: the solubility coefficient  $S$  [ $\text{mol} \cdot \text{m}^{-3} \cdot \text{Pa}^{-1}$ ] and the diffusion coefficient  $D_{\text{mtrl}}$  [ $\text{m}^2 \cdot \text{s}^{-1}$ ]. Generally, these coefficients are temperature dependent. They might also be dependent on concentration. At isothermal conditions the permeability coefficient  $P$  [ $\text{mol} \cdot \text{m}^{-1} \cdot \text{s}^{-1} \cdot \text{Pa}^{-1}$ ] can be calculated as the product of the other two coefficients, assuming the solubility is not concentration dependent.

For foam that is porous, i.e. not altogether solid, the coefficients are replaced by effective coefficients.

The transport rate of gases through polyurethane foam differs between different foams and different gases. Depending on recipe and foaming conditions, polyurethane foams differ from each other concerning the solid polyurethane material itself and its placement in the foam. The gases differ in size and ability to interact with the foam matrix.

The temperature also influences the transport. All coefficients are temperature dependant. A high temperature leads to quicker ageing of the foam, i.e. higher diffusion and permeability coefficients. The solubility decreases as the temperature increases. Arrhenius relationships (eq. 64 a, b and c), characterized by pre-exponential factors  $D_0$  [ $\text{m}^2 \cdot \text{s}^{-1}$ ],  $S_0$  [ $\text{mol} \cdot \text{m}^{-3} \cdot \text{Pa}^{-1}$ ] respectively  $P_0$  [ $\text{mol} \cdot \text{m}^{-1} \cdot \text{s}^{-1} \cdot \text{Pa}^{-1}$ ] and activation energies  $E_D$  [ $\text{J} \cdot \text{mol}^{-1}$ ],  $E_S$  [ $\text{J} \cdot \text{mol}^{-1}$ ],  $E_P$  [ $\text{J} \cdot \text{mol}^{-1}$ ] are usually used to describe the temperature dependencies. The constants are determined by fitting to measurement data.

$$D_{\text{eff},c} = D_0 \cdot e^{-\frac{E_D}{R \cdot T}} \quad (\text{a}), \quad S = S_0 \cdot e^{-\frac{E_S}{R \cdot T}} \quad (\text{b}), \quad P_{\text{foam}} = P_0 \cdot e^{-\frac{E_P}{R \cdot T}} \quad (\text{c}) \quad (64)$$

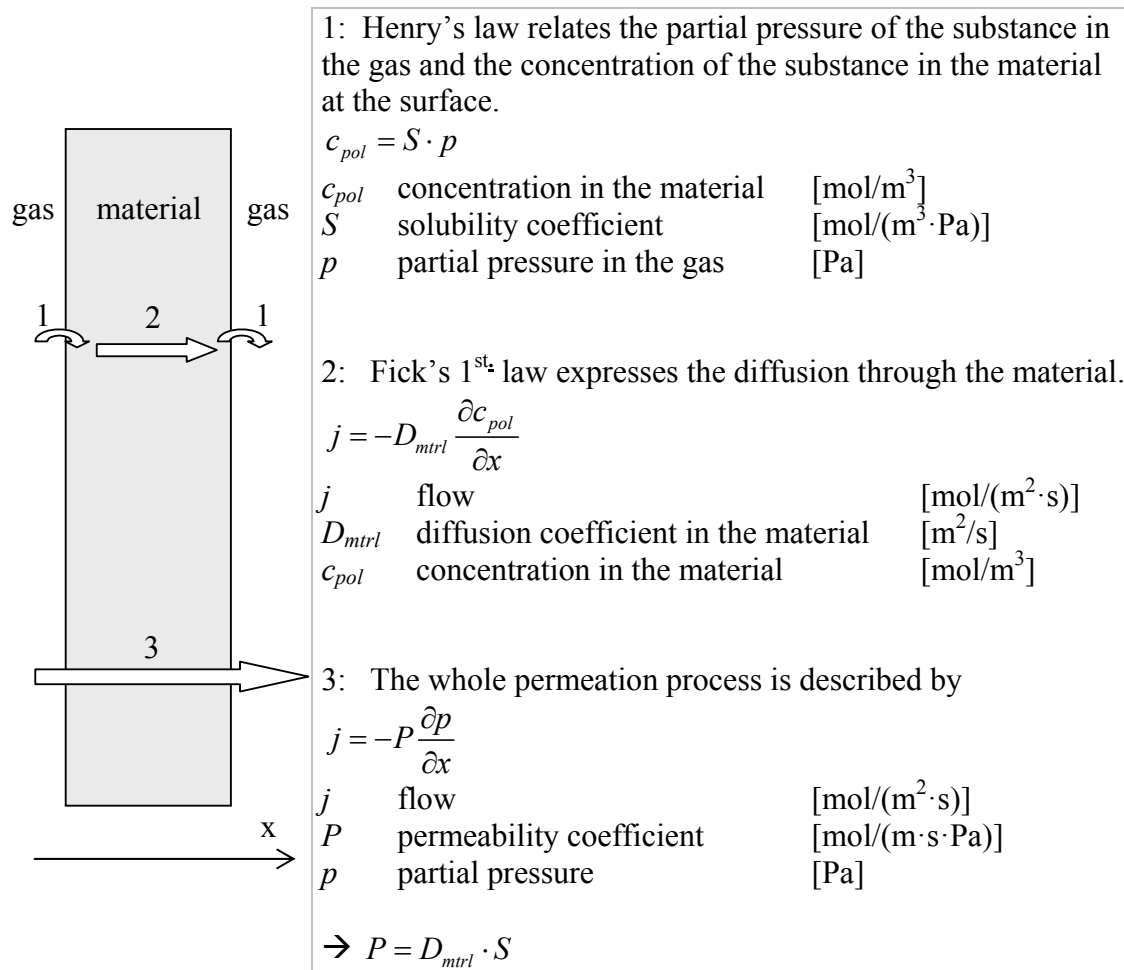


**Figure 13.** Gas transport through a homogeneous layer of isothermal solid material.

Sometimes an accelerated ageing test, i.e. ageing at a higher than usual temperature, is used to try to describe the performance of the foam at a later point in time. This method does not consider that the transport coefficients of the different gases change at different rates as the temperature is increased [Singh et al. 2003]. As a rule of thumb, the diffusion rates of the gases roughly double for a temperature increase of around 20°C.

When a gas is absorbed in the polymer matrix, it may interact with the matrix in a way that changes the transport properties [Comyn 1985]. The coefficients can therefore depend on the concentration or partial pressure of the gas. Such an influence is most likely to be seen at high concentrations [Hilyard and Cunningham 1994] and for large dissolved molecules [Krevelen 1990, Duda and Zielinski 1996]. For the cell gas mixture this would thus be most relevant for the physical blowing agents. Some studies have found a concentration dependence of coefficients for these [e.g. Brodt 1995, Mangs 2005].

#### 4.2.1 Diffusion coefficient ( $D_{eff,c}$ or $\delta_{eff,c}$ )

Of the cell gas components carbon dioxide diffuses fastest, followed by oxygen and nitrogen, while cyclopentane (or some other physical blowing agent used) is the slowest diffusing component. Table 5 presents diffusion coefficients determined by the research group at Chalmers.

**Table 5.** Effective diffusion coefficients  $D_{\text{eff,c}}$  of gases in polyurethane foam determined at Chalmers [ $10^{-13} \text{ m}^2 \cdot \text{s}^{-1}$ ].

Gas	Temperature [°C]			
	Room temperature	40	60	90
Cyclopentane	$0.6^1, 1-5^3, 30^4, 20-300^5$	$4^1$	$7^1$	$10^2$
Carbon dioxide	$500^1, 820-2400^3, 2000^4, 900-1200^5$		$1300^1$	$14000^2$
Oxygen	$150^1, 120-840^3, 600^4, 250-600^5$		$650^1$	$4500^2$
Nitrogen	$25^1, 20-120^3, 80^4, 50-380^5$		$220^1$	$2000^2$

<sup>1</sup>Olsson et al. (2002) Diffusion of cyclopentane in polyurethane foam at different temperatures and implications for district heating pipes, *Journal of Cellular Plastics*, 38, 177-188. Foams of densities 58-71  $\text{kg} \cdot \text{m}^{-3}$  studied.

<sup>2</sup>Mangs S. (2005) Insulation materials in District Heating Pipes – Environmental and Thermal Performance of Polyethylene Terephthalate and Polyurethane Foam, *Doctoral Thesis*, Department of Chemical and Biological Engineering, Chalmers University of Technology, Göteborg, Sweden. Foam density 58  $\text{kg} \cdot \text{m}^{-3}$ .

<sup>3</sup>Svanström M. et al. (1997) Determination of effective diffusion coefficients in rigid polyurethane foam. *Cellular Polymers*. 16:182-193. Foam density 43-49  $\text{kg} \cdot \text{m}^{-3}$ .

<sup>4</sup>Persson et al. 2006 Insulating performance of flexible district heating pipes, *Proceedings of the 10<sup>th</sup> International Symposium on District Heating and Cooling*, Hannover, Germany. Measured on semi-flexible polyurethane foam.

<sup>5</sup>Reidhav C. et al. 2008 Insulating properties of semi-flexible polyurethane foams, *Proceedings of the 11<sup>th</sup> International symposium on District Heating and Cooling*, Reykjavik, Iceland. Foam density 62-70  $\text{kg} \cdot \text{m}^{-3}$ . The diffusion effective coefficient of cyclopentane in all of the studied foams but one was  $20-35 \cdot 10^{-13} \text{ m}^2 \cdot \text{s}^{-1}$ .

For comparison, the following additional values for the diffusion coefficient [ $10^{-13} \text{ m}^2 \cdot \text{s}^{-1}$ ] at room temperature have been reported in the literature; for cyclopentane: 0.5 [Thijs 1994], 8.3 [Bazzo et al. 1994], 6.2 [Capella et al. 1996], for carbon dioxide: 9.8 [Bazzo et al. 1994], 150 [Fan and Kokko 1991], 700-3850 [Nazelle 1995] and for oxygen and nitrogen: 56-1300 respectively 7.8-180 according to various references mentioned in [Svanström et al. 1997].

Diffusion coefficients in semi-flexible foams used in flexible district heating pipes have been found to be higher than in ordinary rigid foam, especially the diffusion coefficient for cyclopentane [Persson et al. 2006, Reidhav et al. 2008, see also Table 5]. Foams made from various polyols have been proven to have different transport coefficients [Kaplan and Tabor 1994]. The flexibility of semi-flexible foams is obtained by mixing short and long polyols. The long polyols increase flexibility whereas the short polyols enhance the diffusion resistance [Kellner and Zarka 2000].

Determining diffusion coefficients is quite time consuming. The effective diffusion coefficients of the gases in the foam are generally established by fitting analytical diffusion equation solutions to measured mean cell gas compositions over time [Svanström 1997, Hilyard and Cunningham 1994]. In order to obtain a good fit sufficient time must have passed to allow changes in content to take place in the foam. Foam samples with simple geometry for which the diffusion equation solution is known are used, such as boards or cylinders with the diffusion in the direction of the

cylinder axis hindered. The diffusion coefficients are determined at isothermal conditions.

Cylindrical samples have mainly been used at Chalmers. To determine the diffusion coefficients a number of sample cylinders were aged at a constant temperature with sealed ends to hinder longitudinal diffusion. The seal consisted of aluminium plates glued to the ends with epoxy or a layer of a beeswax and paraffin mixture. After different storage times the cell gas content of the cylinders was analysed using the special equipment depicted in Figure 14.

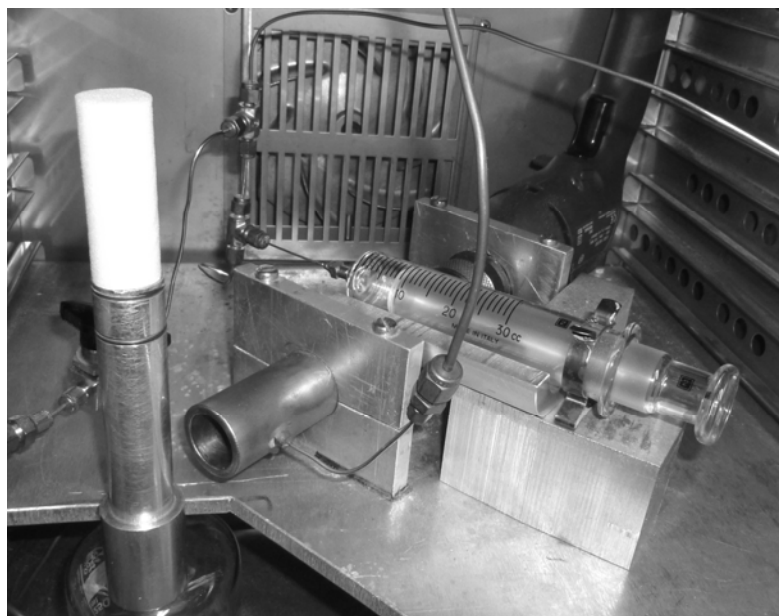


**Figure 14.** Sampling equipment for determination of the cell gas content of polyurethane foam.

The samples were ground in a controlled environment<sup>4</sup> and the released cell gas was collected in a syringe with a readout of the collected volume, after which it was analysed by gas chromatography for percental composition. The total cell gas pressure of the sample was calculated from the volume of the closed cells and the volume of the released cell gas.

The effective diffusion coefficients were then determined by fitting the analytical solution to the radial diffusion equation stated in eq. 65 to the partial pressures obtained from the measurements, which correspond to the mean pressures in the cylinders. The analytical solution to eq. 65 for the mean partial pressures is stated in

---

<sup>4</sup> Dinitrogen oxide is used to flush the sampling equipment before grinding. During flushing, the sample is under a dinitrogen oxide pressure of roughly 150-200 kPa. It has been found that dinitrogen oxide can penetrate some polyurethane foams, in particular new semi-flexible ones. However, it does not penetrate or only to a minor extent penetrate old rigid foams. The penetrated dinitrogen oxide is released after foam grinding, resulting in a volume of collected gas that is too high, corresponding to determination of an unduly high cell gas pressure. Today, foam cylinders are ground both without and after dinitrogen oxide flushing. The difference between the collected volumes is used for correction so that the true partial pressures can be calculated.

eq. 66, where  $p_0$  is the initial partial pressure,  $\beta_{0j} \cdot a$  is the root of the zero order Bessel function and  $a$  is the radius of the cylinder. The diffusion coefficients  $D_{\text{eff}}$  [ $\text{m}^2/\text{s}$ ] were chosen as they gave the best fit between the analytical solution for the mean partial pressures and the measured values.

$$\frac{1}{D_{\text{eff},c}} \frac{\partial p}{\partial t} = \frac{\partial^2 p}{\partial r^2} + \frac{1}{r} \cdot \frac{\partial p}{\partial r} \quad (65)$$

$$\bar{p} = p_0 \cdot \sum_{j=1}^{\infty} \frac{4 \cdot e^{-\beta_{0j}^2 \cdot D_{\text{eff},c} \cdot t}}{(\beta_{0j} \cdot a)^2} \quad (66)$$

Eq. 65 only takes into account the amount of the substance in the gas phase. For an ideal gas at a constant temperature it is equally valid to exchange the partial pressure  $p$  [Pa] in the equation with the concentration  $c$  [ $\text{mol}/\text{m}^3$ ] as in eq. 67. In order to also take into account the dissolved and condensed amounts of the substance, the total concentration  $c_{\text{tot}}$  should be used on the left hand side as in eq. 68. This equation assumes that the substance may be present in the foam in all three phases, but that it is the gas phase that contributes to the transport.

$$\frac{1}{D_{\text{eff},c}} \frac{\partial c}{\partial t} = \frac{\partial^2 c}{\partial r^2} + \frac{1}{r} \cdot \frac{\partial c}{\partial r} \quad (67)$$

$$\frac{1}{\delta_{\text{eff},c}} \frac{\partial c_{\text{tot}}}{\partial t} = \frac{\partial^2 c}{\partial r^2} + \frac{1}{r} \cdot \frac{\partial c}{\partial r}, \quad c_{\text{tot}} = [f_g + S \cdot R \cdot T \cdot (1 - f_g)] \cdot c + c_{\text{liq}} \quad (68)$$

With  $D_{\text{eff},c}$  determined for a foam without condensed cyclopentane according to the first equation (eq. 67), the effective diffusion coefficient  $\delta_{\text{eff},c}$  in the second equation (eq. 68) is given by eq. 69. The difference between the diffusion coefficients for cyclopentane is a factor of about two at room temperature and of around 1.6 at 50°C.

$$\delta_{\text{eff},c} = [f_g + S \cdot R \cdot T \cdot (1 - f_g)] \cdot D_{\text{eff},c} \quad (69)$$

A deviation from the ideal diffusion model for blowing agents was identified during determination of the diffusion coefficients by Mangs (2005). Mangs studied foam sample cylinders up to 16000 h. The diffusion for these gases seemed to become slower over time, which could indicate a concentration dependence of the diffusion coefficients. The diffusion coefficients reported by Chalmers in Table 5 were determined for the first 100-3500 hours depending on the gas studied.

#### 4.2.2 Permeability coefficient ( $\delta_{\text{eff},p} = P_{\text{foam}}$ )

The permeability coefficient for an ideal gas through a foam at isothermal conditions is given by eq. 70. Here, the general gas law eq. 61 is used.

$$\delta_{\text{eff},c} = R \cdot T \cdot \delta_{\text{eff},p} \quad (70)$$

#### 4.2.3 Solubility coefficient (*S*)

The relationship between the concentration in the matrix and the partial pressure in the surrounding gas can be described by Henry's law (eq. 71). Henry's law assumes immediate equilibrium between the dissolved concentration and the surrounding gas pressure and is valid for weakly soluble gases that have no interaction with the matrix [Comyn 1985]. For example, this means that there should be no swelling that causes solubility concentration dependence at a given temperature.

$$c_{pol} = S \cdot p \text{ [mol}\cdot\text{m}^{-3} \text{ polymer]} \quad (71)$$

The solubility of the blowing agent in the foam is of primary interest, as it is present to the largest extent in the matrix. The solubility of cyclopentane is large in comparison to that of nitrogen and oxygen, while the solubility of carbon dioxide is between that of cyclopentane and nitrogen and oxygen. It is not unusual to find around 50 % of the total cyclopentane content in the matrix at room temperature [paper IV, Brodt 1995]. About 10-20 % of the carbon dioxide is dissolved, while only a few % of the nitrogen and oxygen is present in the matrix [Alsoy 1999, Brodt 1995]. The solubility decreases as the temperature increases. At 60°C the fraction of cyclopentane in the matrix decreases to about 35 % [paper IV].

The amount of cyclopentane dissolved in the polyurethane matrix can be determined by heating pulverised foam, e.g. from the cell gas analysis samples, in a closed vessel. Upon heating, the cyclopentane leaves the solid material and the dissolved concentration can be determined by analysis of the gas in the vessel. This method was used in paper IV where the cyclopentane distribution in four foams with a different total amount of cyclopentane was studied at five temperatures. The amount in the gas and the liquid phase was determined by foam pulverization, collection and analysis of the released cell gas, as described earlier in the diffusion coefficient subchapter. Any remaining condensed cyclopentane vaporises at pulverisation and is collected with the rest of the gas.

The solubility coefficient of cyclopentane in the polyurethane matrix at different temperatures was determined by fitting straight lines according to Henry's law to the concentration in the matrix plotted against the partial pressure of the cell gas. The resulting solubility coefficients are listed in Table 6 together with data from the literature. The least square fit Arrhenius parameters (eq. 64) to the determined solubility coefficients in paper IV are  $S_0=1.3\cdot 10^{-5} \text{ mol}\cdot\text{m}^{-3}\cdot\text{Pa}^{-1}$  and  $\Delta E_s=-16\cdot 10^3 \text{ J}\cdot\text{mol}^{-1}$ .

The use of Henry's law for blowing agent solubility in polyurethane foams has been questioned, as strictly speaking the equilibrium is not instant and some studies have revealed a pressure dependence of the solubility. In paper IV, the cyclopentane solubility coefficient in the polyurethane matrix was independent of the partial pressure of cyclopentane in the cell gas (20-66 kPa) (Figure 15). Brodt (1995) found that the solubility coefficient of carbon dioxide and chlorodifluoromethane (HCFC-22) in polyurethane decreased with partial pressure and that the partial pressure dependence was reduced at higher temperatures.

**Table 6.** Solubility coefficients in polyurethane [ $\text{mmol}\cdot\text{m}^{-3}\cdot\text{Pa}^{-1}$ ].

Gas	Room temperature	30	40	50	60	70
Cyclopentane	8.8 <sup>IV</sup> 12.3 <sup>2</sup> 18.5 <sup>3</sup> 23.6 <sup>3</sup> 11.4 <sup>4</sup> 13 <sup>5</sup>	7.7 <sup>IV</sup>	6.6 <sup>IV</sup>	5.3 <sup>IV</sup>	4.2 <sup>IV</sup> 8.4 <sup>2</sup>	5.2 <sup>4</sup>
Carbon dioxide	0.89-1.3 <sup>1</sup> 1.7- 2.2 <sup>4</sup> 0.91 <sup>8</sup> 1.6 <sup>9</sup> 1.7 <sup>9</sup>					0.35- 0.70 <sup>4</sup>
Oxygen	0.066 <sup>1</sup> 0.14- 0.30 <sup>4</sup>					0.10- 0.18 <sup>4</sup>
Nitrogen	0.043 <sup>1</sup> 0.13- 0.22 <sup>4</sup>					0.075- 0.14 <sup>4</sup>

<sup>1</sup>du Cauzé de Nazelle (1995) Thermal conductivity ageing of rigid closed cell polyurethane foams. Doctoral thesis. Technical University of Delft, the Hague, the Netherlands

<sup>2</sup>Mangs S (2002) HFC-365mfc and cyclopentane as blowing agents in polyurethane insulation of district heating pipes. Licentiate thesis. Chalmers University of technology, Göteborg, Sweden

<sup>3</sup>Hong SU. et al. (2001) Transport of blowing agents in polyurethane, Journal of Applied Polymer Science, 70, 2069-2073

<sup>4</sup>Brodth K. H. (1995) Thermal insulations: cfc-alternatives and vacuum insulation, Thesis, Technical University, Delft, the Netherlands

<sup>5</sup>Reidhav C. et al. (2008) Insulating properties of semi-flexible polyurethane foams, Proceedings of the 11<sup>th</sup> International Symposium on District Heating and Cooling, Reykjavik, August 31-September 2.

<sup>7</sup>Hong S.-UK and Duda J. L. (1998) Diffusion of CFC 11 and Hydrofluorocarbons in Polyurethane, Journal of Applied Polymer Science, 70, 2069-2073

<sup>8</sup>Lund, A.E.A. et al. (1990) A performance evaluation of environmentally acceptable foam blowing agents, Journal of Cellular Plastics, 26, 143-160

<sup>9</sup>Du Cauze de Nazelle et al. (1989) A fundamental characterisation of the ageing of polyurethane rigid foam, International workshop on long-term thermal performance of cellular plastics, Sept 28-29.

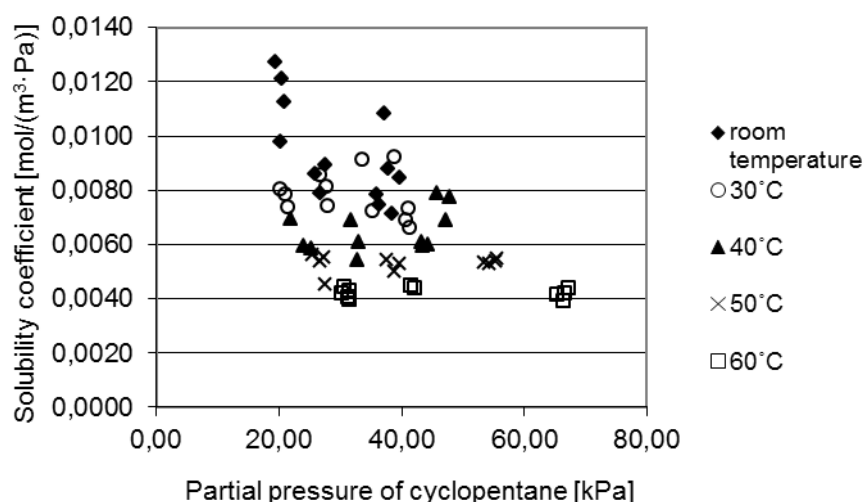


**Figure 15.** Solubility coefficient of cyclopentane in the polyurethane matrix compared to the partial pressure of cyclopentane in the cell gas at different temperatures.

### 4.3 Permeability coefficients for the polyethylene casing

In 2003 requirements on stress crack resistance of the casing material were added to the European standard EN253. As a consequence, the second generation uni-modal high density polyethylene material that had been used for the casing had to be replaced by a third generation bi-modal high density polyethylene material [Ting Larsen C et al. 2009]. This meant that from 2003 a material with two peaks instead of one in the molecular weight distribution was used. The bi-modal material is more stress crack resistant, but has higher permeability to gases (Table 7). At 15°C the permeability of oxygen is increased by 72%, nitrogen by 59% and carbon dioxide by 23%. In the publications for this thesis pipes with uni-modal polyethylene were studied.

**Table 7.** Temperature dependence of the permeability of polyethylene materials used for casings.

Gas	Permeability		Permeability	
	Old uni-modal (HE2467-BL) [Olsson M. E. et al. 2002, cyclopentane at 70°C Brodt K.H. 1995]		New bi-modal PE80 (Borstar HE3470) [Ting Larsen C. et al. 2009]	
	[mol·m <sup>-3</sup> ·s <sup>-1</sup> ·Pa <sup>-1</sup> ]	@ 15°C	[mol·m <sup>-3</sup> ·s <sup>-1</sup> ·Pa <sup>-1</sup> ]	@ 15°C
Cp	1.31·10 <sup>-13</sup> · exp(-1196/T)	2.1·10 <sup>-15</sup>		
CO <sub>2</sub>	5.58·10 <sup>-11</sup> · exp(-3248/T)	7.1·10 <sup>-16</sup>	2.85·10 <sup>-7</sup> /T· exp(-4017/T)	8.7·10 <sup>-16</sup>
O <sub>2</sub>	2.97·10 <sup>-10</sup> · exp(-4186/T)	1.5·10 <sup>-16</sup>	3.55·10 <sup>-7</sup> /T· exp(-4439/T)	2.5·10 <sup>-16</sup>
N <sub>2</sub>	5.44·10 <sup>-10</sup> · exp(-4715/T)	4.2·10 <sup>-17</sup>	1.28·10 <sup>-6</sup> /T· exp(-5185/T)	6.7·10 <sup>-17</sup>

### 4.4 Ageing of single pipes

The steel fluid pipe is gas tight, but the polyethylene casing is permeable. Thus, the gas diffusion in a single pipe takes place in the radial direction through the foam and casing. Depending on the concentration gradient the transport is directed either out, as is the case for cyclopentane and carbon dioxide, or in as for oxygen and nitrogen. If the pipe has a copper fluid pipe it is also diffusion tight, but for a plastic fluid pipe, a flow over a transport resistance has to be accounted for at the inner insulation boundary.

#### 4.4.1 Diffusion in radial coordinates

The diffusion equation in the radial coordinate is given in eq. 72. The total molar mass concentration in the foam  $c_{tot}$  is obtained by the sum of the gas ( $c$  [mol·m<sup>-3</sup> gas]), as well as dissolved ( $c_{pol}$  [mol·m<sup>-3</sup> polymer]) and liquid ( $c_{liq}$  [mol·m<sup>-3</sup> foam]) amounts (eq. 73). The ideal gas law and Henry's law may be used to rewrite the concentration in the matrix into an expression of the gas phase concentration. At the inner boundary of the insulation  $r_f$  [m] the steel fluid pipe is impermeable to gases (eq. 74). At the outer boundary there is a diffusive flux through the casing (eqs. 75-76). The polyethylene casing between the outer radius of the insulation  $r_{ins}$  [m] and the outer radius of the casing  $r_c$  [m] with temperature  $T_c$  [K] acts as a resistance to gas transport between the foam and the exterior of the pipe<sup>5</sup>. The permeability of the

casing material is  $P_{PE}$  [ $\text{mol}\cdot\text{m}^{-3}\cdot\text{s}^{-1}\cdot\text{Pa}^{-1}$ ] and the concentration outside the pipe  $c_e$  [ $\text{mol}\cdot\text{m}^{-3}$ ].

$$\frac{\partial c_{tot}}{\partial t} = -\frac{1}{r} \cdot \frac{\partial}{\partial r}(r \cdot j) \quad (72)$$

$$\begin{aligned} c_{tot} &= c \cdot f_g + c_{pol}(1 - f_g) + c_{liq} \\ &= c \cdot f_g + S \cdot p \cdot (1 - f_g) + c_{liq} = [f_g + S \cdot R \cdot T \cdot (1 - f_g)] \cdot c + c_{liq} \end{aligned} \quad (73)$$

$$j|_{r=r_f} = 0 \quad (74)$$

$$2 \cdot \pi \cdot r_{ins} \cdot j|_{r=r_{ins}} = \frac{c(r_{ins}, t) - c_e}{R_{casing}} \quad (75)$$

$$R_{casing} = \frac{1}{2 \cdot \pi \cdot P_{PE} \cdot R \cdot T_c} \cdot \ln\left(\frac{r_c}{r_{ins}}\right) \quad (76)$$

The solution to the problem presented in eqs. 72-76 may be determined numerically with the aid of the explicit finite difference method. Note the similarity between the heat and diffusion problems. The mass balance in eq. 72 is given by eq. 77 in discrete form.

The net molar mass inflow into cell n during a time step, between  $t^{nr+1}$  [s] and  $t^{nr}$  [s] of length  $\Delta t$  [s] ( $t^{nr+1} = t^{nr} + \Delta t$ ) increases the concentration in the cell. The concentration changes from  $c_{tot,n}^{nr}$  [ $\text{mol}\cdot\text{m}^{-3}$ ] to  $c_{tot,n}^{nr+1}$  [ $\text{mol}\cdot\text{m}^{-3}$ ]. The calculation is based on the flows  $J_{n-1 \rightarrow n}^{nr}$  [ $\text{mol}\cdot\text{m}^{-1}\cdot\text{s}^{-1}$ ] and  $J_{n \rightarrow n+1}^{nr}$  [ $\text{mol}\cdot\text{m}^{-1}\cdot\text{s}^{-1}$ ] at time  $t^{nr}$ .  $J_{n \rightarrow n+1}$  [ $\text{mol}\cdot\text{m}^{-1}\cdot\text{s}^{-1}$ ] is the molar mass flow from cell n to cell n+1. It is given by the conductance with regard to diffusion between cell n and cell n+1  $KD_{n \rightarrow n+1}$  [ $\text{m}^2\cdot\text{s}^{-1}$ ] times the concentration difference (eq. 78). For cells in the inner part of the insulation the conductance is given by half of cell n's resistance and half of cell n+1's resistance (eq. 79)<sup>5</sup>. The conductance at the inner boundary is zero as no diffusion takes place through the steel fluid pipe (eq. 80). The conductance at the outer boundary is the sum of half of the last cell N's resistance and the resistance of the casing (eq. 81). The pipe's total

<sup>5</sup> In radial coordinates the diffusion resistance of a material with diffusion coefficient  $\delta$  [ $\text{m}^2\cdot\text{s}^{-1}$ ] between inner radius  $r_i$  [m] and outer radius  $r_e$  [m] is given by:

$$R_D = \frac{1}{2 \cdot \pi \cdot \delta} \cdot \ln\left(\frac{r_e}{r_i}\right)$$

The diffusion coefficient  $\delta$  may be approximated with the permeability coefficient  $P$  [ $\text{mol}\cdot\text{m}^{-3}\cdot\text{s}^{-1}\cdot\text{Pa}^{-1}$ ] multiplied by the gas constant and the temperature at isothermal conditions;  $\delta \approx P \cdot R \cdot T$ . The resistance thus depends on the place and extent of the material as well as its permeability and temperature.

transport resistance is the sum of all annular cell resistances. By adding part resistances an effective (or equivalent) transport resistance of the foam cross section may be determined. The flows through each cell are assumed to be stationary during the time step.

$$2 \cdot \pi \cdot r_n \cdot \Delta r \cdot (c_{tot,n}^{nr+1} - c_{tot,n}^{nr}) = (J_{n-1 \rightarrow n}^{nr} - J_{n \rightarrow n+1}^{nr}) \cdot \Delta t \quad (77)$$

$$J_{n \rightarrow n+1}^{nr} = KD_{n \rightarrow n+1} \cdot (c_n^{nr} - c_{n+1}^{nr}) \quad (78)$$

$$KD_{n \rightarrow n+1} = \frac{1}{\frac{1}{2 \cdot \pi \cdot \delta_n} \cdot \ln\left(\frac{r_n + 0.5 \cdot \Delta r}{r_n}\right) + \frac{1}{2 \cdot \pi \cdot \delta_{n+1}} \cdot \ln\left(\frac{r_{n+1}}{r_n + 0.5 \cdot \Delta r}\right)}, \quad n = 1, 2, \dots, N-1 \quad (79)$$

$$KD_{f \rightarrow 1} = 0 \quad (80)$$

$$KD_{N \rightarrow c} = \frac{1}{\frac{1}{2 \cdot \pi \cdot \delta_N} \cdot \ln\left(\frac{r_{ins}}{r_N}\right) + \frac{1}{2 \cdot \pi \cdot P_{PE} \cdot R \cdot T_c} \cdot \ln\left(\frac{r_c}{r_{ins}}\right)} \quad (81)$$

The temperature dependence of the effective diffusion coefficient is accounted for (eq. 82).

$$\delta_n = \delta_{eff,c}(T_n), \quad n = 1, 2, \dots, N \quad (82)$$

At every time step the change in molar mass concentration in each cell  $n$  is calculated. The total concentration in a cell at a new time  $t^{nr+1} = t^{nr} + \Delta t = t_0 + (nr+1) \cdot \Delta t$  is given by eq. 83.

$$c_{tot,n}^{nr+1} = c_{tot,n}^{nr} + \Delta t \cdot \frac{(J_{n-1 \rightarrow n}^{nr} - J_{n \rightarrow n+1}^{nr})}{2 \cdot \pi \cdot r_n \cdot \Delta r} \quad (83)$$

As a first step towards taking account of the total amount of cell gases, the three phases of the physical blowing agent are considered in papers III and IV. The total cyclopentane content is thus divided between phases valid for the new time step  $(nr+1)$ . If the total concentration at the new time step determined by eq. 83 divided by  $f_g + S_n \cdot R \cdot T_n \cdot (1 - f_g)$  (from eq. 73) is less than the concentration corresponding to the saturation vapour pressure, no condensed cyclopentane exists at  $n$ . Otherwise the gas phase concentration corresponds to the saturation vapour pressure and the over-concentration is condensed.

The total amount of the other cell gas constituents is assumed in gas phase; the gas phase concentration increases with the change in total concentration divided by the porosity  $f_g$ .

In order for the solution to the diffusion equation to be stable, the time step should not be larger than that stated in eq. 84. The time step should be the shortest obtained for

the different diffusing gases. The stable time step is shortest for the gas that diffuses the fastest; carbon dioxide in the case of a cyclopentane blown pipe.

$$\Delta t \leq \min_{1 \leq n \leq N} \frac{2 \cdot \pi \cdot r_n \cdot \Delta r \cdot [S \cdot R \cdot T \cdot (1 - f_g) + f_g]}{KD_{n-1 \rightarrow n} + KD_{n \rightarrow n+1}} \quad (84)$$

#### 4.4.2 Complete radial model with coupled heat and mass transfer

Strictly speaking, the heat and mass transfer through the pipe is a coupled phenomenon. In the heat balance the thermal conductivity of the foam depends on the temperature and cell gas composition, while in the mass balance the diffusion rates and states of the gases depend on the temperature. The temperature in the cell thus influences the equilibrium between the different phases of cyclopentane, at the same time as the concentration in the gas phase influences the temperature.

Using explicit finite differences for both heat conduction and diffusion, the shortest time step should be chosen, in this case the time step for heat conduction. However, this makes calculations time consuming, as much iteration has to be performed. The time scales of the heat and mass transfer processes differ greatly. Heat conduction is a much faster process. At 40°C the decline time for diffusion, which is a characteristic time scale for equalisation, is thousands to one hundred thousand times that of heat conduction depending on the gas in question [Claesson 2001]. For the DN100/225 pipe studied in papers III and BIII/IV, the time step limit for calculating the heat conduction with explicit finite differences and the insulation divided into ten 5.2 mm cells is about 20 seconds, for diffusion the corresponding time step limit is about 10<sup>7</sup> s for cyclopentane, 10<sup>4</sup> s for carbon dioxide and oxygen and 10<sup>5</sup> s for nitrogen. The time step for explicit finite difference calculations of the heat conduction is thus very much shorter than that needed for the calculation of the diffusion and makes the calculations slow.

A way to make the calculation less demanding, while still taking the coupling into account, is to use a quasi-stationary solution that instead of a temperature profile calculated with explicit finite differences employs a steady state temperature profile that is updated at regular intervals. The diffusion is determined by explicit finite differences (according to eq. 83) over time for the fixed temperature profile and the amounts in the different phases are determined based on the temperature profile. The equilibrium temperature is determined at pre-defined times. The equilibrium calculation can be done with the aid of a loop function in which calculation of the gas phase concentration, thermal conductivity and temperature is repeated until there is negligible difference between the results of the iterations.

The fact that the temperature is less frequently updated in the quasi-stationary solution dramatically speeds up the calculations and has little impact on the results. Over time the temperature change in the pipe due to the coupling is small, a change of less than 1.5°C was predicted over 30 years for the DN100 Series 2 pipe in paper III. Different update times were tested and it was found that it is sufficient to update the temperature annually. Using the same temperature profile during the whole ageing time, i.e. totally neglecting the temperature feedback, gave an error of less than 1% for the predicted mean flows from the forward and return pipes when installed in the ground.

#### 4.4.3 Example of an ageing single pipe

Figure 16 presents a typical ageing curve for the insulation of a district heating pipe without a diffusion barrier over the pipe's 30 year nominal life span. The figure shows the predicted contributions of the different heat transfer mechanisms over time and how the thermal conductivity is altered due to the change in cell gas composition. The thermal conductivity decreases slightly during the first few years before it starts to increase. The change in the average gas concentrations in the pipe are illustrated in Figure 17. Carbon dioxide quickly leaves the foam and initially its escape leads to a higher share of cyclopentane in the cell gas, lowering the thermal conductivity. Finally the in-diffusion of air together with the slow out-diffusion of the cyclopentane increases the thermal conductivity of the cell gas.

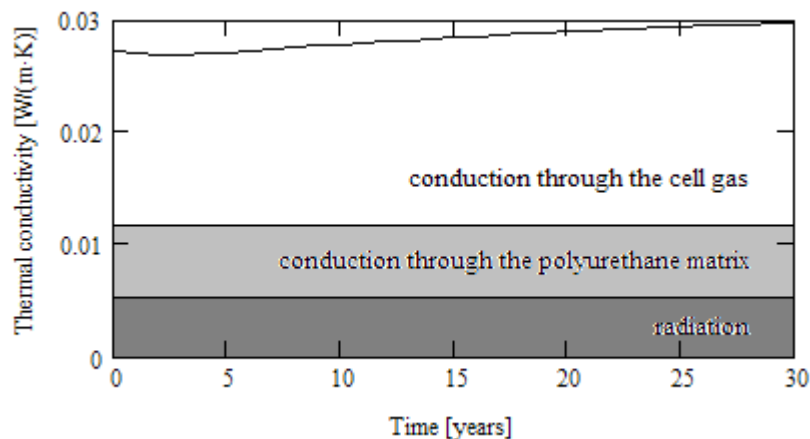


**Figure 16.** Equivalent thermal conductivity over time of the insulation of a DN100/225 pipe without a diffusion barrier aged at 80-15°C [paper III].

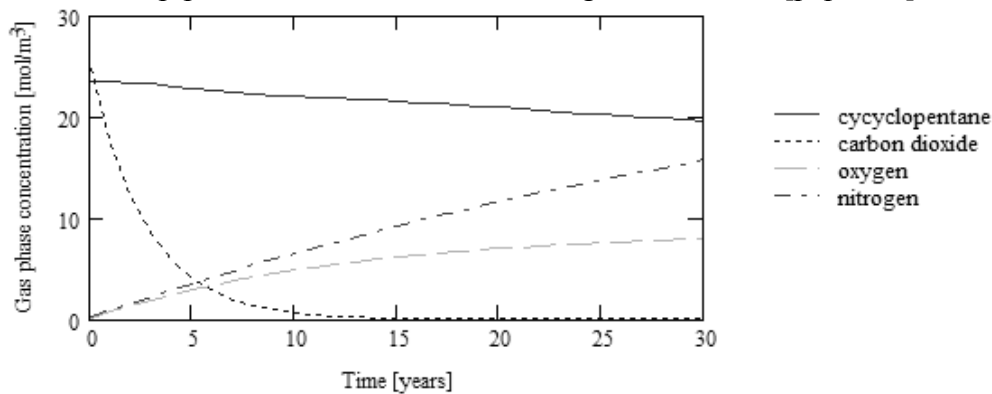


**Figure 17.** Change in average gas concentrations over time in the insulation of a DN100/225 pipe without a diffusion barrier aged at 80-15°C [paper III].

Figure 18 presents the gas concentration profiles over the foam cross section for carbon dioxide, oxygen and nitrogen at different stages of ageing. The slopes of the concentration profiles indicate the direction of gas transfer; out through the casing on the right for carbon dioxide and into the foam through the casing for oxygen and nitrogen. Figure 19 shows the distribution of cyclopentane in the foam. The cyclopentane is divided between different phases. Less cyclopentane is dissolved in the matrix where the foam close to the fluid pipe is hot (to the left in the figure) than in the middle where the foam is merely warm. The saturation vapour pressure for

cyclopentane is lower close to the cold casing, giving a smaller dissolved amount in the matrix. At the same time condensed cyclopentane is present.

Studies of the gas phase concentration profiles through the foam over time reveal that for the studied DN100/225 pipe, which has about 5 cm thick insulation aged at 80-15°C, it takes a couple of years for the carbon dioxide concentration next to the fluid pipe to decrease by 90% from its initial value. It takes some ten years for 90% of the oxygen transport to take place into the foam next to the fluid pipe and about 100 years for 90% of the change in the corresponding nitrogen concentration. The change is even slower for cyclopentane. The specific times vary for different pipes; the carbon dioxide transport may take some ten years for a large pipe with a prolonged diffusion time, which is also the case for the other gases. As a general rule, short and intermediate term ageing is due to out-diffusion of carbon dioxide and in-diffusion of air constituents, while the long term ageing is due to depletion of the physical blowing agent. If the foam has a large fraction of open cells the ageing is more rapid.

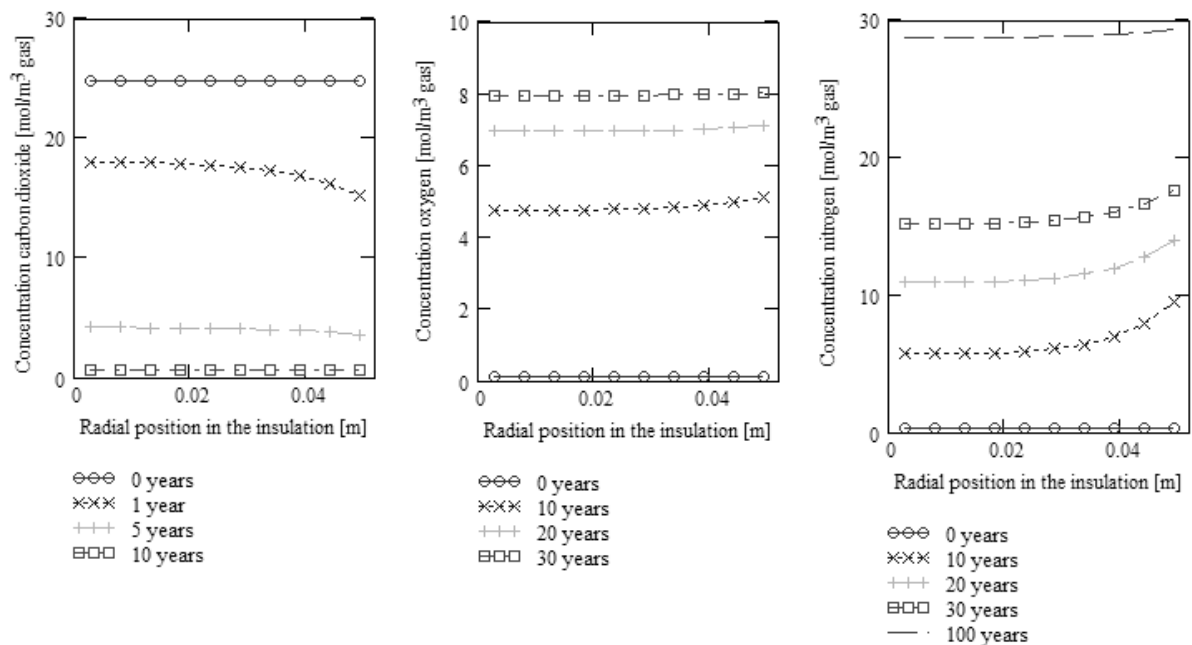


**Figure 18.** Cell gas concentration profiles in the foam of an ageing DN100/225 pipe [paper III].

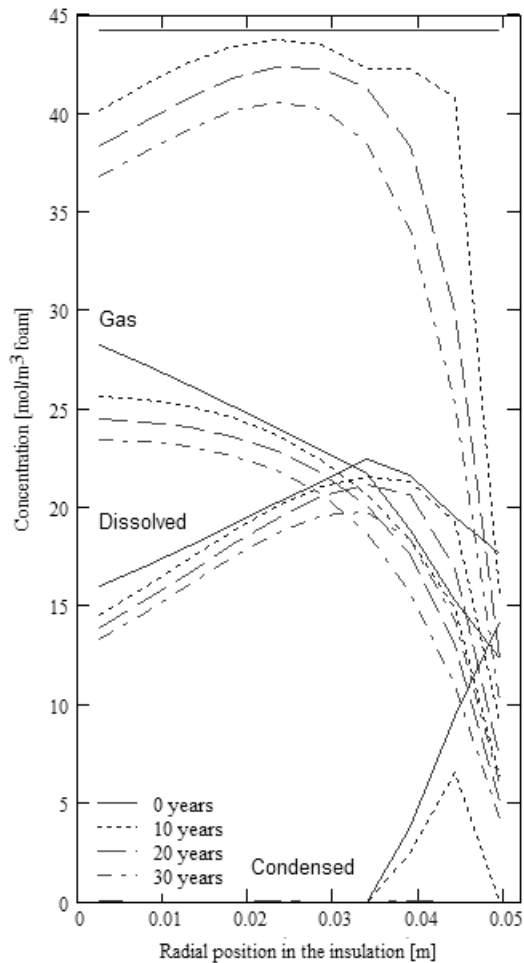


**Figure 19.** Distribution of cyclopentane in the foam of an ageing DN100/225 pipe [paper III].

#### 4.5 Ageing of twin pipes

Modelling the ageing of district heating twin pipes is more complicated than single pipes due to the greater complexity of the geometry. In paper I a simplified method to determine the ageing of district heating pipes was used both for the single and twin pipes to obtain a rough estimation of the change in heat loss. The model ascribes all gas transport resistance to the polyethylene casing, hence does not consider spatial variation of the cell gas composition in the foam. In paper V a more realistic method was used. The coordinate transformation described in chapter 3.3.1 was applied to solve the diffusion problem with the aid of explicit finite differences. As the heat and diffusion equations have the same structure, the transformation may equally well be applied to solve the diffusion problems.

##### 4.5.1 Model ascribing all transport resistance to the casing.

A simplified model of ageing that ascribes all transport resistance to the casing is described in Figure 20. This is the model used in the Swedish district heating association's Ekodim calculation program. The permeability coefficients applied in paper I were determined for a DN80/180 pipe at room temperature for cyclopentane and for two DN150/280 pipes in common use for carbon dioxide, nitrogen and oxygen. For gases that do not accommodate the total transport resistance in the casing, the effective permeability coefficient is dependent on the pipe's geometry and dimension, as well as temperature dependent. For the model to be accurate it is thus

important that the correct pipe dimension data are used, which makes this model less suitable.

foam

$p_{\text{outside casing}} = p_1 \sim p_{\text{air}}$

$J = -P \frac{(p_1 - p(t))}{L_b}$

Mass balance:

$$\left\{ \begin{array}{l} -\frac{V}{R \cdot T} \frac{dp}{dt} = -A \cdot P \frac{p_1 - p(t)}{L_b} \\ \text{decrease in foam} = \text{flow out through the casing [mol/s]} \\ p(0) = p_0 \end{array} \right.$$

$$\rightarrow p(t) = (p_0 - p_1) \cdot e^{-t/t_c} + p_1$$

$$t_c = \frac{L_b \cdot V}{P \cdot A \cdot R \cdot T}$$

$p(t)$ partial pressure in the foam	[Pa]
$p_1$ partial pressure outside the casing	[Pa]
$J$ gas flow	[mol/(m <sup>2</sup> ·s)]
$P$ effective permeability coefficient, including foam and casing	[mol/(m·s·Pa)]
$L_b$ barrier thickness	[m]
$V$ polyurethane foam volume	[m <sup>3</sup> ]
$R$ gas constant = 8.314	[Pa·m <sup>3</sup> /(K·mol)]
$T$ temperature	[K]
$A$ barrier area	[m <sup>2</sup> ]

**Figure 20.** Simplified model of ageing used in paper I.

#### 4.5.2 Model of ageing using conformal coordinates

The coordinate transformation  $w(z)=u(x,y)+i \cdot v(x,y)$  treated in chapter 3.3.1, eqs. 33-35 with the strengths determined by eqs. 36-38, can be applied to solve the diffusion problem. The transformation maps the (x,y)-plane on the (u,v)-plane in which the twin pipe geometry becomes rectangular. The first quadrant of the twin pipe is mapped on  $u \in [0, u_{pav}]$  and  $v \in [0, \pi]$  (see Figure 11). The transformation is extended by imaging to account for the rest of the pipe. The diffusion equation in the (u,v)-coordinates is given in eq. 85. The left hand side is due to the conformal transformation involving an area factor  $A(u,v)=h(u,v)^2$  [-] [see BV].

$$A(u,v) \cdot \frac{\partial c_{tot}}{\partial t} = \frac{\partial}{\partial u} \left( \delta_{eff,c} \cdot \frac{\partial c}{\partial u} \right) + \frac{\partial}{\partial v} \left( \delta_{eff,c} \cdot \frac{\partial c}{\partial v} \right) [\text{W} \cdot \text{m}^{-3}] \quad (85)$$

The problem is solved numerically with the explicit finite difference method (eqs. 86-88). The region is divided into cells i,j. The increase of the total concentration in a cell is caused by the net inflow to the cell (eq. 86). Eqs. 86-88 are valid for internal cells that do not border on the boundary.

$$\underbrace{h_{i,j}^2 \Delta u_i \Delta v_j}_{\approx A_{i,j}} \cdot (c_{tot,i,j}^{nr+1} - c_{tot,i,j}^{nr}) = (J u_{i-1 \rightarrow i,j}^{nr} - J u_{i \rightarrow i+1,j}^{nr} + J v_{i,j-1 \rightarrow j}^{nr} - J v_{i,j \rightarrow j+1}^{nr}) \cdot \Delta t \quad (86)$$

$$Ju_{i \rightarrow i+1,j} = Ku_{i \rightarrow i+1,j} (c_{i,j} - c_{i+1,j}) [\text{W} \cdot \text{m}^{-1}], \quad Ku_{i \rightarrow i+1,j} = \frac{2 \cdot \Delta v_j}{\frac{\Delta u_i}{\delta_{i,j}} + \frac{\Delta u_{i+1}}{\delta_{i+1,j}}} [\text{W} \cdot \text{m}^{-1} \cdot \text{K}^{-1}] \quad (87)$$

$$Jv_{i,j \rightarrow j+1} = Kv_{i,j \rightarrow j+1} (c_{i,j} - c_{i,j+1}) [\text{W} \cdot \text{m}^{-1}], \quad Kv_{i,j \rightarrow j+1} = \frac{2 \cdot \Delta u_i}{\frac{\Delta v_j}{\delta_{i,j}} + \frac{\Delta v_{j+1}}{\delta_{i,j+1}}} [\text{W} \cdot \text{m}^{-1} \cdot \text{K}^{-1}] \quad (88)$$

From eq. 86 the new total concentration in cell i,j is calculated according to eq. 89. The time step limit is stated in eq. 90.

$$c_{toti,j}^{nr+1} = c_{toti,j}^{nr} + \frac{(Ju_{i-1 \rightarrow i,j}^{nr} - Ju_{i \rightarrow i+1,j}^{nr} + Jv_{i,j-1 \rightarrow j}^{nr} - Jv_{i,j \rightarrow j+1}^{nr})}{A_{i,j}} \cdot \Delta t [\text{K}] \quad (89)$$

$$\Delta t < \min_{i,j} \left( \frac{A_{i,j} \cdot [S \cdot R \cdot T \cdot (1 - f_g) + f_g]}{Ku_{i-1 \rightarrow i,j} + Ku_{i \rightarrow i+1,j} + Kv_{i,j-1 \rightarrow j} + Kv_{i,j \rightarrow j+1}} \right) [\text{s}] \quad (90)$$

## 4.6 Factors that influence the ageing of pipes

The ageing is slow for large pipe dimensions with thick insulation and casing, while it is fast for small pipe dimensions with thin insulation and casing.

### 4.6.1 Transport resistance of the different materials

For pipes without a diffusion barrier the polyethylene casing constitutes the main diffusion resistance for nitrogen, oxygen and carbon dioxide. The polyurethane foam is the principal resistance to cyclopentane diffusion. The Biot number  $Bi$  [-] given by the quotient of the diffusion resistances of the foam and casing may be used to relate them (eq. 91). The transport resistance of the materials depends on their permeability coefficient ( $P_{foam}$  [ $\text{mol} \cdot \text{m}^{-1} \cdot \text{s}^{-1} \cdot \text{Pa}^{-1}$ ] respectively  $P_{PE}$  [ $\text{mol} \cdot \text{m}^{-1} \cdot \text{s}^{-1} \cdot \text{Pa}^{-1}$ ]), their temperature and their thickness. For high Biot numbers ( $>1$ ) the main transport resistance is attributable to the polyurethane foam, while the polyethylene casing constitutes the principal resistance for low Biot numbers ( $<1$ ). Generally, the polyethylene casing represents a comparatively major part of the resistance of large pipes of a low insulation series, i.e. pipes with low  $Bi$  numbers.

$$Bi = \frac{R_{foam}}{R_{PE}} \quad (91)$$

The  $Bi$ -numbers of two pipes are presented in Table 8, demonstrating the extremes by means of a small pipe of a high insulation series (most resistance from the polyurethane foam) and a large pipe of a low insulation series (most resistance from the polyethylene casing).

**Table 8.** Bi-numbers of two district heating pipes at 80-15°C (-10°C within parenthesis)\*. The permeability of cyclopentane for the bi-modal polyethylene casing material is lacking.

Pipe dimension	Bi-number (uni-modal)	Bi-number (bi-modal)
DN20/125		
Cyclopentane	420 (430)	?
Carbon dioxide	0.64 (0.62)	0.78 (0.73)
Oxygen	0.38 (0.35)	0.65 (0.59)
Nitrogen	0.55 (0.54)	0.87 (0.83)
DN800/900		
Cyclopentane	45 (47)	?
Carbon dioxide	0.069 (0.067)	0.084 (0.078)
Oxygen	0.040 (0.037)	0.069 (0.064)
Nitrogen	0.058 (0.057)	0.093 (0.088)

\*The numbers were calculated based on the single pipe model.

For pipes with a diffusion barrier it constitutes the main diffusion resistance, hindering radial diffusion. Measurements of the permeability through an ordinary diffusion barrier of multilayer laminate film PE/PETP/Alu/PE have demonstrated that it significantly reduced diffusion [Ting Larsen et al. 2009]. The barrier proved to have a diffusion resistance for carbon dioxide at 22°C equivalent to that of an 8 m thick polyethylene casing. The barrier reduced the permeability of oxygen at 22°C by at least a factor of 160. The use of a diffusion barrier is therefore recommended to prevent the foam from ageing.

District heating pipes with PEX fluid pipes are a special case, as the PEX-pipes are not diffusion tight in themselves. An EVOH barrier on the fluid pipe can be used to prevent oxygen from diffusing into the transported water and causing corrosion in the network [Logstor product catalogue 2013, Uponor 2013]. Care must be taken to ensure that the pipe construction is more open to water vapour diffusion towards the ground than towards the centre in order to prevent accumulation of water in the insulation [Zinko et al. 2002]. Instead of an aluminium diffusion barrier at the casing, a multilayer polymer barrier can be used to reduce diffusion of insulating gases when the fluid pipe contains no metal [Logstor product catalogue 2013].

#### 4.6.2 Cyclopentane content

How the cyclopentane content of the foam influences the heat loss from pipes over time was investigated in papers IV and V. In paper IV single pipes of three dimensions were studied with carbon dioxide blown foam (no cyclopentane), “normal” cyclopentane blown foam without sufficient cyclopentane for initial condensation and “normal” cyclopentane blown foam with enough cyclopentane to be present in condensed form initially. “Normal” here means that the cyclopentane contents are reasonable for new-blown foams. The initial cyclopentane concentration was found to influence the heat loss to the extent that over 30 years the heat loss is about 20-30% higher from the studied carbon dioxide blown pipes compared to the cyclopentane blown ones. The difference between the two cyclopentane blown pipes is less; 3-4 % heat loss. The cyclopentane blown pipe with the most cyclopentane contained barely double the amount per m<sup>3</sup> compared to the other. A few percent difference in the estimated heat loss over a pipe’s nominal life is typical for pipes of different manufacturers on the market due to differences in the initial cell gas

composition [paper III]. In paper V the variation caused by the different cyclopentane contents is studied for a small twin pipe. The difference is here estimated at 6% for the heat loss over 30 years from the return and at 3% for the heat loss over 30 years from the forward pipe.

Table 9 presents the average thermal conductivity of the insulation of a pipe for four different insulation scenarios; “normal” cyclopentane blown insulation with sufficient cyclopentane for initial condensation, the same insulation with the cyclopentane transport prevented, a pipe insulation with double the amount of cyclopentane and a pipe insulation saturated with cyclopentane the whole time but without condensation. The second and fourth cases are hypothetical, but included to provide a picture of the effect of cyclopentane out-diffusion and the optimal situation caused by a large amount of cyclopentane. Figure 21 illustrates how the thermal conductivity of the pipe insulation changes over time.

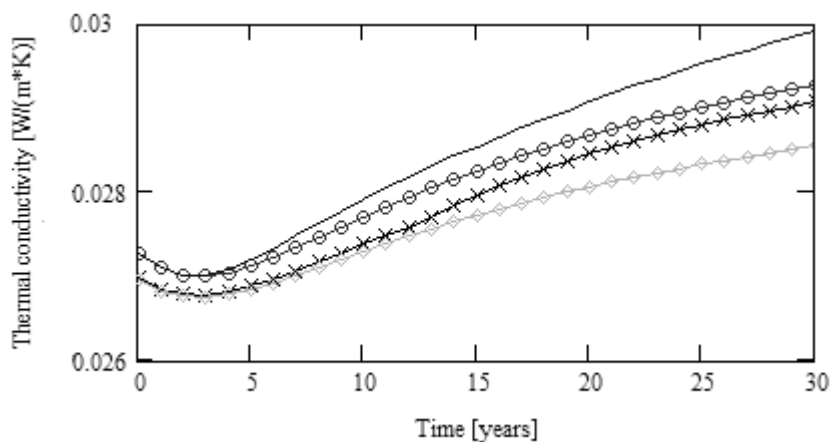


**Figure 21.** Thermal conductivity over time of the insulation of a DN100 pipe with Series 2 insulation (about 5 cm. thick) aged with 80°C at the service pipe and 15°C at the casing; solid line – normal pipe insulation, line with o:s – normal pipe insulation with cyclopentane transport prevented, line with x:s – insulation with the cyclopentane content doubled, line with <>s – insulation saturated with cyclopentane the whole time.

**Table 9.** Average thermal conductivity of different insulations over various ageing times [ $\text{mW}\cdot\text{m}^{-1}\cdot\text{K}^{-1}$ ].

	Normal	Normal prevented	Doubled	Saturated
0 years	27.3	27.3	27.0	27.0
10 years	27.3	27.2	27.0	26.9
15 years	27.6	27.5	27.2	27.1
20 years	27.9	27.7	27.5	27.3
30 years	28.5	28.2	27.9	27.7

Adding more cyclopentane both lowers the initial thermal conductivity and decreases the rise of thermal conductivity over time. The average thermal conductivity of the insulation with the cyclopentane content doubled over 15 years of ageing is lower than the initial value of the normal insulations (Table 9), i.e. over a time period of 15 years double the amount of cyclopentane would be preferable from an insulation point

of view compared to a diffusion barrier hindering all gas transport. The best is, of course, a combination of a high level of cyclopentane and a diffusion barrier. After 20 years it is better to use a diffusion barrier that hinders all ageing than adding more cyclopentane, as was demonstrated by the last case studied, which was calculated with the saturation vapour pressure of cyclopentane the whole time.

#### 4.6.3 PE-material

The speed of ageing is affected by the quality of the polyethylene used. The casing constitutes the principal resistance against the diffusion of oxygen, nitrogen and carbon dioxide, where bi-modal polyethylene increases the permeability of the casing (see section 4.3). In the publications for this thesis pipes with uni-modal polyethylene casing were studied. With bi-modal casing material the pipes would have aged more quickly. For 90% of the concentration changes next to the fluid pipe to have taken place with bi-modal casing for the DN100/225 pipe with about 5 cm thick insulation aged at 80-15°C studied in paper III and section 4.4.3 it would take: for carbon dioxide between 5-6 years (instead of 6-7 years with uni-modal casing), for oxygen about 18-19 years (instead of 30 years) and for nitrogen 73-74 years (instead of about 100 years). The total heat flow over 30 years from the pipe increases by about 1.8% when bi-modal casing is used compared to when uni-modal is employed. For a network with this pipe type, with 80°C forward, 40°C return and a ground temperature of 8°C, the increase in the heat flow from the two pipes is about 1.7% with bi-modal casings compared to uni-modal.

Table 10 illustrates the ageing of the studied pipes in papers III and V. The heat flow from the pipes differs by a few % or tenths of  $W \cdot m^{-1}$ .

**Table 10.** Ageing of pipes with different casing materials.

Pipe	Initial heat flow [ $W \cdot m^{-1}$ ]		% change in heat flow over 30 years	
III				
DN100/225 uni-modal	17.2		9.5% @ 80-15°C	
DN100/225 bi-modal			11% @ 80-15°C	
V				
	Forward	Return	Forward	Return
2xDN25/140 uni-modal, Foam 1	9.39	0.999	3.7% @ 80-15°C	12% @ 80-15°C
2xDN25/140 bi-modal Foam 1			6.2% @ 80-15°C	17% @ 80-15°C
2xDN25/140 uni-modal Foam 2	9.17	0.972	2.2% @ 80-15°C	5.6% @ 80-15°C
2xDN25/140 bi-modal Foam 2			4.4%	11%

#### 4.7 Modelled cell gas content after ageing compared to measured content of used pipes

In order to check the ability of the models to predict the actual ageing of district heating pipes, the measured cell gas content of aged pipes was compared to the modelled cell gas content based on assumptions of the initial composition and ageing conditions. The study is further described in paper VI.

The pipes studied are presented in Table 11. The ground surface temperature was assumed to be the annual average temperature in the city with the network. Figures 22-25 show the results of the comparisons.

**Table 11.** Pipes for which the modelled cell gas content and measured cell gas content have been compared.

Dimension	Casing thickness [mm]	Approx. core density [ $\text{kg}\cdot\text{m}^{-3}$ ]	Type of pipe	Blowing agent	Ageing time [years]
DN40/125	3.2	72	Forward	CFC-11	25
DN250/450	8.7	78	Forward	CFC-11	20
DN300/500	9.3	70	Forward	CFC-11	24
DN300/500	8.8	66	Return	CFC-11	24
DN200/355	5.5-5.6	68	Return	Cyclopentane	4

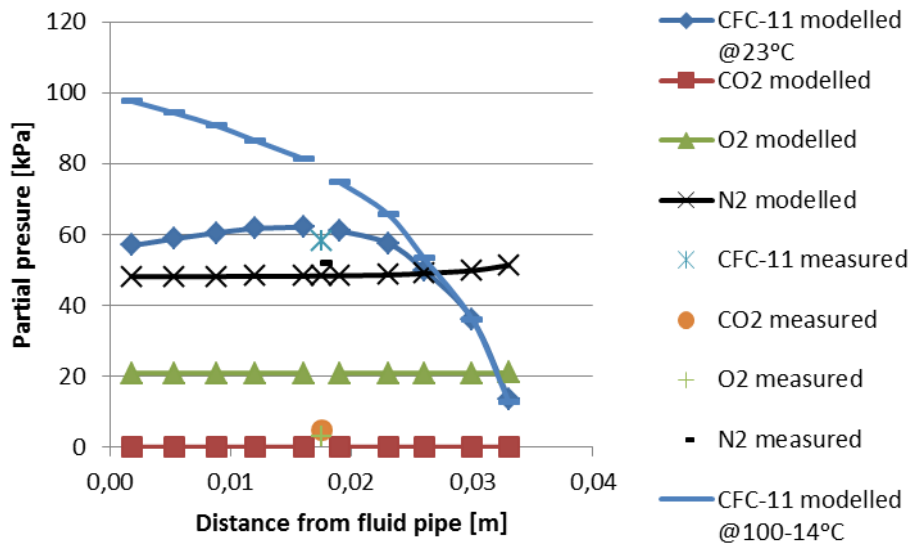


**Figure 22.** Modelled partial pressures in the cross section of the foam of the DN40/125 forward pipe after 25 years ageing in a 100-40°C network based on the initial cell gas content: 68 kPa CFC-11, 48 kPa carbon dioxide, 1.2 kPa oxygen and 2.4 kPa nitrogen, together with measured partial pressures in the aged foam sample. Mean casing temperature during ageing was about 14°C.

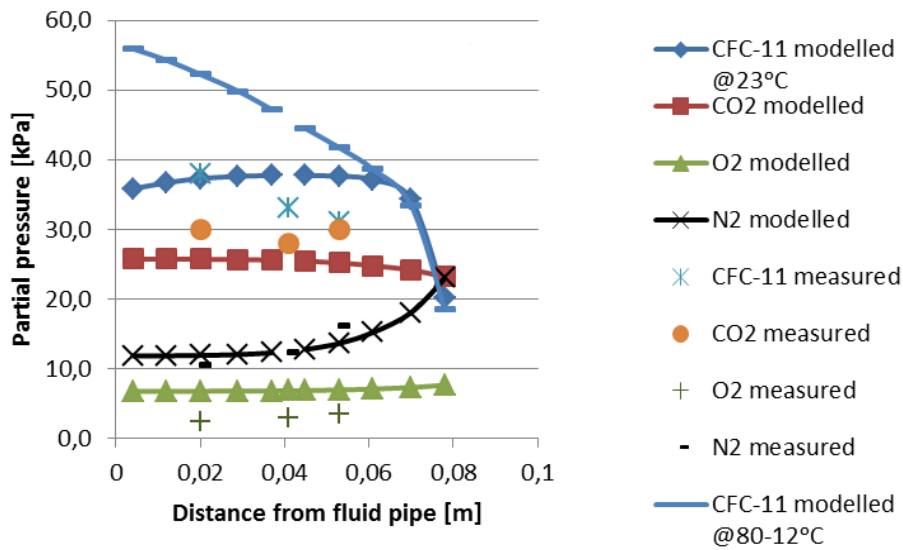


**Figure 23.** Modelled partial pressures in the cross section of the foam of the DN250/450 pipe after 20 years ageing in an 80-40°C network based on the initial cell gas composition: 37.5 kPa CFC-11, 125 kPa carbon dioxide, 1.2 kPa oxygen and 2.4 kPa nitrogen, together with measured partial pressures in the aged foam sample. The permeability of the polyethylene casing has been doubled for nitrogen. Mean casing temperature during ageing was about 12°C.

Comparing modelled and measured results it is obvious that the slopes of the measured CFC-11 and cyclopentane profiles in the pipes match the slopes of the profiles in the hot in-use pipes better than the slopes of the pipes at room temperature. This indicates that equilibrium is thus not instant, but takes time to reach.

It is evident that the model predicts more oxygen and less carbon dioxide in the hot pipes than revealed by the measurements. This is probably due to the fact that oxidation took place in the pipes but was not included in the model. An estimate of how much oxygen could have been consumed by oxidation in each case showed that it could have consumed the over-predicted oxygen [paper VI]. It should be noted that not only the oxygen content is influenced, but also the carbon dioxide content.

The modelling under-predicted the nitrogen content in half of the studied pipes, unless the permeability of nitrogen was increased through the polyethylene casing.

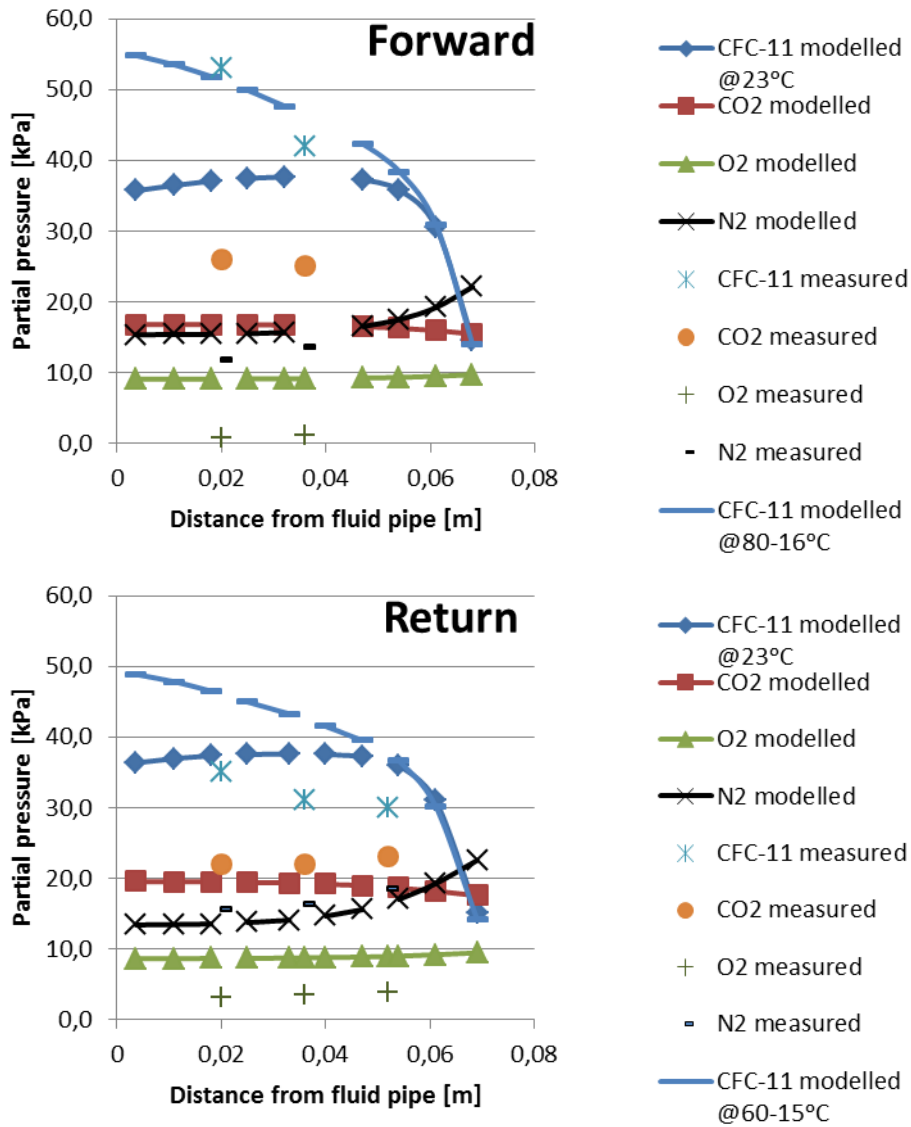


**Figure 24.** Modelled partial pressures in the cross section of the foam of the DN300/500 pipes after 24 years of ageing in an 80-60°C network based on the initial cell gas composition: 37.5 kPa CFC-11, 175 kPa carbon dioxide, 1.2 kPa oxygen and 2.4 kPa nitrogen, together with measured partial pressures in the aged foam sample. The permeability of the polyethylene casing has been increased by 50% for nitrogen. Mean casing temperature of forward pipe during ageing was about 16°C, of return about 15°C.

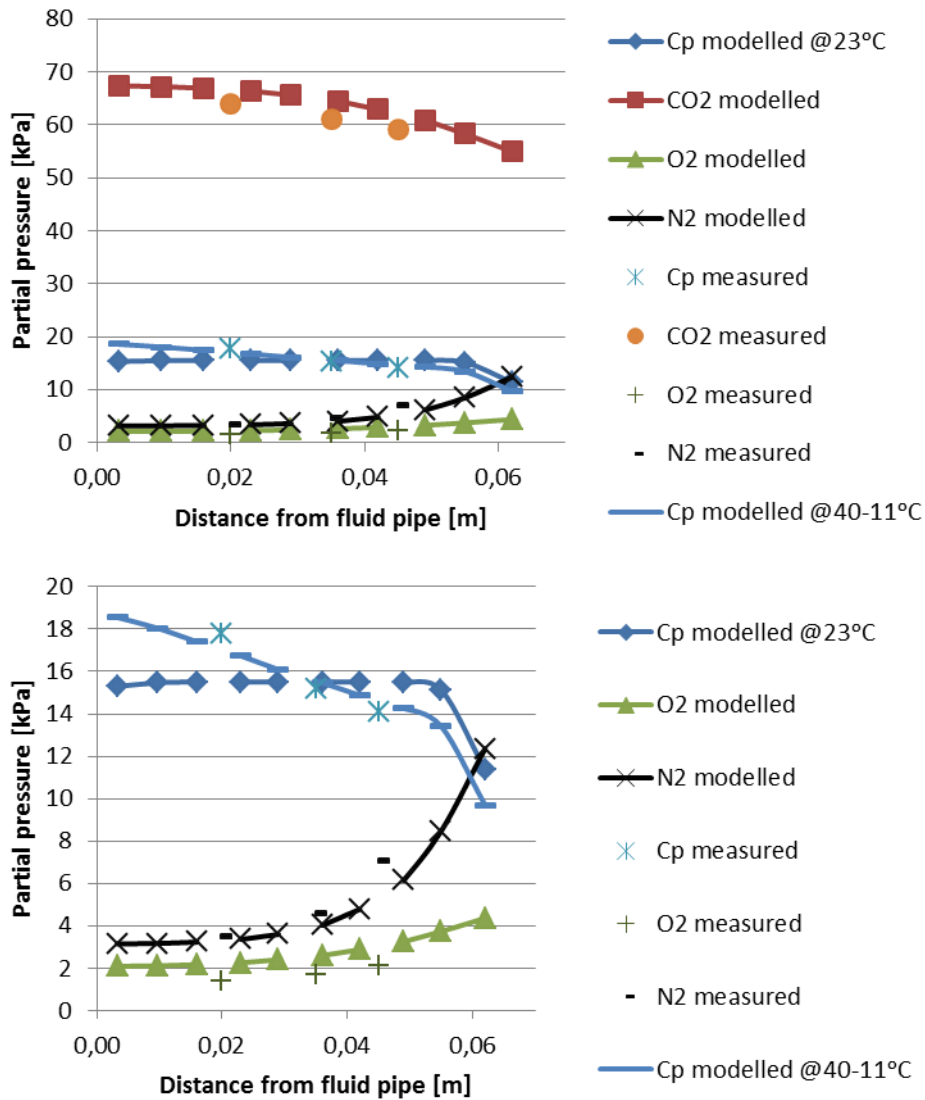


**Figure 25.** Modelled partial pressures in the cross section of the foam of the DN200/355 return pipe after 4 years of ageing in an 80-40°C network based on the initial partial pressures: 15.5 kPa cyclopentane, 110 kPa carbon dioxide, 0.5 kPa oxygen and 3.0 kPa nitrogen, together with measured partial pressures in the aged foam sample. Mean casing temperature during ageing was about 11°C. The upper figure shows the partial pressure interval 0-80 kPa and the lower figure only the interval 0-20 kPa.

## 5 SUMMARY AND DISCUSSION

---

In this thesis the long-term insulation performance of single and twin district heating pipes has been studied. Presented models of ageing of single and twin pipes that give the concentration profiles of the cell gases over the foam cross section over time allow the possibility for detailed study of the cell gas content within the foam and of its insulation performance; for example, it can be seen how the physical blowing agent is divided between phases within the foam, that condensation may occur close to the casing and how long it takes for gas concentration changes to spread from the boundary into the foam. The models enabled the evaluation of different distribution solutions.

In general, the heat loss from the pipe depends heavily on the temperature level used in the network and the amount and thermal conductivity of the insulation. For a district heating pipe buried in the ground, the pipe itself typically constitutes about 90% of the thermal resistance, of which the insulation represents around 99.5% or more. The heat loss can be reduced by using thicker insulation and/or insulation with lower thermal conductivity. The thermal conductivity of the material closest to the fluid pipe is the most important. The heat loss is also reduced if the pipe is buried deeper in the ground. An increased depth of 200 mm, as is normal for pipes in an urban environment compared to in a green area, can make a difference of a few percent in terms of heat loss.

The total heat loss is less from a twin pipe than from a pair of single pipes, as the fluid pipes in the twin pipe are placed closer to each other and the insulation is co-used by them. The return pipe is heated by the forward pipe so that the heat loss from the return is less. The difference is about 25% compared to series 2 pipes and less than one to a few percent compared to series 3 pipes.

Ageing increases the heat loss by about 10% over 30 years. The materials of the pipe hinder ageing by diffusion of gases into/out of the foam to varying degrees. A diffusion barrier inside the casing can be used to prevent ageing. Cyclopentane diffusion is otherwise primarily restricted by the polyurethane foam while carbon dioxide, oxygen and nitrogen diffusion is mainly hindered by the casing. By increasing the cyclopentane content of the foam so that it contains condensed cyclopentane from the beginning, the ageing of the pipe can be slowed down. The liquid cyclopentane vaporises and fills the place of out-diffused gas.

By comparing the modelled and measured cell gas compositions of aged pipes it can be concluded that apart from diffusion, oxidation influences the cell gas composition. From an insulation perspective, the decreased oxygen and increased carbon dioxide concentration caused by oxidation is positive.

### **5.1 Improvements of the models**

The coupling between heat conduction and diffusion within district heating pipes is weak, in the sense that there are only small temperature changes within the foam over time due to the variation in gas content. A quasi-stationary model of ageing can be used without introducing any significant error. In a studied case even calculation with a constant stationary temperature over 30 years of ageing introduced an error of less than 1%. For rough estimates it is thus not necessary to take the temperature coupling into account.

When comparing modelled and measured cell gas compositions of aged pipes it can be concluded that in addition to diffusion, oxidation influences the cell gas composition and thus ought to be taken into account in predictions of ageing. An investigation of its inclusion in the model as a sink term for oxygen and a source term for carbon dioxide is recommended for future work.

It should also be noted that the measured content of CFC-11 and cyclopentane over the foam cross section in aged pipes is more similar to that modelled in hot pipes than the content modelled in pipes at room temperature. The model also predicts less nitrogen in several of the pipes than was found in the aged pipes.

Further comparison of model predictions and true ageing, i.e. results from measurement on ageing pipes, is recommended to analyse the situation more thoroughly.

### **5.2 Discussion of other insulation options**

Polyurethane is the insulation of choice today for rigid district heating pipes. It has several advantages; low thermal conductivity, contribution to the mechanical strength of the pipe construction and self-adhesiveness. On the negative side, the toxicity of diisocyanate, one of the main components of the foam, causes occupational hazards. The foam constituents are also derived from non-renewable fossil resources. Natural oil polyols, i.e. polyols derived from vegetable oils such as castor, sunflower, rapeseed, palm or soybean oil are being developed. However, these alternatives may involve other environmental concerns; e.g. health hazards, devastation of rainforests and use of pesticides.

A couple of insulation options are available on the market for flexible district heating pipes: semi-flexible polyurethane foam, polyethylene foam that may or may not be cross-linked and mineral wool. Flexible fluid pipes installed in insulation blocks of expanded polystyrene are also marketed. The polyurethane foam is rigid, with no significant difference in flexibility between the semi-flexible and the rigid polyurethane foam [Jarfelt and Ramnäs 2008]. The alternative insulations mentioned, with 10-20 mW/(m·K) higher thermal conductivities than polyurethane foam, are chosen for pipe constructions in a compromise between insulation capacity, flexibility (ease of installation) and price. The poorer thermal conductivity of the insulation material can be compensated for by using a thicker insulation layer. Thus the

insulating performance of the whole pipe construction does not have to be inferior to that of the polyurethane foam insulated with an alternative insulation; it depends on the insulation thickness used for the specific pipe.

An insulation alternative that has been investigated but not introduced to the market is polyethylene terephthalate (PET) foam [Jarfelt and Ramnäs 2008, Mangs 2005]. This material has a glass transition temperature of around 80°C, but could be an alternative to polyurethane foam for small pipe dimensions that are not used at a very high temperature (< about 100°C). Investigations have indicated a similar or cheaper price, similar or better short and long-term insulation performance (slower diffusion) and better environmental performance, as the heat losses are expected to be less and recycled PET-material can be used. The use of isocyanates would also be avoided.

Aerogels and vacuum insulations have lower thermal conductivity than polyurethane foam. With these materials it is thus possible to improve the insulation performance without increasing the insulation thickness. Aerogel is available in the form of a blanket ( $\lambda \approx 15-16 \text{ mW}\cdot\text{m}^{-1}\cdot\text{K}^{-1}$ ) that can be wrapped around the pipe. Application of an aerogel blanket or cylindrical vacuum insulation panels with fumed silica as core material ( $\lambda_{\text{min}} \approx 4 \text{ mW}\cdot\text{m}^{-1}\cdot\text{K}^{-1}$ ) between the fluid pipe and an outer polyurethane foam insulation layer has been investigated and shown to have a good result (about 15-25% decrease in heat loss) [Berge 2013]. High performance insulation materials for district heating and cooling applications is a field within which more research will be performed in order to identify well-functioning solutions that provide a superior insulation performance.

## REFERENCES

---

Ahern A. et al. (2005) *The conductivity of foams: a generalisation of the electrical to the thermal case*, Colloids and Surfaces A, Physicochemical and engineering aspects, vol 263, pp 275-279

Alsoy S. (1999) *Modeling of diffusion in closed cell polymeric foams*, Journal of Cellular Plastics, 35 (May), pp 247-271

Arkema (2013) Additives for Polymers, 11 p. 3 (a short notice without author mentioned)

Bayer Material Science (2011) *PUR Nanofoam*, Customer Day, May 19

Bazzo et al. (1994) *Cyclopentane Blown Foam Systems for Domestic Appliances Application*, Journal of Cellular Plastics, 32 (January), pp 46-61

Berge A. (2013) *Novel Thermal insulation in Future Building and District Heating Applications – Hygrothermal Measurements and Analysis*, Licentiate Thesis, Department of Civil and Environmental Engineering, Chalmers University of Technology, Göteborg, Sweden.

Besier R. et al. (2008) *Straight Preinsulated Bonded Pipes – Quality Tests on Preinsulated Bonded Pipe System Components*, EuroHeat&Power English Edition, 1, vol 5, pp 34-45

Biedermann A. et al. (2001) *Analysis of Heat Transfer Mechanisms in Polyurethane Rigid Foam*, Journal of Cellular Plastics, vol 37, 467-483

Brodt K. H. (1995) *Thermal insulations: CFC-alternatives and vacuum insulation*. Doctoral thesis, Delft University of Technology, the Netherlands.

Capella A. et al. (1996) *Advanced hydrocarbon blown formulations for domestic appliances applications*. UTECH 96, the International Polyurethanes Industry Conference, March 26-28.

Claesson J. (2001) *Partial Differential Equations – Engineering Applications*, Mathematical Physics, LTH, Lund and Building Physics, Chalmers, Göteborg, Sweden.

Comyn J. (1985) *Polymer permeability*, Elsevier Applied Science Publishers, London and New York

Contreiras Louro (2007) *Thermal Conductivity of Gases*, Master's Thesis, Universidade Técnica de Lisboa

Dohrn R. (1998) EC, ZT-TE 5.3, Report DHR 60 November

Dohrn R. et al. (2007) *Thermal conductivity of polyurethane foam cell gases: Improved transient hot wire cell - data of isopentane + n-pentane mixtures – Extended Wassiljewa-model*, Fluid Phase Equilibria, vol 261, pp 41-49

Du Cauzé de Nazelle G. (1995) *Thermal conductivity ageing of rigid closed cell polyurethane foams*. Doctoral thesis, the Hague, the Netherlands

Duda J.L and Zielinski J.M. (1996) In *Diffusion in Polymers* by Neogi P, Dekker, New York

EN253:2003. *District heating pipes – Preinsulated bonded pipe systems for directly buried hot water networks – Pipe assembly of steel service pipe, polyurethane thermal insulation and outer casing of polyethylene*, European Committee for Standardisation, Brussels, Belgium.

EN253:2009. *District heating pipes – Preinsulated bonded pipe systems for directly buried hot water networks – Pipe assembly of steel service pipe, polyurethane thermal insulation and outer casing of polyethylene*, European Committee for Standardisation, Brussels, Belgium.

EPBD2: *Directive 2010/31/EU of the Parliament and of the council of 19 May 2010 on the energy performance of buildings*, <http://www.epbd-ca.eu/> (2012-06-09)

ER 2010:39 *Mission 13: National strategy for low-energy buildings (in Swedish: Uppdrag 13: Nationell strategi för lågenergibyggnader)*, Statens Energimyndighet ISSN 1403-1892

Fan Y. and Kokko E. (1995) *Prediction of long-term ageing of cellular plastics*, Environmental International, 21, 441-450

Fleurent H. and Thijs S. (1995) *The Use of Pentanes as Blowing Agent for Rigid Polyurethane Foam*, Journal of Cellular Plastics, vol 31 pp 580-599

Folland G. B. (1992) *Fourier analysis and its applications*, Wadsworth mathematics series, Wadsworth & Brooks/Cole

Frederiksen S. and Werner S. (1993) *District Heating – Theory, technology and function (in Swedish: Fjärrvärme – Teori, teknik och funktion)*, Studentlitteratur, Lund, Sweden.

Fröling M. et al. (2006) *Life Cycle Assessment of the District Heat Distribution System. Part 3: Use Phase and Overall Discussion*, the International Journal of Life Cycle Assessment, 11 (6), pp 437-446.

GEF Ingenieurgesellschaft Chemnitz mbH, IMA Dresden GmbH, IPF Leibniz-Institut (2011) AGFW - Forschung und Entwicklung, Heft 17: *Zeitstandsfestigkeit von Kunststoffmantelrohren - Permeations- und Degradationsverhalten, Wechselbeanspruchung, Alterungsgradient, Muffenbewertung, Versagensverhalten*, AGFW-Projektgesellschaft für Rationalisierung, Information und Standardisierung mbH, Frankfurt/Main, ISBN: 978-3-89999-026-3

Glicksman L. R. and Stewart J. (1997) *Measurement of the morphology of closed cell foams which control the overall thermal conductivity*, Proceedings of the 3rd Symposium on Insulation Materials, Quebec City, USA, May 15-17 1997 (ASTM Special Technical Publication, vol 1320, pp 307-334).

Hagentoft C.-E. (2001) *Introduction to Building Physics*, Studentlitteratur, Lund

Heinemann T. et al. (2000) *Experimental Determination of the Vapor Phase Thermal Conductivity of Blowing Agents for Polyurethane Rigid Foam*, Journal of Cellular Plastics, vol 36, pp. 45-55

Hilyard N. C. and Cunningham A. (1994) *Low density cellular plastics – Physical basis of behaviour*, Chapman & Hall, London, U.K.

Honeywell (2013) *Honeywell Solstice Liquid Blowing Agent – Technical Datasheet*, <http://www.honeywell-solsticelba.com> (Viewed April 2013).

Isberg J. (1988) *The thermal conductivity of polyurethane foam*, Doctoral thesis, Department of Building Technology, Chalmers University of Technology, Sweden

Jarfelt U. and Ramnäs O. (2008) *New materials and constructions for improving the quality and lifetime of district heating pipes*, The 11th International Symposium on District Heating and Cooling, Reykjavik, Iceland, August 31 to September 2.

Jarfelt U. (1998) *Field measurements of Gas Diffusion from District Heating Pipes*, Thermal Insulation Gas Diffusion Report 8, Department of Building Physics, Chalmers University of Technology, Sweden

Jarfelt U. and Ramnäs O. (2006) *Thermal conductivity of polyurethane foam – Best performance*, 10th International Symposium on District Heating and Cooling, September 3-5, Hanover, Germany.

Jonsson E. (2001) *Värmeförluster från fjärrvärmnät i småhusområden – Inverkan av röргеometri och dimensioneringskriterier*, Licentiate thesis, Institution of Heat and Power Engineering, Lund Institute of Technology, Lund University, Lund

Kaplan W. A. and Tabor R. L. (1994) *The Effect of Polymer Structure on the Gas Permeability of Model Polyurethanes*, Journal of Cellular Plastics, 30 (May), pp 242-272

Kellner J. and Zarka P. (2000) *Development of new generation polyols for semi-flexible foam systems for the production of flexible polyurethane pre-insulated pipes*, UTECH Europe 2000, the Hague

Krevelen van D.W. (1990) *Properties of Polymers. Their correlation with chemical structure; their numerical estimation and prediction from additive group contributions*, Elsevier, Amsterdam, Oxford, New York, Tokyo.

Kristjansson H. and Bohm B. (2006) *Optimum Design of Distribution and Service Pipes*, the 10<sup>th</sup> International Symposium on District Heating and Cooling, 3-5 September, Hanover, Germany.

Laying instructions FVF D:211 (2001) *Laying instructions for district heating pipes (in Swedish: Läggningsanvisningar för fjärrvärmerör)*, the Swedish district heating association [www.svenskfjarrvarme.se](http://www.svenskfjarrvarme.se)

Logstor product catalogue (2013), [www.logstor.com](http://www.logstor.com) (Viewed: 2014-09-16)

Loh G. et al. (2012), *Formacel 1100 (FEA-1100) – a Zero ODP and Low GWP Foam Expansion Agent*, Polyurethanes 2012 Technical Conference, Atlanta, Georgia, Sept 24-26, 2012.

Lynch J. (2014), Arkema Inc, Spray Foam Convention and Expo, January 26-29, Palm Springs, California, USA.

Mangs S. (2005) *Insulation Materials in District Heating Pipes, Environmental and Thermal Performance of Polyethylene Terephthalate and Polyurethane Foam*, PhD-thesis, Department of Chemical and Biological Engineering, Chalmers University of Technology, Gothenburg, Sweden.

Marrucho I. M. et al. (2005) *Ageing of Rigid Polyurethane Foams: Thermal Conductivity of N<sub>2</sub> and Cyclopentane Gas Mixtures*, Journal of Cellular Plastics, Vol 41, pp 207-224

McMenamin J. et al. (2009), *Development of Novel Blowing Agents for Polyurethane Foams*, UTECH Europe 2009, Maastricht, Netherlands.

Meigen M. and Schuricht W. (2005) *Zeitstandsverhalten von PUR-Schäumen, KMR altern schneller und anders als bisher angenommen*, EuroHeat&Power, 1-2, pp 50-57

Merten A.-K. and Rotermund U. (1997) *Thermal Conductivity of Gas Mixtures as Blowing Agents for Isocyanate-Based Rigid Foams*, Polyurethanes World Congress, September 29-October 1, pp 317-328

Murphy J. et al. (2005) *Ecomate® Foam Blowing Agent*, API Polyurethanes 2005, Technical Conference

Myrehed M. (1989) *Multipole Method to Compute the Conductive Heat Flows to and between Pipes in a Composite Region: Pipes in a Circle in a Half-Plane*, Notes on

Heat Transfer 1-1989, Dep. of Building Technology and Mathematical Physics, Lund Institute of Technology, Sweden.

Nielsen L. et al. (2000) *Thermal conductivity of nonporous polyurethane*, High Temperatures-High Pressures, 32, pp 701-707

Nielsen L. V. (1998) *Materials for District heating Pipes*, PhD Thesis, Department of Chemical Engineering, The Technical University of Denmark

Nielsen L. V. (2001) *Life Cycle Assessment of district heating*, News from DBDH, 1, pp 14-17.

Nilsson S. et al. (2006) *Shallow burial of district heating pipes (in Swedish: Grund förläggning av fjärrvärmeledningar)*, Report Värmegles 2006:25, the Swedish district heating association ISSN 1401-9264

NIST Chemistry webbook, <http://webbook.nist.gov/chemistry/> (Viewed 2012-03-13).

Oertel G. and Abele L. (1994) *Polyurethane Handbook* 2<sup>nd</sup> edition, Hanser

Oliveira N. S. (2001) *Thermal Conductivity of Gases – An Internship Report for Graduation in Chemistry – Branch of Analytical Chemistry*, Bayer A.G / Universidade de Aveiro

Olsson M. E. (1998) *Long-Term Thermal Performance of Polyurethane Foam – measurements and modelling*, Licentiate thesis, Department of Building Physics, Chalmers University of Technology, Gothenburg, Sweden

Persson C. et al. (2006) *Insulating performance of flexible district heating pipes*, Proceedings of the 10th International Symposium on District Heating and Cooling, Hanover, Germany, September 3-5

Pinto Varanda C. D. G. (2009) *Thermal Conductivity of Gas Mixtures for Polyurethane Rigid Foams*, Universidade de Aveiro

Poling et al. (2001) *Properties of Gases and Liquids* (5th Edition), McGraw-Hill Publishers, Munich, Vienna, New York

Quintero M. (2012), *Alternative Technologies for the Rigid Foam Sector*, UNDP, Sao Paolo, Nov 2012.

Reid et al. (1987) *The Properties of Gases and Liquids* 4<sup>th</sup> edition, McGraw-Hill.

Reidhav C. et al. (2008) *Insulating properties of semi-flexible polyurethane foams*, Proceedings of the 11th International Symposium on District Heating and Cooling, Reykjavik, Iceland, August 31-September 2

Schuetz M. A. and Glicksman L. R. (1984) *Basic Study of Heat Transfer through Foam Insulation*, Journal of Cellular Plastics, vol 20, pp 114-121

- Singh S.N., Nturu M and Dedecker K (2003) *Long Term Thermal Resistance of Pentane Blown Polyisocyanurate Laminate Boards*, Journal of Cellular Plastics, vol 39, pp 265-280
- Smith B.D. and Srivastava R. (1986) *Thermodynamic Data for Pure Compounds. Part A: Hydrocarbons and Ketones*, Elsevier, New York
- Smits G.F. (1994) *Effect of cellsize reduction on polyurethane foam physical properties*, Journal of Thermal Insulation and Building Envelopes, vol 17, pp 309-330
- Svanström M. (1997) *Blowing Agents in Rigid Polyurethane Foam – Analytical studies – Technical and Environmental aspects*, PhD-thesis, Department of Chemical and Environmental Science, Chalmers University of Technology, Göteborg, Sweden.
- Svanström M. et al. (1997) *Determination of Effective Diffusion Coefficients in Rigid Polyurethane Foam*, Journal of Cellular Polymers, 16, pp 182-193
- Sörensen C. F. (2001) *The development of pre-insulated pipes*, News from DBDH, 2
- Takada N. et al. (1998) *Gaseous thermal conductivities of new hydrofluoroethers (HFE:s)*, Journal of Fluorine Chemistry 91, 81-85
- Thijs S. (1994) *Routes to more environmentally friendly rigid polyurethane foams*, UTECH 1994
- Ting Larsen C. et al. (2009) *Extending the Service Life of Pre-Insulated Pipes. Analyses of Diffusion Rates through PE and Impact on Ageing*, EuroHeat&Power English Edition, 6(2), pp 48-53.
- Treckmann R. and Braden C. (1995a) Philips, ZF-TVG5, DI. Report 1594207-1 from 1995-01-05
- Treckmann R. and Braden C. (1995b) EC, ZF-TVG5, DI., Report 1594207-1 from 1995-01-05
- Uponor (2013), [www.uponor.se](http://www.uponor.se) (Viewed: 2014-09-16)
- Volkert O. (1995) *Cyclopentane-Blown Rigid Foams for Refrigerators*, Journal of Cellular Plastics, vol 31, pp. 210-216
- Wallentén P. (1991) *Steady-State Heat Loss from Insulated Pipes*, Department of Building Physics, Report TVBH-3017 (licentiate thesis), Lund Institute of Technology, Sweden.
- Wang J. (2003) *Heat and Mass Transfer in Built Structures - Numerical Analyses*, PhD-thesis, Department of Building Physics, Chalmers University of Technology, Göteborg.
- Werner S (1999) *50 years of district heating in Sweden*, Booklet **issued by the** Swedish district heating association [www.svenskfjarrvarme.se](http://www.svenskfjarrvarme.se)

Zinko et al. (2002) *Moisture diffusion in plastic piping systems (written in Swedish: Fuktdiffusion i plaströrssystem)*, Report FOU 2002:73, Swedish district heating association, Sweden.



## APPENDIX A

### Thermal conductivities and viscosities – an additional literature study

---

#### *Thermal conductivity of nitrogen, oxygen and carbon dioxide*

All thermal conductivity values reported here are given in units of  $\text{mW}\cdot\text{m}^{-1}\cdot\text{K}^{-1}$ .

Nitrogen: The values calculated from the equation  $\lambda = 0.0646\cdot T + 6.4165$  for the temperature range 270-400K deviates  $<0.4\%$  from the tabulated values given in NIST [A1]. The equation  $\lambda = -0.00003371\cdot T^2 + 0.08719\cdot T + 2.724$  for the same range deviates  $<0.05\%$  from the tabulated values given in NIST. The NIST-values agree within  $\pm 2\%$  with the values given in other references for nitrogen [A2-A4].

Oxygen: The values calculated from the equation  $\lambda = 0.0805\cdot T + 2.5004$  for the temperature range 270-400K deviate  $<0.04\%$  from the tabulated values given in NIST [A1]. The equation  $\lambda = -0.00000293\cdot T^2 + 0.08245\cdot T + 2.180$  for the same range deviates  $<0.03\%$  from the tabulated values given in NIST. The NIST-values agree within  $\pm 4\%$  with the values given in other references for oxygen [A2-A3, A5].

Carbon dioxide: The values calculated from the equation  $\lambda = 0.0822\cdot T - 7.8019$  for the temperature range 270-400K deviate  $<0.5\%$  from the tabulated values given in NIST [A1]. The equation  $\lambda = 0.00003032\cdot T^2 + 0.06192\cdot T - 4.481$  for the same range deviates  $<0.3\%$  from the tabulated values given in NIST. The NIST-values agree within  $\pm 1.5\%$  from the values given in other references for carbon dioxide [A3, A6].

The uncertainties of the tabulated values in [A2] for the thermal conductivity of oxygen and nitrogen are  $\pm 3\%$  below 400K and  $\pm 5\%$  above 400K. According to [A3], the estimated uncertainty for the thermal conductivity of nitrogen and carbon dioxide is 1.5% in the range 300-500 K, deteriorating to 3% at lower and higher temperatures. For oxygen these estimates increase to 3% in the range 300-500 K, rising to 5% at lower and higher temperatures. Considering the uncertainties of these inorganic gases, it makes no sense to use higher order polynomials instead of linear approximations for the temperature dependence of the thermal conductivity within the 270-400K range.

#### *Viscosity of cyclopentane vapour*

The viscosity of cyclopentane vapour may be calculated according to a relation suggested by Reichenberg for organic compounds at low pressures [A7].

$$\text{Viscosity } \eta \text{ [Pa}\cdot\text{s]} = \frac{10^{-7} \cdot M^{1/2} \cdot T \cdot T_r \cdot (1 + 270 \cdot \mu_r^4)}{a \cdot \left(1 + \frac{4}{T_c}\right) \cdot [1 + 0,36 \cdot T_r \cdot (T_r - 1)]^{1/6} \cdot (T_r + 270 \cdot \mu_r^4)}$$

M = molecular mass [g·mol<sup>-1</sup>] = 70.1 g·mol<sup>-1</sup>

T = temperature [K]

T<sub>c</sub> = critical temperature = 512 K

T<sub>r</sub> = reduced temperature = T / T<sub>c</sub>

μ<sub>r</sub> = reduced dipole moment = 0

a = a constant for the cyclopentane molecule (contribution from each CH<sub>2</sub>-unit in the ring) = 5·6.91 = 34.55

A linear approximation,  $\eta = (0.024 \cdot T + 0.129) \cdot 10^{-7}$  [Pa·s], was found for the viscosities calculated for cyclopentane within the temperature range 270 – 400K.

In order to check the Reichenberg relation, it was also applied for pentane. About 2.5% lower viscosities than those tabulated in NIST [A1] were calculated for pentane within the temperature range 270 – 400K.

#### *Viscosity of nitrogen, oxygen and carbon dioxide*

All viscosity values reported here are given in units of μPa·s.

Nitrogen: The values calculated from the equation  $\eta = 0.0440 \cdot T + 4.6713$  for the temperature range 270-400K deviates <0.5% from the tabulated values given in NIST [A1]. The equation  $\lambda = -0.00002836 \cdot T^2 + 0.06304 \cdot T + 1.535$  for the same range deviates <0.02% from the tabulated values given in NIST. The NIST-values agree very well (< +/-0.3%) with the values given in other references for nitrogen [A2, A4].

Oxygen: The values calculated from the equation  $\eta = 0.0528 \cdot T + 4.6952$  for the temperature range 270-400K deviate <0.5% from the tabulated values given in NIST [A1]. The equation  $\lambda = -0.000003198 \cdot T^2 + 0.07427 \cdot T + 1.158$  for the same range deviates <0.02% from the tabulated values given in NIST. The NIST-values agree within +/-1% with the values given in other references for oxygen [A2, A5].

Carbon dioxide: The values calculated from the equation  $\eta = 0.0473 \cdot T - 0.8402$  for the 270-400K temperature range deviate <0.5% from the tabulated values given in NIST [A1]. The equation  $\lambda = 0.00001678 \cdot T^2 + 0.05849 \cdot T - 1.016$  for the same range deviates <0.01% from the tabulated values given in NIST.

In [A4] the error in the viscosity tabulation is assigned to be +/-1% for nitrogen in the temperature range 100-1000K and +/-2% for oxygen up to 400K.

#### References:

A1 NIST Chemistry WebBook, [webbook.nist.gov/chemistry/fluid](http://webbook.nist.gov/chemistry/fluid).

A2 Hanley H. J. M. and Ely J. (1973) The viscosity and thermal conductivity coefficients of dilute nitrogen and oxygen, J Phys Chem Ref Data, vol. 2, no. 4, pp 735-755.

A3 Uribe F. J., Mason E. A. and Kestin J. (1990), Thermal conductivity of nine polyatomic gases at low density, *J Phys Chem Ref Data*, vol. 19, no. 5, pp 1124-1136.

A4 Stephan K., Krauss R. and Laesecke A. (1987) Viscosity and thermal conductivity of nitrogen for a wide range of fluid states, *J Phys Chem Ref Data*, vol. 16, no. 4, pp 993-1022.

A5 Laesecke A., Krauss R., Stephan K. and Wagner W. (1990) Transport properties of fluid oxygen, *J Phys Chem Ref Data*, vol. 19, no. 5, pp 1089-1122.

A6 Scalabrin G., Marchi P., Finezzo F. and Span R (2006) A reference multiparameter thermal conductivity equation for carbon dioxide with an optimized functional form, *J Phys Chem Ref Data*, vol. 35, no. 4, pp 1549-1575.

A7 Reid R. Prausnitz J. and Poling B. (1987) *The Properties of Gases and Liquids* 4<sup>th</sup> edition, McGraw-Hill.

